Intensification of Delignification process by Acoustic Cavitational approach for Development of Self-healing Corrosion Inhibition Coatings.

A Thesis Submitted

To

THE NATIONAL INSTITUTE OF TECHNOLOGY WARANGAL
for the award of the degree of

DOCTOR OF PHILOSOPHY

in

CHEMICAL ENGINEERING

By

D.SUSHMITHA

Roll No. 715062

Under the guidance of

Dr.S.SRINATH
Associate Professor

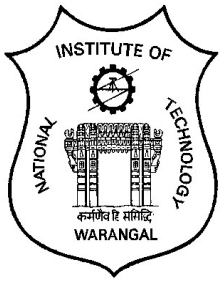

DEPARTMENT OF CHEMICAL ENGINEERING
NATIONAL INSTITUTE OF TECHNOLOGY
WARANGAL - 506004, TELANGANA, INDIA.
MARCH-2021.

DECLARATION

I declare that this written submission represents my ideas in my own words and where others' ideas or words have been included, I have adequately cited and referenced the original sources. I also declare that I have adhered to all principles of academic honesty and integrity and have not misrepresented or fabricated or falsified any idea/data/fact/source in my submission. I understand that any violation of the above will be a cause for disciplinary action by the institute and can also evoke penal action from the sources which have thus not been properly cited or from whom proper permission has not been taken when needed.

Miss Devadasu Sushmitha
Roll No. 715062

Date:

NATIONAL INSTITUTE OF TECHNOLOGY- WARANGAL

CERTIFICATE

This is to certify that the thesis entitled **"Intensification of delignification process by acoustic cavitational approach for development of self-healing corrosion inhibition coatings."** Being submitted by **Miss. Devadasu Sushmitha** for the award of the degree of Doctor of Philosophy (Ph.D) in Chemical Engineering to the National Institute of Technology, Warangal, India is a record of the bonafide research work carried out by her under my supervision. The thesis has fulfilled the requirements according to the regulations of this Institute and in our opinion has reached the standards for submission. The results embodied in the thesis have not been submitted to any other University or Institute for the award of any degree or diploma.

(Dr. S. Srinath)

Thesis Supervisor
Associate Professor& HOD
Department of Chemical Engineering,
National Institute of Technology,
Warangal.

Date : 23 -03-2021

ACKNOWLEDGEMENT

First and foremost I want to thank my supervisor **Dr. S. Srinath.** It has been honor to be, I am his Ph.D. student. He cultivated seed of the research in me and inspired to apply this knowledge not only in laboratories but also in the personal life. His invaluable contributions of time and ideas provides by him during my Ph.D. stay made me wealthy in experiences, which is productive and stimulating in all aspects. He provided me an excellent platform to nourish and grow my professional as well as personal life.

I wish to sincerely thank university authorities, **Prof. N.V. Ramana Rao**, Director, National Institute of Technology, Warangal and other top officials who gave me an opportunity to carry out research work.

I also sincerely thank **Dr. A. Shirish H Sonawane**, Professor Chemical Engineering Department, National Institute of Technology, Warangal for his continuous support towards carrying out research work. I also sincerely thank **Dr.Gogate** Professor Chemical Engineering Department, Institute of Chemical Technology, ICT Mumbai for giving me an opportunity to perform experiments in their laboratory.

I wish to express my sincere and whole hearted thanks and gratitude to my doctoral scrutiny committee (DSC) members professor **Dr. K. Anand kishore, Dr.S.Vidhaysagar, Associate professor, Dr. G. Uday baskar Babu , Assistant Professor,** Department of Chemical Engineering and, **Dr. Narshimhulu** Associate Professor Department of Biotechnology, National Institute of Technology, Warangal for their kind help, encouragement and valuable suggestions for successful completion of research work.

I would like to extend my thanks to all the faculty members in Department of Chemical Engineering for their valuable suggestions and encouragement.

I am also thankful to all the supporting and technical staff of Department of Chemical Engineering who has directly or indirectly helped during the course of my work.

I am thankful to all my fellow research scholars who helped me directly and indirectly to boost my confidence to during my Ph.D.

I take this opportunity to sincerely acknowledge the **MHRD Government of India** for providing the financial assistance in the form of stipend.

Last but not the least, I would like to thank my parents and brothers, who are surely the happiest to see me complete this endeavor. To them, I owe all my accomplishments.

DEVADASU SUSHMITHA.

Abstract:

Valorization of agricultural wastes is one of the critical current research areas due to the abundantavailability of crop residues. All types of crops and plant residues belong to lignocellulosic biomass, and its main composition is 30-35% cellulose, 28-32% hemicellulose, and 18-22% lignin and the remaining extractives, silica and ashes. Delignification is the important step for further utilisation of lignocelluloses material for different applications. Different pre-treatment methods are available for fractionation of lignocellulosic biomass to individual components, i.e., cellulose, hemicelluloses, and lignin. Cavitation plays a crucial role in the efficient removal of lignin in the pre-treatment of lignocellulosic biomass. The structure and compositions of the extracted lignin and cellulose, are more suitable to be used as natural corrosion inhibitors. The phenolic group and methoxy functional groups present in the lignin act as free radical scavenges to form inert complexes that chelate to the metal ion to inhibit a metal's corrosion reaction.

The thesis aims at an intensified process for delignification of teak sawdust (Tectona grandis) for higher lignin yields and further extraction of cellulose from delignified sawdust for the development of self-healing corrosion inhibition coatings.

Delignification process was intensified with different configurations of ultrasound reactors assisted with alkali peroxide approach and the efficacy compared with more commonly used configurations of ultrasonic reactors. Comparison with the conventional approach based on stirring has also been presented to establish the process intensification benefits. Effect of different operating parameters such as sodium carbonate concentration (0.1, 0.15, 0.2, 0.25 M), hydrogen peroxide concentration (0.2, 0.4, 0.6, 0.8, 1 M) and biomass loading (2, 4, 6, 8, 10 wt %), on the efficacy of lignin extraction has been investigated for different ultrasonic reactors by varying operating times (from 10 to 80 minutes).The maximum removal of lignin and lignin yield as87.4 % with an error of$\pm$ 2.6 % for longitudinal horn (optimum conditions of 150 W, 0.2M Na_2CO_3, and 1 M H_2O_2, 10 wt % biomass loading, and operating time of 70 minutes). Followed by probe-type ultrasonic horn with 85.1 % lignin yield were established at 150 W, 50% duty cycle, and 80% amplitude with optimum process conditions as0.2M Na_2CO_3, and 1 M H_2O_2, 10 wt % biomass loading, and 70 minutes of operating time. Longitudinal horn resulted in best efficacy (both in terms of yield and energy requirements) followed by the ultrasonic horn and ultrasonic bath, whereas the conventional approach was least effective. The extracted lignin was confirmed with

different characterization techniques. The presence of peaks at a wavelength range of 875–817, 1123–1110, and at 1599 cm^{-1} for the extracted sample confirmed the presence of lignin. An increase in the crystallinity index of the processed sample (maximum for longitudinal horn) confirmed lignin is amorphous. Overall it has been concluded that ultrasound can be effectively employed for delignification with the longitudinal horn as the best configuration.

Since the extracted lignin has more hydroxyl and phenolic ions used for the Chelation of metal, for good corrosion inhibition. It is proposed to show effectiveness of lignin as a corrosion inhibitor when it is combined with epoxy. The results are compared with the hybrid coatings, such as combination of synthetic corrosion inhibitor benzotriazole and organic polymer, especially cellulose.

Further fractionation of cellulose from delignified biomass was carried out using the ultrasonic horn. Sulphuric acid treatment was adopted for cellulose extraction from delignified sawdust. Further the extracted lignin and cellulose were reduced to required nano size through sonochemical approach.

Smart coatings with Self-healing property were prepared for corrosion inhibition through in-situ polymerization techniques. Coatings have been developed using natural healing materials such as a combination of lignin and safflower oil and sillane coupling agents, i.e., APTES, in the waterborne epoxy curing agent. Successful encapsulation of lignin and safflower oil was done via in-situ polymerization with the aid of urea-formaldehyde pre-polymer solution in the presence of surfactant polyvinyl alcohol (PVA). TEM and FE-SEM images confirm nanoparticles' encapsulation, and its histogram gives the average particle size distribution of the lignin nano particle and lignin nanocapsules as 106 and 146 nm. Polarization studies revealed that the current density decreases to a minimum of 3.703E-8A/cm^2, with the increasing weight percentage of lignin nanocapsules. Electrochemical Impedance spectroscopy and immersion studies gave a better corrosion rate for 1 wt% LNC coatings when compared to bare and standard coatings.

Benzotriazole loaded cellulose reinforced 2k polyamide coating system was developed to check the Corrosion inhibition performance of mild steel in 3.5 wt% NaCl solution for time period of 120 hours. Self-healing coatings were prepared to utilize cellulose nano fiber as a carrier for the Benzotriazole (BTA) with different loadings of 2, 4, and 6 wt%. Cellulose consists of hydroxyl groups and has sulfate and half ester groups on its surface acquired during sulphuric acid hydrolysis of delignified sawdust. These hydroxyl and sulfate groups are negatively charged and provide anions to develop a patina on the site of mild steel's

damaged coatings for providing corrosion protection. TEM images confirmed that the extracted cellulose nano fibers had cylindrical hollow shapes with an average length of 176 nm and a lumen of 23 nm in size.

The Electrochemical Impedance Spectroscopy (EIS) following 120 h of immersion proved that corrosion rate was decreased for BTA stacked cellulose reinforced coatings compared to coatings without reinforcement. At the same time, Potentiodynamic studies reveal the decrease in current density with an increase in corrosion potential (E_{corr}) for bare, standard, and different compositions of CNB. It was also observed that the decrease in corrosion rate from the weight loss studies for epoxy modified with encapsulated BTA in cellulose nano fibers implies better corrosion inhibition when compared to Bare and standard coatings of mild steel.

Sustainable eco-friendly hybrid organic coatings with high solid content came into existence which are capable of competing with the fourth generation coatings. The gravimetric analysis proved that the corrosion rate is nearly equal to both coating system for higher loadings of corrosion inhibitor that is for 1.5% LNC is 0.1022 ± 0.4 and for 6% CNB is 1.76 ± 0.6 mm/year. The Polarisation and EIS results revealed better corrosion inhibition for modified epoxy than epoxy alone.

Tables of Content

Appendix

List of Figures

List of Tables

List of Abbreviations or Symbols or Units

O/W	- Oil by water
UF	- Urea formaldehyde
TEA	-Tri-Ethanol Amine
PVA	-Poly Vinyl Aniline
IPDI	-Isophorone diisocyanate
MDI	- Diphenyl Methane Diisocyanate
APTES-3	-Aminopropyl triethoxy silane
LNC	- Lignin Nano Capsule.
FTIR	- Fourier Transform Infrared Radiation
FE-SEM	-Field Emission Scanning Electron microscopy.
TEM	- Transmission Electron Microscopy
TGA	- Thermo Gravimetric Analysis.
EIS	- Electrochemical Impedance Spectroscopy
NC	- Nano Cellulose.
NCB	- Benzotriazole loaded Nano cellulose

Symbol

|Z|	- Magnitude of Impedance
Ω	- Ohm
I_{cor}	- Corrosion current.
E_{cor}	- Corrosion potential
C_C	- Coating Capacitance
C_{edl}	- Electric Double layer Capacitance.
R_s	- Solution Resistance
R_P	- Polarization Resistance.

Rc	Coating Resistance

Units

M	- Molarity
k	- Rate constant
A/cm^2	- Amperes per centimeter square
µm	- micrometer
nm	- nanometer
W	- Watts
V	- Volts
kHz	- kilo Hertz
Mm/year	- milli meter/ year.
$F.cm^{-2}$	-Faraday per centimeter square
$\Omega.cm^2$	- Ohm per centimeter square.
Pbw	-Parts by weight.

Chapter 1

Introduction

Chapter 1 Introduction

1.1General

1.1.1Agricultural waste as a Raw material

Waste valorization is one of the important subjects to be investigated in order to recover valuable chemicals or products. Waste valorization increases the countries capital, and also reduces the greenhouse emissions and toxic evolution during their conversion process. Agricultural wastes are easily available, which are renewable and sustainable low cost raw material. Major quantities of agricultural wastes are mainly of lignocellulosic biomass type. The Pretreatment / fractionation / separation of lignocellulosic biomass gives valuable components.

Investigation has been initiated from several years, and gradual development in the technologies made the pretreatment process very interesting and easy by integrated and intensified approaches along with multiple value added by products. The waste valorization has given more insight in to increase the economy. Therefore agriculture waste is used as a raw material for extraction of value added products such as lignin and cellulose for checking corrosion inhibition performance of mild steel.

1.1.2 Types of Biomass Available

Biomass can be available from hard/soft wood or from living micro-organisms like algae, bacteria, fungi. Different types of biomass could be from forest, agricultural, industrial resources, and municipal, sewage, animal wastes. The twigs, sawdust, bark can be extracted from hard wood and stalks, cobs/leaves, manure are could be obtained from agricultural resources. Lignocellulosic biomass can be broadly classified into virgin biomass, waste biomass and energy crops. Virgin biomass includes all naturally occurring terrestrial plants such as trees, bushes and grass. Waste biomass is produced as a low value byproduct of various industrial sectors such as agriculture (corn stover, sugarcane bagasse, straw etc.) and forestry (saw mill and paper mill discards). Energy crops are crops with high yield of lignocellulosic biomass produced to serve as a raw material for production of second generation bio-fuel; examples include switch grass (*Panicum virgatum*) and Elephant grass. The status of solid waste generation in India was shown in figure 1.1. Bagasse, municipal wastes, rice husks, jute fiber, rice wheat straw, groundnut shell contribute more than 19% of all solid wastes produced in India. Therefore agricultural wastes are produces more when

compared to all the solid wastes in India. Hence attempts were made to decrease the solid wastes either by converting it to any useful products, or just to burning or to fill the lands.

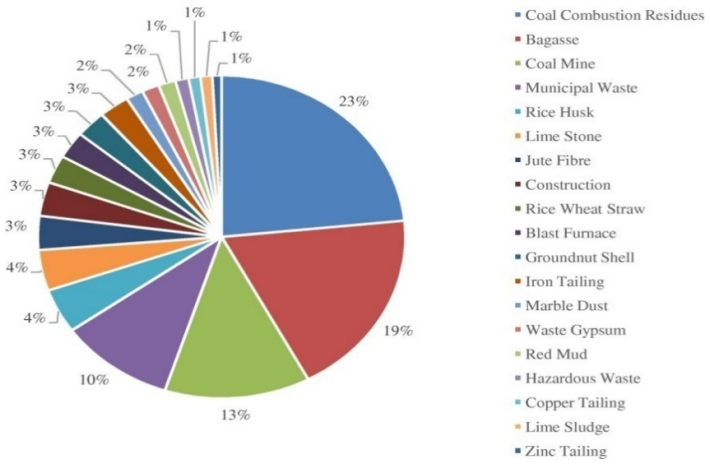

Figure 1.1. Status of solid waste generated in India (Madurwar et al., 2013).

Valorization of wastes has become attractive since it decreases the solid wastes, and in turn increases the economy of an country. Especially this is very much important to the developing countries like India. Even though pollution control board has set some limits to decrease the green house emissions into the atmosphere. The pollution control board has reported that during 2000–2011, atmospheric CO_2 levels increased to 390.5 ppm in India (champa et al., 2016). Both the aspects of limited availability as well as concerns for climate change and greenhouse gas emissions have led to enhanced interest in the alternate resources and development of the processes.

1.1.3 Structure and composition of Lignocelluloses biomass

Valorization of agricultural wastes is one of the important current research areas due to abundant availability of solid wastes like agricultural wastes. The most common type is Lignocellulosic biomass and is composed of three polymeric compounds which occupy 99 % of total composition and are classified into structural (cellulose and hemicellulose) and non-structural carbohydrates (lignin, extractives, silica, and ashes). Selection of lignocelluloses biomass is mostly depending up on the high cellulose, hemicelluloses and low lignin content. Considering a plant material, which is not a food crop, will be an economic way to for its valorization. Teak sawdust consist of more amount of cellulose 36.6% and hemicellulose 35.3% , 26.7 % of lignin (Gasperic., 2019). Lignin is in the form of Klason lignin and acid soluble lignin (ASL).

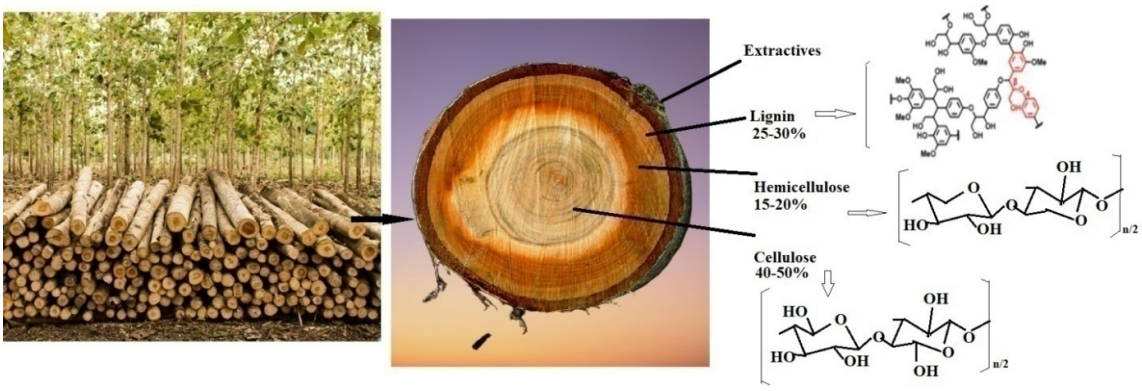

Figure 1.2.Structure of Tectona grandis Lignocelluloses biomass.

The structure and compositions of cellulose and acid soluble lignin (ASL) are required and important to be used as a natural corrosion inhibitors. Since Lignin (ASL) has good amount of phenolic OH^- and methoxy components which acts as a chelating agent to inhibit corrosion rate of a metal. Interestingly cellulose surface contains hydroxyl and sulfate groups that are negatively charged are responsible for chelating with metal ions.

Table 1.1.The typical composition of lignocellulosic biomass.

Lignocelluloses biomass	**Cellulose (Wt%)**	**Hemicellulose (Wt%)**	**Lignin (Wt%)**	**Reference**
Teak wood	36.6	26.7	35.3	Gasperic., 2019
Beech	20	33	45	Di Blasi et al., 2010
Poplar	20	24	49	Di Blasi et al., 2010
Aspen	19.5	21.7	52.7	Taherzadeh et al., 1997
Cherry wood	18	29	46	Di Blasi et al., 2010
Willow softwood	29.3	16.7	41.7	Taherzadeh et al.. 1997
Pine	27.3	20.3	46.9	Taherzadeh et al., 1997
Franch	24.1	17.8	48.4	Wang et al., 2016
Spruce	27.6	29.4	43	Demirbas et al., 2005
Japans cedar	33.8	23.1	38.6	RabemanolontsSaka., 2013
Fir	30	22	45	Di Blasi et al., 2010
Hardwood	20-25	45-50	20-25	Karthik rajendra et al., 2018
Softwood	27-30	35-40	25-30	Karthik rajendra et al., 2018

The pretreatment of biomass and resultant byproduct valorization is crucial in deciding the cost of the product. The typical structure of lignocelluloses biomass is shown in the Figure 1.2 and the composition of lignocelluloses biomass varies for different plants and trees materials as shown in table 1.1. Hardwood and softwood has different compositions and are vary from place to place, and surrounding climatic conditions.

1.1.4 Classification of Fractionation methods

Different types of fractionation methods are available to effectively fractionate/separate cellulose, hemicellulose, and lignin from lignocelluloses biomass. Pretreatment process could be physical, chemical, thermo chemical and enzymatic process as explained in the figure 1.3. Most of treatment processes are used in bio fuel production, to make availability of cellulose to the enzymes. Since structural carbohydrates (like cellulose and hemicellulose) are covered by unstructured carbohydrates (like lignin).

Most utilized physical process could be dry milling or wet milling process, among these two, wet milling is most popular process because of high costs of by-products obtained during bio fuel production. In this process lignocelluloses biomass are soaked for 10-20 days, and in dry milling process biomass was soaked for 1or 2 days, and further milling takes place. This process makes availability of cellulose from lignocellulosic biomass by removing lignin. (Ramezanzadeh et al., 2011).

Since lignin is a complex structure it is difficult to extract at the same time it has different names depend up on its characteristics. Generally to extract lignin from lignocelluloses biomass is to first try to solubilize the lignocellulose biomass in any solvent to weaken the linkages between structural and unstructured carbohydrates. The solvent could be anything water, acid, salt solution etc. Therefore the processes are named accordingly to the pretreatment process. If lignin is extracted by Kraft process, then it is termed as “Kraft lignin”. If lignin is extracted by alkali solution, it is termed as “alkali lignin”. If extracted lignin is soluble in 72% of sulfuric acid it is termed as “acid soluble lignin” ASL. (Rahman et al., 2018)

Efforts have also been directed to improve the efficiency of lignin extraction process and to obtain a high percentage of structural carbohydrates. Some of the specific examples of the pretreatment processes are high pressure treatments, microwave processing, hydrothermal liquefaction, torrification (both dry and wet approach), steam explosion, ozonolysis etc. (Goyelsetu et al., 2016). Large shear and turbulence effects play a crucial role in the efficient

pretreatment of lignocelluloses biomass and these effects can be effectively obtained using cavitational reactors (Moretti et al., 2014).Emerging technologies for intensified processes such as pretreatment with microwave irradiation, Pyrolysis, wet oxidation, dry oxidation Pretreatment, saccharification and fermentation using ultrasound, hydrodynamic cavitation, Gama ray Electron beam irradiation, Pulsed electric field, High Hydrostatic pressure, High pressure homogenization, High pressure Autoclave reactor, steam explosion. Some of these pretreatment intensified processes are explained in the literature review section along with references.

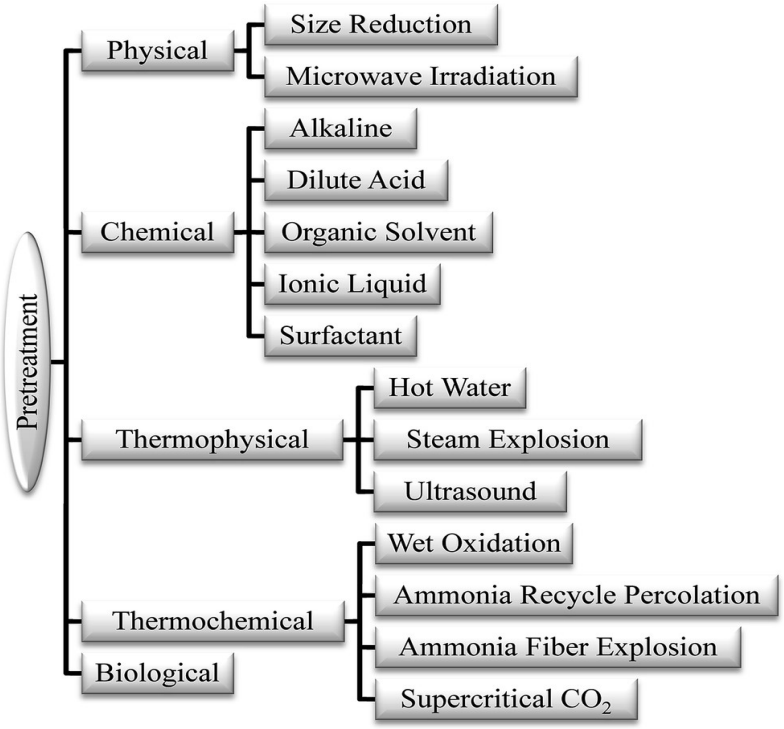

Figure 1.3. Classification of pretreatment processes for lignocelluloses biomass.

1.1.5 Limitations of Conventional Fractionation processes

One of the main limitations of conventional fractionation processes is energy, operating time and large processing volumes for with yields of the required fractions. So there is a need to search or develop fractionating process for pretreatment of lignocelluloses biomass process for processes intensification. Even though some existing process gives good results in yields, but those processes are lacks in reducing operating costs there by increasing the cost of the final product which is not acceptable for a middle class people. Every process has its own pros and cons. subsidizing all the disadvantages by improving the process at each

single stage and finally integrating the process reduces the several steps to get the final product.

There are several pretreatment process exits as explained above for instance considering steam explosion process require high energy for treatment, but gives quality product in terms of lignin as well as cellulose. There are several similar kind of treatment process, like using high pressure Autoclave reactor, and some biological process which are cost effective if the enzymes and micro-organisms are available at reasonable cost. Therefore interests have been shifted to intensification of delignification process.

1.1.6 Natural polymers as Corrosion resistant material

Natural polymer consists of several hetero atoms, and some functional groups such as hydroxyl, nitro and heterocyclic compounds which are responsible for corrosion inhibition. These components present in natural polymer will replace anions that are lost due to the dissolution of metal during corrosion. So that a natural polymer can behave as a corrosion inhibitor by providing self-healing characteristics (G. and F. 2014)

Biomass consists of carbohydrate polymers (such as cellulose and hemicelluloses) and aromatic polymers (lignin) which can be easily converted to value added products (Division et al. 2019). Since nano cellulose has hallow like structure it can accommodate any active chemicals which can be released whenever necessary and needed (Vijayan and AlMaadeed 2016; Zhao et al. 2017).

Valorisation of natural materials has been started to enhance ones economy with low cost products with sustainable eco-friendly raw materials. Lignin and cellulose containing functional groups such as hydroxyl (OH-), methoxy (CH_3O-), and sulphate (SO_4^{-2}) (Neumann et al. 2014) which are responsible for chelating with metal ions, by sharing its lone pair of d-electrons (Olad et al., 2013).Interests have been shifted for the formulation of corrosion resistant paints from synthetic corrosion inhibitors like chromates, benzotrialze with natural polymers to enhance the corrosion inhibition rate. The inclusion of natural polymers converts the hazardous paints to eco-friendly paint by reducing the release of harmful gases, and harmful voltaic materials (Zhao et al. 2017).

Intestingly natural materials structure also helps to act as a carrier for corroion inhibitor. Even though surveys has shown the combination of natural and synthetic corroison inhibitors has given best performance as compared ro the syntheic corroion inhibitor alone and natural polymer alone ((Frankel 2016).

1.2 Process Intensification

Lignocellulosic materials are considered as effective and sustainable source of other value added products. The fractionation of lignocelluloses materials into cellulose, hemicellulose and lignin typically involves pre-treatment steps, which can be cost intensive and also requires the use of environmentally benign chemicals, leading to interest in application of process intensification approaches.

Industries are focusing on the intensified processes such as sonication. Process Intensification (PI) is about a change made to a process to make it work in a smaller volume for the same performance.

Intensification in the current context is referred to as any improvement leads to enhanced rates possibly with lower energy and chemical as well as enzyme requirement for delignification or hydrolysis. Some of the intensified processes for delignification are also discussed based on use of different reactors such as microwave irradiation, gamma ray radiation, electron beam irradiation, high pressure autoclave, steam explosion, photo chemical oxidation, hydrodynamic cavitation, acoustic cavitation.

Different oxidation processes for intensification of delignification processes, using different oxidizing agents such as, oxygen, ozone, hydrogen peroxide, per acetic acid, Organic peroxides etc were also discussed.

Therefore this section introduces the alkali peroxide process (AHP) and acoustic cavitation and its importance in delignification, and discuss about the mechanisms and working principle.

1.2.1 Lignin and its separation techniques

A. Lignin

Lignin typically consists of mono-lignols, also known as aromatic alcohol precursors (p-coumaryl alcohol, coniferyl alcohol, sinapyl alcohol etc) and phenyl propane units (aromatic constituents) such as p-hydroxyphenyl, guaiacyl and syringyl units. These units are linked with structural carbohydrates like hemicellulose with phenyl ether,α-O-4 and β-O-4 linkages. Lignin consist of 60-80 % of β-O-4 linkages(Neumann et al. 2014) and the typical structure of lignin is mentioned in the **figure 1.4** (Rauber et al. 2018). The main objective of any pretreatment process is to provide maximum cleavage of phenyl ether α-O-4 and β-O-4 linkages to remove lignin fragments easily.

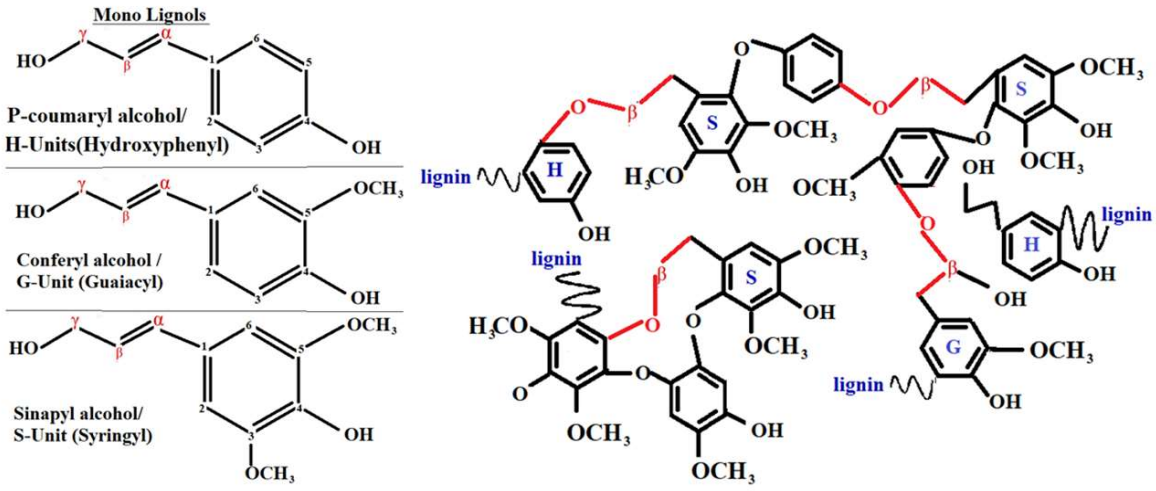

Figure 1.4.Structure of Mono Lignols and a typical structure of Lignin containing S, G, H Units liked with ether β–O-4 linkages.

B. Lignin separation techniques

There are two main techniques for lignin separation they are filtration and precipitation. However, precipitation of lignin by lowering the pH is the most common method for the separation of kraft and soda lignins (Jönsson and Wallberg, 2009; Vishtal and Kraslawski, 2011b). It is difficult to separate soda lignin though filtration due to its highly hydrophilic structure (Doherty et al., 2011).

Lignin from black liquor can be obtained by precipitation with acid in two steps. The Ligno Boost process is used to recover lignin from kraft black liquor by acidifying it with carbon dioxide (Beis et al., 2010; Li, 2011). However capturing of Co2 is one of the important step to be considered which increase the cost of operation. The Lingo Boost process is briefly explained as follows. In the first step, carbon dioxide is used to reduce the pH of the liquor to 9-10 (Vishtal and Kraslawski, 2011b). In this step, about 75% of the lignin is precipitated as a sodium salt. Lignin is obtained by suspending the salt in water and decreasing the to pH below 3 with sulfuric acid (Li, 2011; Vishtal and 21 Kraslawski, 2011b).

Finally, lignin is separated through a filtration process (Vishtal and Kraslawski, 2011b). The cost for the extraction of lignin by carbon dioxide precipitation is about $32- $50 per ton of lignin (Axelsson et al., 2006).

1.2.2 Delignification processes.

Industries have shown interest on the intensified processes such as sonication. Process Intensification (PI) is about a change made to a process to make it work in a smaller volume for the same performance.

Some of the process intensified delignification processes are microwave irradiation, gamma-ray radiation, electron beam irradiation, high-pressure autoclave, steam explosion, photochemical oxidation, hydrodynamic cavitation, acoustic cavitation (Jerold et al., 2018)

A. Conventional

According to the tappi method of lignin removal, 72% sulphuric acid was used to treat wood, sulfate pulp, and sulfite pulps. Acid insoluble lignin was measured and reported as 19-30, 2.6-19.1, 6.5-28 (Tappi T-222 om-02 method) similarly, acid-soluble lignin was 30, 24, 24 respectively for wood, sulfate pulp, and sulfite pulps, respectively (measured spectrophoto metrically [Tappi UM 250]. Lignin 48% was removed from sugarcane bagasse after de-polymerization of polysaccharide at processing conditions of 28% v/v ammonium hydroxide solution, and with an operating temperature of 130°C for 1 h (walker et.al 2012). In another paper, Morritis used the same sugar cane bagasse, irradiated with microwave for 5min with distilled water, phosphoric acid of pH3, and 100% glycerol, was reported that the highest separation of hemicelluloses and cellulose was occurred (Morrit et al 2014)

B. Microwave Irradiation

There is a difference between microwave heating and conventional heating. The traditional heating method takes place from the outer surface. It then reaches the core of the processing material, whereas microwave heating is volumetric heating that is heating takes place from the core of the material. A microwave reactor uses borosilicate glass (tan δ = 0.0010) which is transparent to microwave irradiation (De Souza et al., 2015). The scientific microwave has a flexible probe for temperature measurement with an I.R sensor.

Bussemaker and co-workers used a combination of ultrasound in oxidative environments to depolymerize the lignocellulosic biomass in alkali presence. Their studies are performed on specialized equipment that merges the use of ultrasound and microwave then compares, the results with those obtained with microwave alone. He reported combination of equipments for pretreatment gives better performance than microwave alone, but explained the importance of

microwave irradiation for pretreatment (Bussemaker et al., 2013). Therefore from the previous studies, proves that simultaneous use of microwave and ultrasound for less residence time, and thereby utilizing non-oxidizing compounds gives higher yields of main compounds (i.e. cellulose, hemicellulose, and lignin) but with less purity. The pretreatment with oxidizing compounds results in lesser yields but with higher purity. The production of nano cellulose composites and derivatives, using microwave irradiation along with 3% (w/v) NaOH, at 120 °C for 10 min was studied (Ming-Guo Ma et.al 2005) he separated nearly 85% lignin from Mission grass. And from the solid residue of treated mission grass, they observed an excellent reducing sugar content (34.3 ±1.3 g per 100 g of dried biomass), mainly of 31.1 ± 0.8 g of reducing sugar per 100 g of dried biomass.

C. Gama ray Radiation

Gamma beam radiation is acquired from radioisotopes (Cobalt-60 or Cesium-137) and has tried as a lignocellulosic pretreatment. Ionizing radiation can undoubtedly reaches inside of the lignocellulosic structure, causing cleavage of the lignin and structured carbohydrate bonds. The further cleavage was done with the aid of free radicals which will decay biomass rapidly at amorphous region after/at end of radiation. Exposure of radiation for a particular period can degrade the crystalline regions.1200killo Grays (KGy) gamma radiation on rapeseed straw was applied to obtained better cleavage of lignin and cellulose bonds, with good thermal stability with 80% cellulose and 50% lignin removal (Zhou et al., 2016).The impact of 891 killo Grays (KGy) gamma irradiation was used for better bioconversion of lignocellulosic biomass to microcrystalline cellulose (Liu et al., 2015).

D. Electron Beam Irradiation

Electron beam processing or Electron Beam Irradiation (EBI) is a procedure that utilizes beta radiation with a high energy, to treat lignocellulosic biomass and also EBI was used for variety of purposes. This may occur under maximum temperatures and also in inert environment like nitrogen. Conceivable utilizations for electron beam radiation involve cleavage of lignin and carbohydrate bonds in lignocellulosic biomass.

Electron energies typically vary from the keV to MeV range, depending on the depth of penetration required. The irradiation dose is usually measured in grays but also in Mrads (1 Gy is equivalent to 100 rad).Using electron beam accelerator with Different dosage of 100-1000 kGy was used for cellulose degradation (Jusri et al., 2018). Water soaked rice straw is

treated with Electron beam irradiation at a dose of 1MEV at 80 kGy for 120 hours of hydrolysis to obtain 70.4% of delignification (Bak et al., 2014).

E. High pressure hydrothermal treatment

Selective fractionation of biomass can be obtained from high temperature and pressure processes like water extractives and hemicellulose and lignin can be removed at temperature of 120 to 180°C and at a pressure of 1 -5 bars. Eucalyptus is used for hydrothermal treatment at 181°C for 37.5 minutes with a liquid to solid ratio of 6:1 w/w, with lignin yield of >70% (Aditiya et al 2016). More than 60 % lignin removal was obtained with hydrothermally treated eucalyptus sawdust for a set of operating parameters such as 150°C, 113 minutes, with L/S ratio 5:1 w/w (Alfaro et al., 2009). So the optimum conditions for lignin and hemicellulose removal is at 180°C and at a pressure of 1 -5 bars.

F. Steam explosion.

Steam pretreatment in a batch reactor involves heating wood chips at high temperatures and pressures, followed by mechanical disruption of the pre-treated material either by violent discharge into a collecting tank (explosion) (Schwald wt al.,1989; Ramos et al.,1992)or by mild blending after bleeding the steam pressure down to atmospheric (no explosion)(Ramos et al.,1992; Harold 1987).The high-pressure steam radically modifies the plant cell wall structure, yielding residue that is chemically modified lignin that can be further extracted by mild alkali (Schwald wt al.,1989; Ramos et al.,1992) dioxane, ethanol(Brownell et al.,1989) or oxidative agents such as alkaline hydrogen peroxide (Schwald wt al.,1989; Ramos et al.,1992) and sodium chlorite. Steam explosion of empty fruit bunch using auto hydrolysis for bio-refinery approach tells about the solubilization of hemicellulose in the form of xylose an arabinose obtained as a hydrolysate. There is an increase in porosity and crystallinity after steam explosion of empty fruit bunch (Medina et al., 2016) with 50-70% lignin removal.
Bioethanol and along with bio-oil co-production experiments were conducted with steam exploded wheat straw through a bio-refinery approach. Cellulose and hemicellulose were utilized for ethanol fermentation for better yield by increasing the inoculums size from 1g/l to 3 g/l. Pyrolytic conversion of remaining 70% lignin to bio-oil (Tomas pejio et al., 2017).

Table 1. 2. Different types of pretreatment processes

Biomass type & reference	**Equipment**	**Operation conditions**	**Result**
Bagasse (Yuan et al. 2018)	Chemical	0.25 M NaOH at 30°C for 6 h as the first step followed 40 mg of H_2O_2 per g of biomass at 50°C, 15 h.	54.1 % acid soluble lignin precipitated
rapeseed straw (Zhou et al., 2016).	1200killo Grays (kGy) **gamma radiation**	water	80%Cellulose, 50 % of lignin removal.
Eucalyptus (Aditiya et al., 2016)	**High pressure auto clave reactor**	181 °C for 37.5 minutes, 1 bar, S/L 6:1	lignin yield of 70%
Hybrid polar, silver birch, hybrid aspen and sugar maple) (Bansal et al. 2016)	fed-batch, two-stage Cu-AHP pretreatment process	5M NaOH 125µL of a 40mM CuSO4 solution, 160mM 2,2´-bipyridine 150µL of 30% H2O2 (w/w) 10% loading)	enhanced Klason lignin 0.17, 0.12, 0.12, 0.18 g/g respectively. ≥ 90% lignin
Bagasse Ruly (2016)	1mm of orifice Diaphragm pump **hydrodynamic cavitation**	0.48 M of NaOH, 4.27% of S/L ratio and 44.48 min	52.1% of glucan content, 60.4% of lignin removal
Bagasse (Nakashima et al., 2016)	narrow throat **hydrodynamic cavitation**	sodium percarbonate for pre-treatment	glucose and xylose with minimum inhibitor conc.. that is furfural
empty fruit bunch (Medina et al., 2016)	**Steam explosion** using auto hydrolysis	water	80% solubilization of hemicellulose 50-70% lignin removal
sugarcane bagasse Huang et al., 2016).	**High pressure Autoclave reactor**	180 °C 1 -5 bars	Water extractives and hemicellulose and lignin
Mission grass (Ming-Guo Ma et.al 2005)	**microwave irradiation**	3% (w/v) NaoH, at 120 °C for 10 min.	85% lignin

G. Photochemical Oxidation

This process involves UV light, hydrogen peroxide and ozone for pretreatment of biomass. However this process on combination with steam exploded biomass reported for higher fermentable sugars and better crystallinity of treated biomass.

Combination of ultrasound and ozonation can improve the lignin yield but not as effective as a microwave and seam exploded treated biomass. On comparison of techno economic analysis steam exploded or high pressure auto clave reactors gave best results with minimum operating and maintenance costs (Gomes et al., 2012).

1.2.3 Ultrasound assisted Alkali biomass pre-treatment

The fractionation of lignocelluloses biomass into individual components involves very costly chemicals or the high energy process which increases the cost of the final product. Decreases the yields with long operation time are also one of the drawbacks. An intensified process like sonication can increase the hydrolysis reaction's by producing free-radical chemicals (sono-chemical effects) as well as mechanical effects (mechano-acoustic effects) inside the reactor. This synergetic effect of both sono-chemical and mechano-acoustic effects will help in efficient generation of free-radicals that helps to attacks on hydroxyl groups of cellulose–lignin linkages. Ultrasonic de-polymerization, separation, degradation and condensation of lignin takes places in one reaction with less time of operation. The shear forces generated inside the reactor due to sonication also helps in de-polymerization of the biomass. The structure and morphology of treated biomass through SEM images, product yields from the literature review have shown the importance of sonochemical effects in the pre-treatments.

The depolymerization and solubilization of lignin, hemicellulose and bleaching of cellulose due to radical generation also reduces the steps for producing high quality cellulose.

Sonication not only helps in separation of lignin but also solubilization and bleaching of cellulose. The extent of degradation of the components has to be considered during a pretreatment of polysaccharides (lignocelluloses biomass) to mono saccharides. However this can be controlled by optimizing the ultrasound equipment parameters such as power, frequency, amplitude, and duty cycle along with experimental operating parameters such as concentrations of solvent, temperature, maintaining desirable solid to liquid ratio.For better understanding of the degree of polymerization one should know the mechanism of sonication and how it works. So a brief introduction to mechanism and working principle of sonication was done.

1.2.4 Cavitation Processes and its types

Cavitation is a process of generating cavities filled with vapour or gas that dissolves in surrounding fluid by sudden collapse releasing large amount of temperature and pressure. Sonication takes place continuous and in discontinuous mode. Sonication waves produce compression and rarefaction cycles. During its compression cycle bubble formation starts and it continues to grow until there is a large pressure difference between the inside bubble and its surrounding liquid. At a large pressure difference it will collapse generating large amount of heat and pressures. This sudden release of gas generates radicals in presence of sonication in liquid medium. The release of free radicals such as hydroxyl ions (OH-), superoxide radicals ($O_2^{\bullet}$), and ozone are responsible for chemical affects (Ramadoss et al., 2016). Therefore this process of radical generation for possible chemical reactions in homogenous or heterogeneous reaction in presence of sonication is termed as "sonochemical reaction". The shear forces that produces due to compression and rarefaction cycles produces mechanical effects and these effects in presence of sonication are termed as "mechano-acoustic cavitation".(Ramezanzadeh et al., 2011)

There are two types of cavitations one ***Natural cavitation*** and the other ***Artificial cavitation***

Natural cavitation is characterized by two phases: initial bubble cavitation and oscillation of bubbles. Bubble cavitation has a cavitation field with a low pressure zone, filled with cavitation bubbles in clusters. At high pressure zone, cavitation bubbles are broken to form a micro-flow at 50-1500 m / s and the pressure of 102 MPa.

The bubbles oscillate and grow slowly in size or shape, larger than the cavitator by 1-5 times or more. The pressure pulse produces a periodic growth and collapse of cavitation bubbles. The bubble oscillation mode is widely used in the processes of mixing, degassing, evaporation and contact heating. Natural cavitation occurs in liquids when pressure falls below vapour pressure. It creates cavities and cavitation bubbles in liquid filled with steam and diffused gases.

Artificial cavitation occurs by venting liquid flow with gas. The gas is generated under pressure. Artificial cavitation is characterized by two types of gas-leakage: the pulsating or portion-leakage, and the constant gas-leakage with continuous gas flow. Artificial cavitation mode is used for the aeration of sewage, for mixing gas and liquid, for contact heat transfer, flotation, it is also used in ejection equipment.

In natural cavitation the pressure in the cavity is equal to the vapour pressure of the liquid at the constant liquid temperature. In artificial cavitation, the pressure is formed in the cavity due

to the enhanced gas-leakage. It is always higher than the vapour pressure. This allows to simulate a wide range of cavitation, for example, increasing the flow of liquid would cause cavitation on the walls of the cavity(energy.Globecore.de).

Cavitation devices are based on the processes of cavitation, effective mixing, activation, dispersing and homogenization. They are new generation equipment greatly intensifying and accelerating the processes in liquid environments, significantly lowering the cost of energy and resources.

These devices can be classified according to operation mode, input and output of the gas phase, the type of design and features, and the types of cavitation process, which could be natural and artificial.

Different types of cavitation such as hydrodynamic cavitation, acoustic cavitation, particle cavitation, and optic cavitation (Pandith et.al., 2011, Parag et.al., 2014) can be used for the processing of lignocelluloses biomass. Generally, hydrodynamic cavitation is reported to generate much higher cavitational intensity (Kuldeep et al., 2011).

Hydrodynamic cavitation is produced by pressure variation in a flowing liquid caused by the velocity variation in the system by changing the flow geometry of the flow system.

Acoustic cavitation is same process like hydrodynamic process but the difference is that it Vapors/ bubbles/ voids are formed due to sound waves that are generated by piezoelectric transducers. It is a result of pressure variation in a liquid when ultrasound (sound with frequency greater than 16 KHz) waves pass through it.

Particle cavitation is produced from the rupture of a liquid due to high-intensity light or a laser.

Optic cavitation is produced by any type of elementary particle beam (e.g, a proton) rupturing a liquid, resulting in cavitation.

Acoustic cavitation has a wide range of applications in the intensification of various processes such as emulsification, dispersion, crushing, separation, mixing, energy production, encapsulation of nanoparticles, wastewater or sludge treatment, enzymatic reactions, oxidation of unsaturated oils, biodiesel production from non-edible oil etc. (Yonemoto et al., 2015; Subedare et al., 2016; Prajapat et al., 2016)). In general, for the heterogeneous systems, acoustic cavitation is most effective under low frequency and high power operation.

1.2.5 Mechanism and working Principle of Acoustic Cavitation

Acoustic cavitation is most likely to occur under low frequency and high signal amplitude ultrasonic waves. Crystals of materials such as quartz vibrate very fast when electricity is passed through them an effect called "piezoelectricity." As they vibrate, they manipulate the air around them and the fluids they come in contact with, producing ultrasound waves.

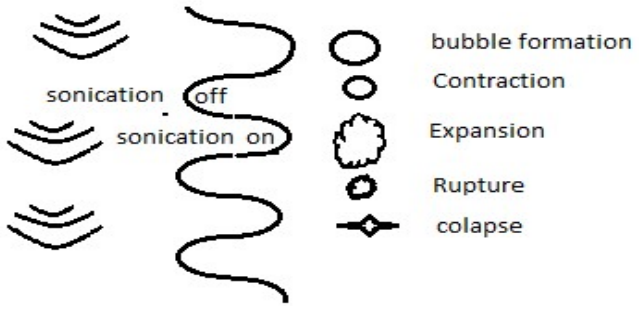

Figure 1. 5. Illustration of compression and rarefaction cycles in cavitation reactor.

The ultrasound waves causes cavitation, it is formation of voids or bubbles in the aqueous environment induced by the pressure fluctuations by passage of sound waves (Hodge et al., 2008; De Souza et al., 2015). The growth of voids occurs continuously to a certain maximum extent, where the growing void is unable to hold onto the accumulated energy leading to the adiabatic collapse within microsecond time intervals. When particle comes in the territory of the cavitation range, the collapse of bubble or cavity occurs and it may occur in asymmetric or symmetric position. When the solid particles are in contact with the bubble territory, then the bubble cannot collapse symmetrically and forms micro-jets, this phenomenon is known as asymmetric cavitation. When the solid particles are not in the range of cavitation bubble, then the bubble collapse symmetrically and this phenomenon is known as symmetric cavitation. The net result is the sudden release of the accumulated energy coupled with generation of high temperature and pressure pulses as well as intense liquid circulation and turbulence (Brebu et al., 2010).

Mechanism of acoustic cavitation was explained with the common radical generation reactions that takes place in the cavitation reactor in the presence of water, and hydrogen peroxide. Generally hydrogen peroxide readily decomposes in alkali medium to give hydroxyl ($OH^{\bullet}$) and superoxide radicals ($O_2^{\bullet}$) which are helpful in delignification. The step by step reactions occurring in the presence of hydrogen peroxide under alkaline conditions are given as follows:

$$H_2O_2 + H_2O \rightarrow HO_2^- + H_3O^+ \qquad \text{(eq 1. 1)}$$

$$H_2O_2 + HO_2^- \rightarrow OH^{\bullet} + O_2^- + H_2O \quad \text{(eq 1.2)}$$

$$OH^{\bullet} + O_2^- + H^+ \rightarrow O_2 + H_2O \quad \text{(eq 1.3)}$$

Application of ultrasound also generates radicals in the presence of water by dissociation of water molecules based on the cleavage of hydrogen−oxygen (H−O) bonds. The radicals can give a series of reactions as represented by equations 1.4-1.7 possibly forming H_2O_2 and ozone which are also oxidizing agents.

$$H_2O \xrightarrow{)))} H^{\bullet} + {}^{\bullet}OH \quad \text{(eq 1.4)}$$

$${}^{\bullet}OH + H_2O \rightarrow H_2O_2 + O^{\bullet} \quad \text{(eq 1.5)}$$

$$O_2 \rightarrow 2O^{\bullet} \quad \text{(eq 1.6)}$$

$$O_2 + O^{\bullet} \rightarrow O_3 \quad \text{(eq 1.7)}$$

The hydroxyl radicals and other in-situ formed oxidants have capability to degrade the phenolic parts in lignin, delivering low-atomic weight compounds, and causing lignin depolymerization (K.S Suslick et al 2008, R.M Wagterveld et al 2011).

1.2.6 Oxidation processes

Oxidation process for delignification or saccharification is to oxidize the lignocelluloses biomass such that it effectively converts polysaccharides to monosaccharide's without or less degradation of components owing to more yields. An oxidation process are occurred by oxidizing agent that have ability to oxidize those are mostly free radicals such as (OH, OOH, Ozone etc) (T.Y.Wu et al., 2019)

In any fractionation of lignocellulosic biomass mainly involves physical / chemical / biological methods or in combination pre-treatment methods to remove lignin, and to separate cellulose from biomass. An oxidative pre-treatment process of lignocellulosic biomass removes lignin easily and bleaches the delignified biomass and makes availability of cellulose.

1.2.7 Alkaline Hydrogen Peroxide (AHP) process

Alkaline Hydrogen Peroxide (AHP) process is a combination of alkali and hydrogen peroxide process. AHP processes also called as bleaching process since it involves hydrogen peroxide as a bleaching agent for bleaching of lignocelluloses biomass. It reduces several steps in pre-treatment for delignification and saccharification process.

1.2.8 Mechanism of AHP process

AHP process proceeds until the good amount of radical generation by decomposition of hydrogen peroxide. The intermediate radicals are the initiators for various oxidative reactions. In presence of alkaline environment the decomposition reactions of hydrogen peroxide will increase especially at pH 11.5.

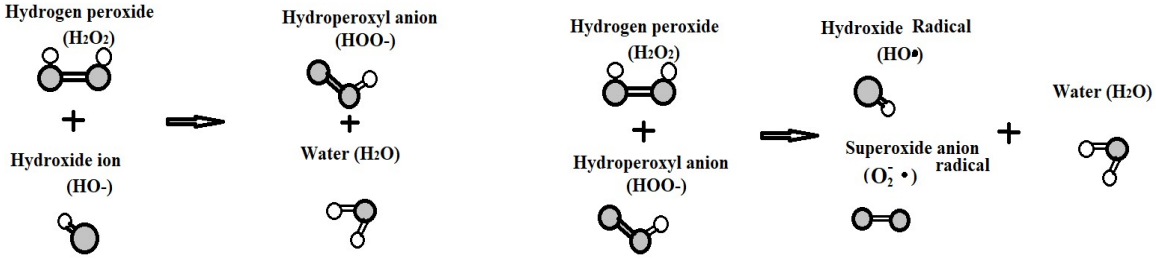

Figure 1. 6. Illustration of radical generation in AHP process.

The important reactions that are involved in the AHP process are illustrated in the figure 1.6. This explains the formation of hydroperoxyl anion (HOO^-), during decomposition of hydrogen peroxide (H_2O_2) will help to accelerate oxidative reactions. This hydroperoxyl anion (HOO^-) acting as a initiator and reacts with hydrogen peroxide (H_2O_2) to form highly reactive hydroxide (HO*) radicals, and superoxide anion radicals (O_2^{-*}) (Parag et al., 2011).

Lignin consist of 60-80 % of β-O-4 linkages that are linked with structural carbohydrates like hemicellulose with phenyl ether, α-O-4 and β-O-4 linkages. These β-O-4 linkages are effectively cleaved in AHP process at pH 11.5-11.6. Hence AHP delignification process is said to be strong pH dependent.

Hydroxide (HO*) radicals, and superoxide anion radicals (O_2^{-*}) are known as strong oxidizers for depolymerization or defragmentation of low molecular weight biomass fractions (Sonawane et al., 2008).

AHP Process not only removes lignin but also solubilise hemicellulose and isolates high crystalline cellulose from lignocellulosic biomass with less inhibitors generation like furfural. The acetic acid formed during AHP process helps to cleave the lignin and hemicellulose bonds and solubilise hemicellulose. The radical generation during AHP process will help to fractionate effectively lignin, and some amount of solubilised hemicellulose and cellulose. Therefore AHP process can effectively fractionate all the structural and unstructured components of lignocelluloses biomass.

1.3 Self-healing Corrosion Inhibition Coatings

Corrosion generally occurs when steel or an alloy exposed to environment this could be due to the electrochemical reaction that takes place between the metal and environment (M.G Fontana et al., 1986).Corrosion generally occurs at a rate determined step by equilibrium, that occurs due to the two opposing electrochemical reactions that is anodic and cathodic reaction, when these two reactions are in equilibrium, and there is no net flow of electrons. When a steel, iron or a metal is exposed to air or water molecule it gets oxides by losing electrons converting iron to fe^{+2} fe^{+3} ions (pitting). The anodic action causes pitting of iron, so this particular site corresponds to anodic site. The electron reduces the oxygen and hydrogen from water molecules or environment to form OH^- ions. The cathodic action reduces the oxygen from air forming OH^- ions. These OH^- ions are highly reactive with Fe^{+2} to form iron hydroxide FeOH rust. The electrochemical cell action driven by the energy of oxidation continues the corrosion process. (Raja et al 2016).

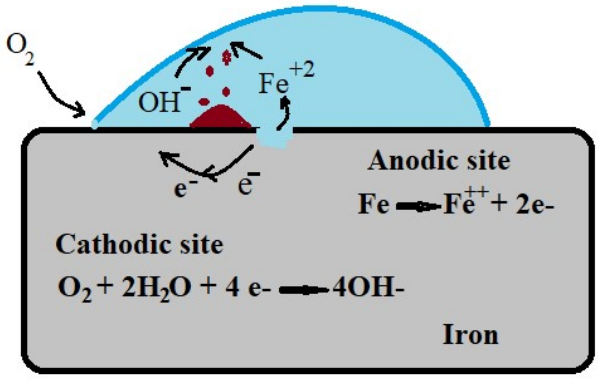

Figure 1. 7. Schematic diagram of Corrosion processes

Every corrosion process is an accelerating process. Since all metals (in periodic table) except gold (Au), Platinum (Pt), Palladium (pd) are exists in combined form as oxides, sulphides, chlorides, Sulphates. Metals in combined form are known as mineral ores (M.G Fontana et al., 1986). Theses mineral ores are reduced to the metallic state by any extraction process. During this extraction process from ores to metallic state large amount of energy is required. As energy is consumed during extraction process the isolated pure metals (products) can be considered to be in highly excited state compared to corresponding the mineral ores (raw material). These isolated metals are highly unstable, with higher energy state and in pure form. Then their exits a tendency to revert back to its stable natural combined form which is lower energy state.

Higher amount of energy required to separate the metal from its mineral, (which is a forward reaction) is equal to energy required for the tendency of the metal to revert back to its natural state which is a back ward reaction resulting in degradation of metal. (Olad et al., 2013)

Therefore when a pure metal is exposed to dry gases, moisture or water molecule, present in the environment /atmosphere. The exposed metal surfaces will tend to decay by reverting back to its natural stable form. This process of converting pure metal form to degrade / decay state is called corrosion.

1.3.1 General forms of corrosion.

There are eight forms of corrosion, they are classified according to the way the corrosion occurs, but all of them are inter related. They are Uniform attack, Galvanic or two metal corrosion, Crevice corrosion, Pitting, Inter granular corrosion, Selective leaching, Erosion Corrosion, Stress corrosion, Hydrogen damage (M.G. Fontana et al., 1986).

Uniform attack: This corrosion occurs uniform on the surface and proceeds uniformly. This occurs mostly due to chemical attack.

Galvanic or two metal corrosion: This is an electrochemical action that occurs between two dissimilar metals which are in contact with each other.

Crevice corrosion: It occurs when metals are in contact with non metals. It is the localized attack on a metal surface at, or immediately adjacent to the gap or **crevice** between two join surfaces

Pitting: This kind of corrosion are said to be localized, and perforation occurs on the metal due to corrosion. In other words the metal was eaten by corrosion at one place by causing perforation and the rest of metal has no or little effect.

Inter granular corrosion: Also known as inter granular attack is a form of corrosion where the boundaries of crystallites of the material are more susceptible to corrosion than their insides. This takes place near grain boundaries of a metal and is imperceptible or slightly perceptible from outside of the metal.

Selective leaching: This is dissolution of an alloying element due to corrosion. It also termed as aka parting or dealloying, demetalification, selective leaching/corrosion.

Erosion Corrosion: A conjoint action involving corrosion and erosion in the presence of a moving corrosive fluid leading to the accelerated loss of material.

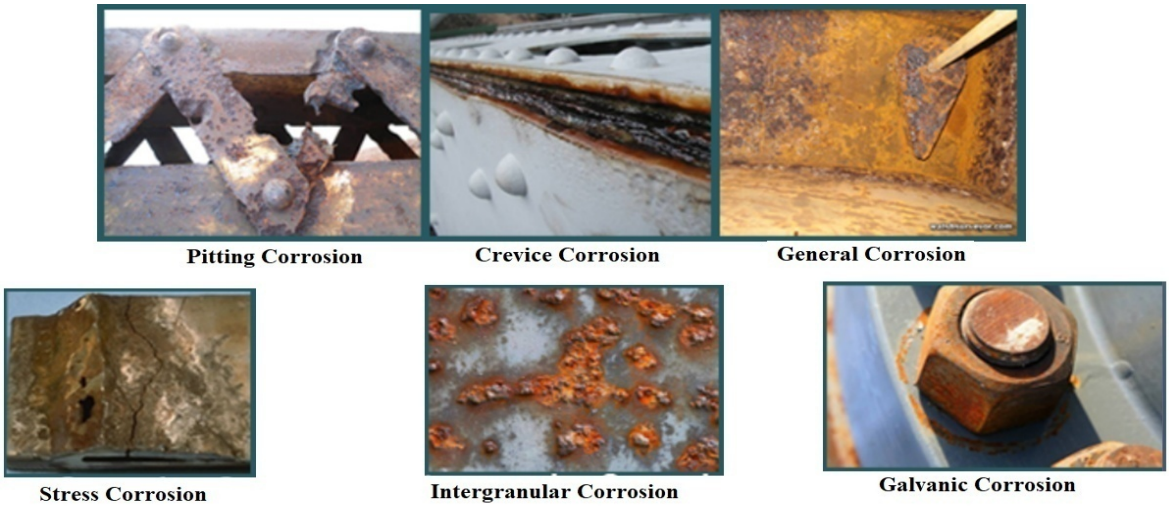

Figure 1. 8. Forms of Corrosion.

Stress corrosion: This is due to the environmental assisted cracking (EAC) is a general term that includes corrosion fatigue and stress corrosion cracking. This occurs along cracks or faults across the crystals in metals and alloys. It follows the pattern of grains in the individual lattices of the material. Stress corrosion of austenitic steels is usually transgranular.

1.3.2 Protective coatings using Self-healing Inhibitors.

Corrosion can be controlled by several techniques such as by environment modification, Potential change, design improvement, coating and plating (M.G. Fontana et al., 1986). One of the most commonly using techniques is by modifying epoxy with synthetic corrosion inhibitors or with natural chelating agents, or combinations of both. The use of corrosion inhibitors in combination will have synergetic effect for corrosion inhibition thereby avoiding earlier deactivation, osmotic blistering, leaching of the coated paint etc (Patil and Radhakrishnan 2006; Padilla-Martinez et al. 2014).

Several authors worked on control of corrosion rate by epoxy modification using synthetic corrosion inhibitors. Some examples of this kind are the combination of polyaniline and oxides such as ZnO, TiO_2, Fe_2O_3 have shown excellent corrosion resistance properties (Patil and Radhakrishnan 2006; Sathiyanarayanan et al. 2007a, b; Ramezanzadeh and Attar 2011; Ramezanzadeh et al. 2011; Olad and Nosrati 2013).

The fluoro type silane used as a core material for encapsulation of corrosion inhibitor(Wei et al. 2014; Frankel 2016). Different shell materials for encapsulation purpose, these being urea/phenol/melamine formaldehyde, using in situ polymerization approach(Hussin et al. 2015a).

Natural polymer consists of several hetero atoms, and some functional groups such as hydroxyl, nitro and heterocyclic compounds which are responsible for corrosion inhibition. These components present in natural polymer will replace anions that are lost due to the dissolution of metal during corrosion. So that a natural polymer can behave as a corrosion inhibitor by providing self-healing characteristics(G. and F. 2014)

Biomasses consists of carbohydrate polymers (such as cellulose and hemicelluloses) and aromatic polymers (lignin) which can be easily converted to value added products(Division et al. 2019). Since nano cellulose has hallow like structure it can accommodate any active chemicals which can be released whenever necessary and needed (Vijayan and AlMaadeed 2016; Zhao et al. 2017).The controlled release of corrosion inhibitor on to the effected surface of metal depend up on the pH environment of the substrate and containers shape, size these are most important parameters that to be considered which in turn decides the amount of corrosion inhibitor that can be effectively loaded into nano fiber (Frankel 2016).

The electro spun nano fibers were synthesized by dibutyltin dilaurate (DBTL) and Poly (vinyl alcohol) with a size range of 300–400 nm. Coatings were prepared along with the cross linking agent poly(diethoxy siloxane) (PDES) and a catalyst poly(dimethxy siloxane) (PDMS). The coatings were dried and scribed with coo cutter and then immersed in 5 % nacl solution for 48 hours. These have shown 88% corrosion inhibition (Subhedar and Gogate 2014)

The main advantages of High performance coatings, the major outcome of any organic paintings are having qualities such as high corrosion resistance in highly aggressive environments**.** It can be applied in high relative humidity (more than 90%). These coatings has high thickness (DFT) which can be achieved per coat**.** This Provides resistance to weathering, especially UV light**.** These coatings also exhibit good mechanical properties such as high impact strength, abrasion resistance and hardness (Olad et al., 2013).

1.3.3 Mechanism for development of patina

When the oxidizing power of this solution is increased, say, by adding oxygen or ferric ions, the corrosion rate of the metal will increase rapidly. or such a metal the corrosion rate increases as the oxidizing power of the solution increases. The oxidizing power of the solution is controlled by both the specific oxidizing power of the reagents and the concentrations of these reagents. Therefore by addition of any chelating agent can accelerate the corrosion

reaction by forming a complex which is an inert layer. This inert layer is patina/ polymerized layer that controls or stops the fast accelerating corrosion reactions. (Frankel 2016).

The rate of electrochemical reactions are limited by several environmental factors. So the electrochemical reactions are said to be polarized by making metal passive slightly. The mechanism of electric double layer with electric circuit is illustrated in the figure 1.9. Essentially, passivity refers to the loss of chemical reactivity experienced by certain metals and alloys under particular environmental conditions. That is, certain metals and alloys become essentially inert and act as if they were noble metals such as platinum and gold. Fortunately, from an engineering standpoint, the metals most susceptible to this kind of behaviour are the common engineering and structural materials, including iron, nickel, silicon, chromium, titanium, and alloys containing these metals.

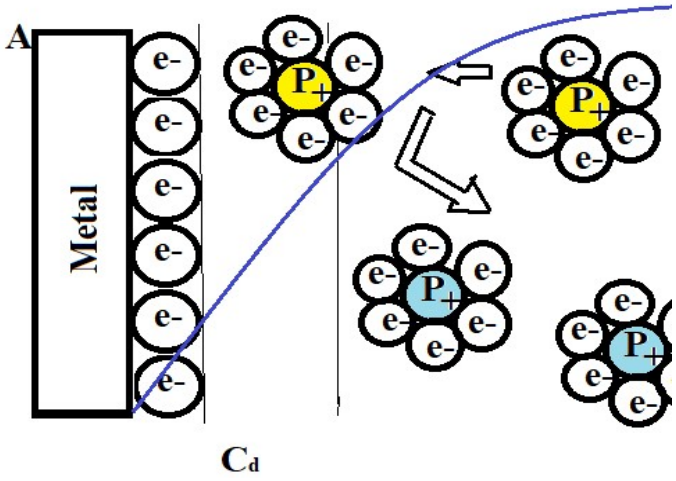

Figure 1. 9. Mechanism for electric double later formation.

Also, under limited conditions other metals such as zinc, cadmium, tin, uranium, and thorium have also been observed to exhibit passivity effects. Passivity, although difficult to define, can be quantitatively described by characterizing the behavior of metals which show this unusual effect (Zhao et al. 2017).

1.3.4 Containers for Corrosion Inhibitor for self healing Approach

Container based smart, green corrosion inhibition substances have pulled attraction in developing patina over a metal, in-order to decelerate corrosion reactions. Investigations are done with the corrosion inhibitors along with the combination of extractives of renewable resources to have synergetic effect on corrosion inhibition (Vijayan and AlMaadeed 2016).The first era of repairing device was mentioned more than a decade(White et al. 2001;

Yiamsawas et al. 2014). Meanwhile, with the aid of this technology into coating industry container-based self-healing substances open up to important subject in smart coatings that can provide immediate remarks over a metal and repairs autonomously to considerably extend the life (Montemor 2014; Wei et al. 2014). Previous studies (Wypych 2017) reveals that active healing reagents are essential to be present in micro-capsules in order to prepare self-healing coatings. In self-healing mechanism the nested microcapsules concurrently rupture to release the recuperation reagents to the damaged part (Trask et al. 2007). Therefore, microcapsule is demanded to possess various features, which comprise high loading of corrosion inhibitor for fast responsiveness towards sudden damages as a result it plays an vital role in repairing using capsule-based smart materials. The utilization of natural organic inhibitors is more efficient for corrosion inhibition than synthetic inhibitors.

1.3.5 Limitations with Inorganic Inhibitors.

Synthetic Corrosion inhibitors are available such as nitrates Chromates are best example of corrosion inhibitor will generate toxic chemical compounds when it reacted with steel by forming a toxic corrosion product. chromates will generate chromium ions which will effects the living organism by causing cancer(Raja et al. 2016).

1.4 Motivation for the Study

The pretreatment of lignocelluloses biomass is the important step in Biorefinery process to obtain maximum accesses to cellulose in-order to produce bio-fuel like bio-ethanol. The valorisation of these by-products could decrease the cost of bio-ethanol. (Ramadoss et al., 2016).

Since lignin is potent of hydroxyl and phenolic ions, it could easily chelate to the metal surface and forms a polymerized layer which is inert and is strongly bounded. The available paints like primers can reduce the corrosion rate but these are mostly chromate based and carcinogenic in nature . Therefore there is a need to developed epoxy which is toxic free, sustainable and eco-friendly. It can be achieved by modifying the epoxy by addition of the natural materials like lignin to decrease the corrosion rate by increasing the metal life.

Lignin can act as a corrosion inhibitor carrier by preparing microcapsules that are encapsulated with corrosion inhibitor(Rauber et al. 2018). It can also act as a stabilizer during encapsulation process by controlling the container size. Similar to lignin cellulose which is hallow in structure can also hold more corrosion inhibitor than a microcapsule. Cellulose contains sulphate groups on its surface that are obtained during the isolation of cellulose using concentrated sulfuric acid process. Sulphate groups can easily chelate to the metal surface by forming a polymerized film therefore easily reduces the corrosion rate.(Frankel 2016)

The inherit characteristic of lignin and cellulose gave motivation to study its corrosion inhibition characteristics on mild steel due to its low cost, high strength, ductility and malleability .

However the studies on novel configured equipment like longitudinal horn and epoxy formulations that are used in for development of self healing high build solid coatings for corrosion inhibition are scarce.

1.5 Scope of the work

1) Fractionation of tectona grandis sawdust to lignin using longitudinal horn and compared the performance of lignin yield with the conventional ultrasonic horn, bath, and chemical approach at different operational parameters.

2) Synthesis and characterization of nano containers such as lignin nano capsules and cellulose nano tubes utilizing sonochemical approach.

3) Development of patina by smart self healing sustainable eco friendly coating on mild steel.

4) Corrosion parameters were analytically measured by electrochemical work station and analyzed gravimetrically by immersion and weight loss studies. Results like Impedance were analyzed by EIS electrochemical impedance spectroscopy measurements using bode and Nyquist plot and polarization studies were done using tafel plot.

The obtained results were compared to establish optimum conditions for suitable materials.

1.6 Organization of Thesis

Thesis is divided into seven chapters, so as to make the contents more comprehensible. The seven chapters include introduction, literature review, materials and methods, experimental procedures, results and discussion, conclusion.

Chapter 1 Introduction

This chapter is divided into two sections. First section discuss about the types of lignocellulosic biomass available as a raw material along with its structure and composition. Classification of fractionation process and its limitations over conventional methods. In brief this section explains about importance of acoustic cavitation and its mechanism for delignification. Second section is about introduction to organic corrosion inhibitors. In brief this section explains about general forms of corrosion and about protective coatings using inorganic and organic inhibitors and for development of patina. Introduction to corrosion inhibitor carriers for self healing approach and their limitations with inorganic inhibitors.

Chapter 2 Literature review.

This chapter is divided into 4 main sections. First one is on literature review on different intensified pre-treatment processes for delignification. Second section is about literature review based on self healing coatings. Categorization of self healing materials. Literature review on lignin and cellulose as a corrosion inhibitor carrier.

Chapter 3 Materials methods

This chapter is divided into 2 main sections. First one is materials and experimental procedures used for delignification. In brief second section deals about materials and characteristic analysis procedures for synthesis and characterization of lignin nano capsules (LNC) and cellulose nano fibers (CNF).And also discusses about the equipment used for corrosion analysis.

Chapter 4 Experimental procedures

This chapter is divided into 3 main sections. First section deals with the experimental setup and procedures for delignification. Section deals with the experimental setup and procedures for lignin and cellulose.

Chapter 5 Results and discussion

This chapter is divided into 4 main sections. First one is about results and discussion for delignification, effect of operational and equipment parameters, and energy requirements on lignin yield from tectona grandis sawdust using different configured acoustic cavitational devices like longitudinal horn, ultrasonic probe and bath and compared the results.

Second and third are about results and discussion self healing coatings with lignin and cellulose as a corrosion inhibitor carrier. Second section discuss about lignin nanocapsules characterization like FTIR, FE-SEM, TEM. The corrosion rate with respect to weight loss and polarization, impedance studies are discussed.

Third section discuss about characterization like FTIR, SEM, TEM of benzotriazole loaded cellulose nano fibers 2k polyamide epoxy coating with ph responsive activity. The corrosion rate with respect to weight loss studies and polarization, impedance studies with tafel, bode and nyquist plots were discussed.

Fourth section discuss about comparison of structure of lignin and cellulose as a corrosion inhibitor carrier. Compares the epoxies and curing agent used for the lignin and cellulose based epoxy coatings. Finally compares about the corrosion rate, polarization, impedance studies to establish the best corrosion inhibition coating for corrosion inhibition of mild steel.

Chapter 6 Conclusion.

Reports the conclusions drawn from the present investigation.

Chapter 7 Scope for future work.

Deals with the direction and scope for the further research related areas of self healing in other applications.

Chapter 2

Literature Survey

Chapter 2 Literature Survey

2.1 Delignification

Lignocellulosic materials are considered an effective and sustainable source that can be processed to give bio-fuels and other value-added products. Due to the limited availability of sustainable raw materials and to reduce the greenhouse effect, specifically in India, the pollution control board has reported that during 2000-2011, atmospheric CO_2 levels increased to 390.5 ppm (Chhabra and Gohel 2017). The processing of lignocelluloses materials into bio-fuels typically involves multiple steps. The first step is the fraction of lignocellulose biomass to cellulose, hemicellulose, and lignin, which can be cost-intensive and require the use of harsh chemicals, leading to an interest in the application of process intensification approaches.

2.1 Role of Acoustic cavitation process for delignification

Acoustic cavitation is most likely to occur under low frequency and high signal amplitude ultrasonic waves. Generally, sonication can be transmitted by a piezoelectric transducer that can convert Alternative Current to ultrasonic energy waves.

The enhancement in the extraction of bioactive compounds achieved using sonication is attributed to cavitation in the solvent. This process involves nucleation, growth, and collapse of bubbles in a liquid, driven by the passage of the ultrasonic waves ((Frankel 2016).

2.1.1 Mechanism for Lignin extraction using sonication

Lignin is composed of there monomers (coniferyl, sinapyl, p-coumeryl alcohol), that are linked with ether linkages at α and β positions to form lignin macromolecule(Rauber et al. 2018). The structure of lignin varies from plant to plant with varying linkages positions. Similarly the composition also varies from plant to plant.

Depolymerization of lignin

To understand the lignin degradation the reactive sites of lignin has to be understand. ***Recative sites*** Lignin is amorphous in nature and is most likely to form hydrogen bonding, by that has most reactive sites they are ether linkages, and functional groups, the C-C bond is said to be covalent bond and is ore resistant to chemical attacks. The most effected site of lignin are hydrolyzable ether linkages (α-alkyl, β-aryl, α-aryl), and functional groups like (OH hydroxyl, -OCH_3 methoxy groups, Aliphatic hydroxyl groups (R-C-OH), R varies in

number it could be 1, 2, 3). Ester groups (RCOOR`), unsaturated groups, and uncondensed groups.

The Lignin-Carbohydrate Linkages are inert to chemicals such as glycosidic, ester, and ether. Some ester groups are easily hydrolyzed in presence of alkali medium. Some ether linkages such as α-0-4,β-0-4, are hydrolyzed at mild alkali peroxide medium through radical generation.

Degradation of lignin

The lignin degradation occurs by its surrounding environments. Generally three types of environments exists, (On the basis of solvents) they are alkali, acid, and oxidation. These are could in combination like alkali peroxide environment etc.

In acidic environment benzyl oxygen can be protonated initiating acid degradations of α- and β-ether lignin units. The protonation is followed by α-ether elimination of the phenol or alcohol giving a benzylic carbonium ion intermediate which can undergo further degradation enabling depolymerization of the lignin compound.

In Alkaline and oxidative environments were used extensively for delignification in the bleaching of pulp in the Kraft process and were looked at as pretreatment options.In alkaline and alkaline-oxidative environments lignin degrades through the cleavage of the α- and β-aryl ether linkages to yield fragmentation units.

However in oxidative environments, unlike in pulping, degradation is driven by the cleavage of carbon−carbon linkages and the formation of acidic groups from ring degradations such as carboxylic acids. Side chains within the lignin may be displaced or cleaved in oxidative reactions through electrophilic substitution at an unsubstituted ring position and α−β-cleavage of the carbon chain (Hon et al., 2001). These three main chemical methods of lignin degradation were the basis for many chemical pretreatments to enhance the enzymatic digestibility of cellulose in lignocellulosic biomass. The pretreatments are not always selective and can sometimes be counterproductive due to the loss of carbohydrates in the process.

Degradation of ultrasound can occur through hydroxyl attack on the lignin structure. The hydroxyl attack on model lignin compounds under ultrasound was found to mostly (75−85%) occur on the aromatic ring (Pranovich et al., 1998). This led to hydroxylated, demethoxylated, and side chain eliminated products. The remaining 25−15% of hydroxyl attack occurred on the side chains leading to the formation of dimers and the oxidation of aromatic aldehydes to carboxylic acids. Additionally, an increased production of hydroxyl radicals, from the

combination of ultrasound with TiO2 and the Fenton reagent, coincided with an increased lignin degradation (Ninomiya et al., 2013). Further evidence of oxidative attack was found in the increased number of non conjugated carbonyls in sonicated pulp fibers under high frequency irradiation (Gadhe et al., 2006).For the purpose of lignin extraction, separation and depolymerization can augment yields, whereas degradation was also observed. In regards to the pretreatment of biomass for utilization of the carbohydrates and/or the lignin (Pranovich et al., 1998) component, lignin depolymerization and separation enhance pretreatment. However, the competing condensation reactions, responsible for the change in molecular weights observed, must also be considered.

Condensation of lignin

Alongside the cleavage of inter unitary bonds within the lignin and lignin-hemicellulose bonds evidence for condensation of lignin in the presence of ultrasound was observed. Condensation was observed in the ultrasonic-enhanced hydrogenolyis of lignin (Goncalves et al., 2002) and the extraction of humic acids from tobacco dust (Qi et al. 2004). Furthermore lignin condensation was shown to occur during lignin extraction and in the treatment of lignocellulosic biomass. (Garcia et al 20011; Sulman et al 2011) Lignin condensation mechanisms without ultrasound depend on the chemical environment, However, with ultrasound, the conditions can favor the accumulation of species at the bubble interface, depending on the solvent properties. This accumulation may enable proton transfer (Ashok kumar et al.2005) or promote radical scavenging (Ashok kumar et al.2000) in the hot inter facial region, which would in turn promote re-condensation and re-polymerization reactions. The behavior of phenol at the bubble interface supports this possible mechanism ofre-condensation of lignin. (Ashok kumar et al.2006) evidence phenol scavenges hydroxide radicals at the bubble surface in aqueous solutions, and this will also occur in the presence of phenol derivatives due to the similarity of types of decomposition products observed (Ashokkumar et al.2000). It is important to note that the behavior would depend on the exact nature of the solvent used and the sonochemical field ultrasound tended to enhance the purity and yield of lignin extraction. The ability of ultrasound to enhance the cleavage of linkages between hemicellulose and lignin increased the purity of the extracts. Ultrasound influenced the molecular weight of the lignin extracted. The influence on molecular weight was not uniform attributed to competing separation, degradation, and re condensation reactions. The condensation reactions of lignin are theorized tooccur in the interfacial region around the collapsing bubble,hence depending on the nature of the treatment solution.

2.1.2 Practical considerations for sonication as a pretreatment.

I. Raw material Characteristics

A. Type and Size of biomass.

Type of biomass Different types of raw materials like agriculture waste such as lignocellulose biomass, municipal waste, and wastewater treatment are available. Different results/responses in the yields are obtained for other biomass under the same ultrasonic operating conditions. Two different biomass, such as sage leaves (Hromadkova et al., 1999) and valerian roots (Hromadkova et al., 2002), are treated with the same treatment gave different polysaccharides yields. Other biomass parts such as stem, leaves, roots have different polysaccharides yields for the same ultrasonic operating conditions. Different operating conditions have shown the different degree of polymerization. For instance, the treatment of biomass with and without ultrasound gives 3-4 folds of increases in yields or degree of polymerization (Gogate et al., 2014)

Hardwood and softwood biomass are different kinds of lignocelluloses biomass; Hardwood such as poplar wood, teak wood (Shiva et al., 2002), bamboo (et al.) and softwood such as wheat straw (Wypych et al. 2017), rice straw and rice bran (Fan et al. 2011)), sugarcane bagasse (Ramadoss and Muthukumar 2016) has a different composition of lignocelluloses biomass.

Size of biomass / raw material. The size of biomass also affects the degree of polymerization. Homogenization or ball milling is used to reduce the size of dried biomass. Generally, smaller particle sizes can directly get lignin. This pretreatment process is only a physical process that takes place by ball milling. Almost all literature surveys reported pretreatment of ultrasound-assisted biomass is less than 1 mm size for effective depolymerization (Hromadkova et al., 1999; Fan et al. 2011). For depolymerization of Olive tree pruning of size 1-8 mm (Sun et al., 2002). However, this size reduction is an expensive step while considering on a large scale. So wet grinding method is preferred for pretreatment.

B. Biomass loading

Biomass loading is an important parameter to be optimized in the pretreatment of biomass. The structure, texture, and recalcitrant nature of the processed biomass are affected by biomass quantity. Typically, there must be enough exposure of biomass particles to the alkali with the best conditions for mixing and mass transfer, dependent on the solid content in the reactor.The enzymatic hydrolysis results were reported that the sequential alkaline-AHP

pretreated WS was efficiently hydrolyzed at 10% (w/v) solids loading using an enzyme dosage of 10mg protein/g glucan. The total sugar conversion of 92.4% was achieved. When wheat straw of size (20-40 mm) was treated at 20 kHz, 150W, 20 minutes, lignin content was reduced to 5.4% in 1/1 (g/ml) straight pulp when compared to 2.4, 4.2, 4.8% in the solid to liquid ratio of 1/70, 1/105, 1/140 (g/ml) (Yuan et al., 2011).

II. Solvent for Delignification

A. Alkaline and Acid Solvents

The pretreatment using dilute acid hydrolysis of 8 different feed stocks was subjected to enzymatic saccharification followed by fermentation with S.cerevisiae and ultrasound at 35kHz at a 10% duty cycle. 220 g/kg of bioethanol per kg of raw biomass with 86.8 delignification and 133g/kg of pentose and hexose fermentation (Ramadoss et al., 2016). A two-step process of treatment using 0.25 M strength of NaOH at 30°C for6 hours as the first step followed by treatment involving 40 mg of H_2O_2 per g of biomass at 50°C for 15 h. It was reported that acid-soluble lignin precipitated from hydrolysate is 54.1 %(Yuan et al. 2018).Olive tree pruning of size 1-8 mm, with 7.5% soda and solid to liquid ratio (SLR) 1/10 (w/w) using an ultrasonic bath, at operating conditions of 60 kHz, 420 W, 50°C, 30-120 min. The recovery percentage of lignin, cellulose, hemicellulose, and ash3.2/8.9; 1.7/-0.3; -3.1/-0.1; -3.5/2.7 (Sun et al., 2002).

Ultrasound-assisted NaOH pretreatment of sugarcane, which was subsequently used for biogas as well as fermentable sugar production. It was reported that 99.6% lignin was removed from biomass under optimum operating conditions of 24 kHz as frequency and 400 W power (Velmurugan and Muthukumar 2012). 80% delignification was achieved using ultrasound-assisted sodium hydroxide treatment of the waste news paper (Gogate et al., 2011). Nearly 2-fold increase in delignification was performed using the ultrasound-assisted approach under best-operating conditions as power dissipation of 100W,frequency of 20 kHz, the temperature of 80°C and 70 min as compared to the conventional treatment (Subhedar and Gogate 2014).

In one of the studies, 3% sulfuric acid pretreatment at ultrasonic power of 120 W followed by saccharification was reported to give 26 g/L as the enhanced sugar yield (94.5% of the theoretical yield) (Theme 2010). Similarly, dilute sulfuric acid treatment of corncob combined with sonication resulted in the efficient extraction of xylan with 14.7% higher yield and reduced operation time from 24 h to 45 min (García et al. 2011).

B. Organic solvents and Ionic liquids

Organic solvents Coconut shells were subjected to 50% ethanol/water (v/v) adjusted to pH 4.5, processed with a solid to liquid ration (SLR) of 1/33 (g/ml),under bath sonication at 25 kHz, 150 W at 30°C, and 20-60 min. Ultrasound extraction time was the most important variable in the yield of lignin for a longer time of more than 50 min maximized the extraction (Rodrigues et al., 2007).Olive tree pruning of size 1-8 mm, with 60% v/v acetic acid and solid to liquid ratio (SLR) 1/10 (w/w) using an ultrasonic bath, at operating conditions of 60 kHz, 420 W, 50 °C, 30-120 min. Water for 60/120 min changed the percentage of lignin, cellulose, hemicellulose and ash by -5.8/-13.8; 0.9/1;1 -1.3/-11.2; -0.3/0.8 in water, -0.9/-9.9; 0.6/-0.4; -6.9/-4.8; -0.1/-0.2 in acetic acid. (Sun et al., 2002). Organosolv lignin's (when extracted with 95% Ethanol, methanol, dioxane and dimethyl sulfoxide using Poplar wood SLR 1/15 (g/ml)) had a lower molecular weight average than the alkaline lignin's. Successive treatments under the operating conditions: Horn, 20-24 kHz, 570 W, 25 °C, 30 min.

Ionic liquids Birch is treated with ionic liquid-like 1-Ethyl-3-methylimidazolium acetate (EmimOAc) at a temperature of 110ºC for 16 hours gave 74 % lignin yield (Achinivu et al., 2014). Similarly, when the cotton stalk is treated with ionic liquid 1-Allyl-3-methylimidazolium chloride (Amim cl) and DMSO solvent at a temperature of 130ºC for 4 hours has been shown 74.4% lignin yield (Zhu et al., 2018). When an ionic liquid (1-Butyl-3-methylimidazolium acetate (Bmim [Ace]) and salt (toluene and sodium hydroxide) are used to treat at reported lignin yield as 74%.(Zhu et al., 2018).

C. Inert environment

Lignin extracted from what straw when it is treated with argon, krypton and xenon were 3.7, 1.2, and 0.8 under sonication of 150 W, 20kHz, at 20 minutes. And this lignin extracted was higher, i.e., 4.2% when treated with water and 5.4% after ultrasonic treatment (Yuan et al., 2011).

D. Oxidizers

Most of the problems in the research are tackled by just mimicking nature. The fragmentation of saprophytes by oxidative cleavage of bonds between pant cell walls is best example (Li et al., 2013). This could be used for the effective pretreatment of lignocellulosic biomass. Selective delignification by free radicals that are generated from hydrogen peroxide by Fenton reaction is also the best example for higher lignin yields. Different Oxidative

pretreatments are available; they are done with the fenton reagent (Dawn M et al., 2014) oxygen (Palone et al., 2004), ozone (Simoes et al., 1999), peracids (Teixeira et al., 1999), organic peroxides (Paszczynski et al., 1988), hydrogen peroxide (Gould 1984). A brief explanation for different oxidation processes for their application in lignocelluloses biomass pretreatment is illustrated in table 2.1.

Table 2. 1. Different Oxidative pretreatment processes

Biomass	**Oxidizer**	**Operating conditions**	**Result**	**Reference**
Miscanthus, corn stover, and wheat straw, but switch grass	***Fenton reagent***	(10g biomass, 176mmol H_2O_2 and 1.25mmol Fe(2+) in 200mL of water)	**Delignification of Miscanthus(6.63%) corn stover (14.1%) wheatstraw (8.76%) Switchgrass(3.59%)**	(Dawn M et al., 2014)
Pine & Kraft pulp Eucalyptus	***Ozone***	Temperature 4°C	**Delignification**	(simoes et al., 1999)
Soft wood	***Oxygen***	Wet oxidation Temperature: 200 °C Time:10 minutes	**enzymatic hydrolysis**	(Palone et al., 2004),
Agriculture residue	***Hydrogen peroxide***	1% w/v H_2O_2, Temperature: 25°C Time:18-24hours	**Delignification and enzymatic saccharification**	(Gould et al., 1984)
Wheat straw	***NaoH and H_2O_2***	0.2 mole/L NaoH for 30°C @ 5 h. $H_2O_2$40mg/g biomass 50 °C @7 h.	**80% of lignin and 91% silica.**	(yuan et al., 2018)
Hybrid polar	***Peracids***	15 % Peracids Solid to liquid : 1:6 Time 7 days	**Enzymatic digestibility**	(Teixeira et al., 1999),
Wood chips and pulps	***Organic peroxides***	Refluxed boiling using 70% tert-butyl H_2O_2, Time 24 h. S/L ratio: 500:1.	**Delignification**	(Paszczynski et al., 1988),

i. Alkaline Hydrogen Peroxide (AHP) Process

Several authors (Dawn M et al., 2014; Gould et al., 1984; yuan et al., 2018) have shown oxidative treatment gives efficient removal of lignin and hemicellulose while separating high crystalline cellulose, with the release of low inhibitors. The operating conditions also play a vital role in the delignification of biomass. Alkaline hydrogen peroxide attacks only aliphatic lignin groups under normal conditions give rise to selective depolymerization of lignin carbohydrate linkages. While in alkaline oxidative process at high temperatures gives degraded lignin, selective cleavage of phenolic groups of lignin gives rise to carboxylic groups.

The production of bioethanol and value-added compounds from wheat straw was achieved through combined alkaline/alkaline-peroxide pretreatment (yuan et al., 2018). The work explained as follows wheat Straw was pre-extracted with 0.2mol/L sodium hydroxide at 30 °C for 5hours and was reported to remove 80% of lignin and 91% silica. The residue of alkaline-pretreated solids was subjected to alkaline hydrogen peroxide (AHP) pretreatment with 40mg hydrogen peroxide (H2O2)/g biomass at 50 °C for 7 hours for a highly digestible substrate.

ii. Parameters affecting the AHP process

Reaction Initiators

Temperature

Temperature is one of the initiators for the depolymerization reaction. Corn bran sieved to 0.25 mm. Solid to liquid ratio (SLR) 2/50, 3/50, 5/50 (g/ml) Horn, 20 kHz, 100 W, 8 W cm-1, 10 min intervals, 30, 50, 60, 70°C, 5 and 10 min. Distilled water, 1% and 5% NaOH. The total polysaccharides yields increased with ultrasound by 10% and 30% for the 1% and 5% NaOH solutions, respectively (Ebringerova et al., 2002).

Metal salts

The hydrogen peroxide composition in the presence of metal ions such as Cu 2,2'-bipyridine complexes (Bansal et al. 2016), Titanium dioxide (Ramadoss and Muthukumar 2016), etc. to form radicals that can improve depolymerization of lignocellulosic biomass.

In brief, 1% hydrogen peroxide and metal salt (TiO2) to treat sugarcane under sonication (24 kHz, 400Wwith 50 % amplitude and 70 % duty cycle for 60 minutes) reported 78.72 ± 0.86% lignin removal (Ramadoss and Muthukumar 2016).

Bansal used a combination of metals in the form of Cu 2,2'-bipyridine complexes with alkali peroxide pretreatment of biomass and reported enhanced Klason lignin in the pretreated biomass with an actual amount as 0.17, 0.12, 0.12, 0.18 g/g of total content for different sources as hybrid poplar, silver birch, hybrid aspen, and sugar maple respectively(Bansal et al. 2016).

pH is one of the important parameter to be considered**.** The effectiveness of pretreatment with alkaline H2O2 is largely dependent on pH, as it is combined with the generation of the hydroperoxide anion, as described in Eq. (1).

Studies by (Gould et al., 1985) have shown that the optimal pH value is 11.5.Studies have reported that the use of H_2O_2, without pH correction, results in less efficiency in the release of sugars during enzymatic hydrolysis. In a comparative study of the chemical pretreatment of aquatic plants used in water purification, pretreatment with H_2O_2 was not effective in improving enzymatic hydrolysis (10% w/v total solids; 1% (v/v)H_2O_2;room temperature for 2 h). However, the combination with NaOH solution achieved the best enzymatic hydrolysis results (1% NaOH w/v, room temperature for 12 h followed by the addition of 1% (w/v) H2O2, at room temperature for 12 h) (Mishima et al., 2006).

Alkaline hydrogen peroxide for pretreatment seaweed biomass with pH 4, 6, 8, and 10 (Li et al. 2016).The results showed that the yields obtained, from reducing sugar and glucose in pretreated groups, were higher than those of the control group. The optimum pH was 4.0 with a maximum rate of reducing sugar. The lowest yield of glucose and sugar reduction was obtained at pH 6.0. A smaller increase was observed at pH 8.0 and 10.0. The authors suggested that, when compared with another lignocellulosic biomass, the differences with the best condition are pH 11.5. The lower content of lignin might be the reason why the yield of sugar reduction was sensitive to the pretreatment of pH.

Operating time is most crucial parameter. However as treatment time is increased the effect is not always accumulative. For example, 120 min rather than 180 min was the optimum treatment for delignification of bon bogori and moj trunks (Yuan et al. 2018) and the lignin content of sunflower husks decreased with ultrasonic treatment upto 15 min, after which it increased (I.I. Savin et al., 2007). These observations were probably due to re condensation reactions of the lignin occurring with ultrasonic treatment. Furthermore the sonication of pretreatment liquor was found to decrease the hemicellulose content after 60 min but then to increase the hemicellulose content after 120 min.

Meanwhile, the acid insoluble lignin was increased after 15 min of ultrasound, after which the lignin content gradually decreased ((Fan et al. 2011) These observations were explained by hemicellulose and lignin degradation reactions, lignin condensation reactions, alongside the cleavage of the lignin-hemicellulose complex.

Reaction Inhibitors

Stabilizers

The hydrogen peroxide decomposition in the absence of stabilizers such as MgSo4 or sodium silicate etc. can improve depolymerization of lignocellulosic biomass (Mittal et al., 2017).

III. Configuration of Reactor

A. Design of Reactor

Different types of ultrasonic reactors reported in the Literature for a variety of applications include probe type (different diameters with various intensities), ultrasonic bath, ultrasonic flow cell with dual frequency or triple frequency operation, continuously operating flow cell and longitudinal horn (I.I. Savin et al., 2007), though there are not many studies reporting multiple configurations in single investigation.

In a lab scale operation for ultrasonic probe type can utilize small diameter and large length reactor for maximum/better results for mixing and dispersion.

B. Power

Ultrasonic waves delivers energy that could be utilized for efficient pretreatment that increases the delignification to 3-4 folds. Optimum utilization of an ultrasound intensity can increase the enzyme activity. Simultaneous Saccharification and Fermentation (SSF) of bioethanol yields can be enhanced with sonication (Gogate et al., 2011).

Application of ultrasound for the pretreatment of rice stalks used in production of biogas under operating parameters of power dissipation as 400 W, frequency as 30 kHz and time of 60 min was reported to enhance the production of biogas by about 35-48%compared to the use of only NaOH and by about 67-77% as compared to use of rice stalks directly without any pretreatment(Fan et al. 2011). Similar to lignin separation, it is also reported by number of authors that increased sugar yields and xylan yields are obtained with ultrasound assisted approach. Some of the literature review of ultrasound assisted pretreatment process are presented in the bellow table 1.4.

C. Frequency

The effect of ultrasonic frequency is mainly on the cavitational intensity which in turn affects the production of hydroxyl radicals that act on ether linkages such as β-aryl, α-aryl, and α-alkyl. On increasing the frequency, cavitational intensity and hence the production of the hydroxyl radicals is favored due to enhanced hydrogen peroxide and water dissociation reactions. These radicals mainly act to depolymerize lignin giving rise to higher lignin separation. The effect of frequency is similar to that reported for extraction of various polyphenols and antioxidants from spinach (altemimeetal., 2015)

D. Amplitude and Duty Cycle

Amplitude and duty cycle are the crucial parameters for probe type ultrasonic reactors affecting the processing conditions and the net effects. Duty cycle means the time for which the sonication is on. Typically the duty cycle ranges from 10-100 % or can be represented as 0.1 to 1. If the duty cycle is said as 60% (or 0.6), then it implies that sonication is on for 6 seconds and off for the next 4 seconds (Gogate et al., 2011). Power delivered to the system is affected by the amplitude. Amplitude can be explained as the intensity with which the ultrasonic waves are delivered. (Pinjari et al., 2011)

Summary

Overview of the presented studies clearly established that though the use of ultrasound for intensification has been reported, there are no studies dealing with effect of different configurations of ultrasonic reactors. Also, most studies have dealt with the lignin removal using strong alkali and acid which also gives environmental concerns as not all the acid/alkali used is completely utilized in the process. The main objective of the current work is isolation of lignin from biomass using ultrasound assisted approach with comparison of the different configurations of ultrasonic reactors, which clearly forms the novelty of the current work. The efficacy of different configuration of ultrasonic reactors for delignification has been compared in terms of the energy requirement for the process. The present work also focused on the use of mild alkali and oxidizing agent as sodium carbonate and hydrogen peroxide respectively so as to have lesser impact on environment compared with strong alkali as sodium hydroxide. The sustainable source of lignocellulosic biomass considered in the work is sawdust, which is most abundantly available in India due to large scale usage of wood. The quality of the recovered lignin has been confirmed with different characterization methods, which also is not routinely studied in the Literature.

Table 2. 2. Literature review on Ultrasound assisted delignification.

Biomass type & Reference	**Equipment**	**Operation conditions**	**Result**
Sugarcane bagasse (Ramadoss and Muthukumar 2016)	24 kHz, 400W with 50 % amplitude and 70 % duty cycle for 60 min)	1% hydrogen peroxide along with metal salt (TiO_2)	78.72 ± 0.86% delignification
Corn stover (Y.Q. Zhang 2008)	40 kHz, 80 W, 25 °C, 1 h vertical probe	Sodium hydrate	Decomposition % of ultrasound-assisted Corn strover were 7%, 15%, 43%, conventional treatment 8%,30%, 55% for cellulose, hemicellulose,& lignin, respectively
Corncob (García et al. 2011)	ultrasonic bath 420 W, 50/60 Hz.	Organosolv (acetic acid 60% v/v), alkaline (NaoH 7.5%w/w)	26% of lignin yield obtained with NaoH, 22% with acetic acid
Sugarcane (Velmurugan and Muthukumar 2012)	Optimum operating conditions 24 kHz 400 W power	NaOH (2.89 w/v%)	It was reported that 99.6% lignin was removed from biomass
Waste newspaper. (Subhedar and Gogate 2014)	Power of 100W, freq of 20 kHz, temp of 80°C, 70 minutes.	Sodium hydroxide treatment (1 M)	80% delignification
Rice stalks (Fan et al. 2011)	power dissipation as 400 W, frequency as 30 kHz and time of 60 min.	NaoH (2 w/v%)	delignification 67-77% with 35-48% increase in biogas compared to the use of only NaoH 41.01% lignin in stalk degraded.
Sugar cane bagasse (Theme 2010)	20 kHz, 50-200 W	3% Sulphuric acid	26 g/L sugar yield (94.5% of the theoretical yield)

2.2. Self healing coatings

Materials can degrade due to time, environmental factors …etc for the continuous usage during conversion processes.A material is required which can sense a problem, prevent it from getting worse and repair itself as quickly as possible. This is the concept on which self-healing materials are based.

Earlier from egyptian erathe smart materials were used for construction of pyramids which are proved to be long-lasting material (Olad et al., 2013). In recent days, (Malinskii et al. 1969) reported the first smart material in the laminated form (aluminum foil-poly (vinyl acetate)). They discover that self-repair take place at edge of crack of unloaded specimen. Later in 1970s various studies appeared on crack healing with help of human interference such as silica glass with soda lime (Raja et al 2016), in which they reported that crack recover around 80% is possible of unloaded specimen.

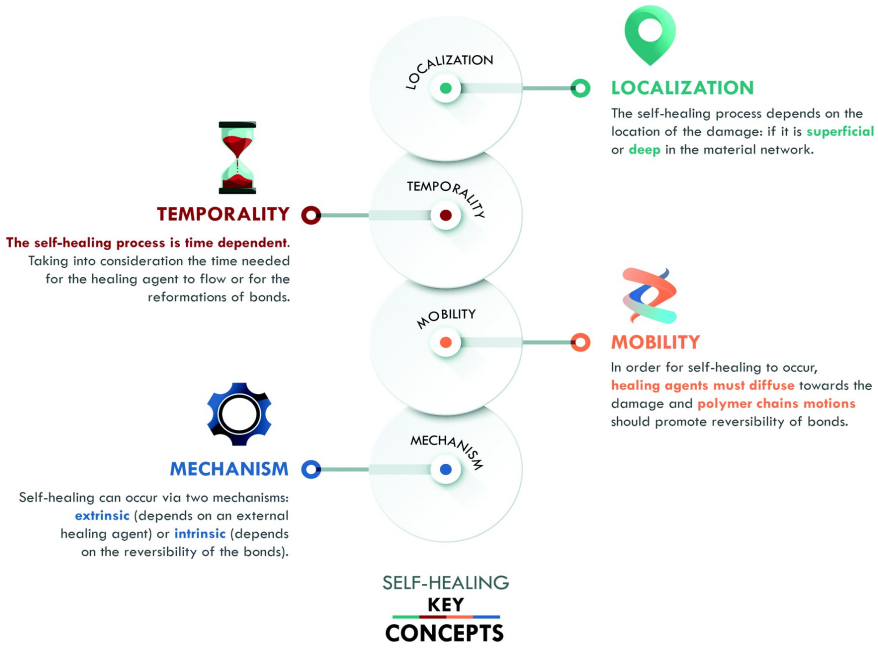

Figure 2. 1. Key concepts of Self healing.

The concept of localization refers to the position and/or scale of the damage in the material. It can be superficial, such as scratches, (micro) cracks, or cuts; it can be deep, such as the propagation of surface damage, fiber de-bonding or de-lamination, ending up in catastrophic damage; or it can be molecular scale damage, *e.g.* breakage of the material network. The localization and scale of these types of damage play an essential role when considering the self-healing capability of the material. The key concepts of self healing is also explained in figure 2.1.

2.2.1 Categorization of self healing materials

Self-healing materials are now a reality, with such materials able to restore their structural integrity if damaged (eg, components used in mechanical processes, the scratches on automobile bodies and cracks in paints, which can close on their own).

Based on the self healing mechanism the materials are divided into two divisions. They are intrinsic and extrinsic self healing materials. Self-healing can be used for different types of material (eg, polymers) but is not limited to metals, alloys, ceramics and composites. The design strategies for self-healing materials include: the release of a healing agent, reversible cross-link, electro hydrodynamics, the shape-memory effect, nano particle migration, and co-deposition.

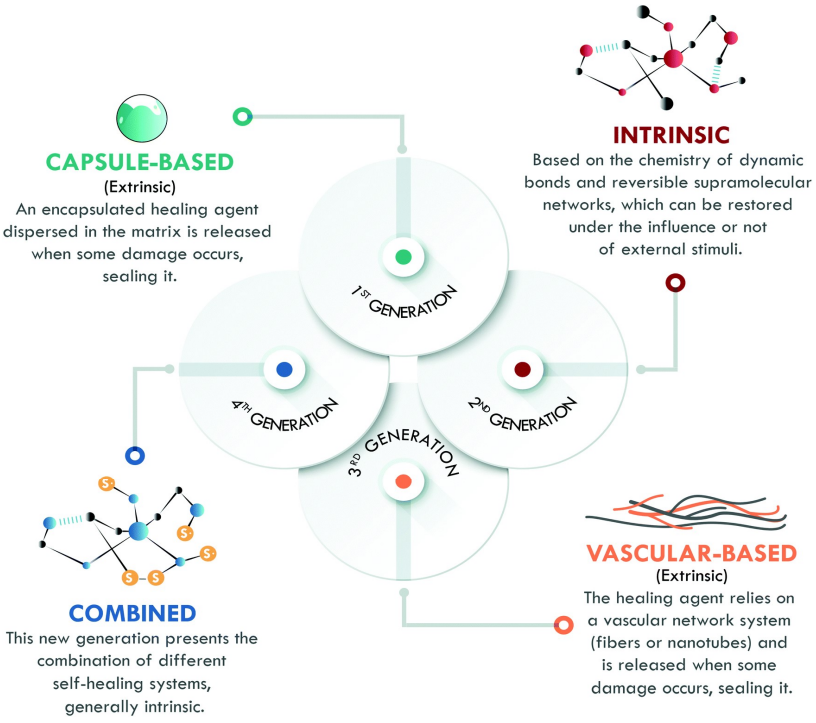

Figure 2. 2.Generations of healing materials according to the healing material involved.

Figure 2.2 explains about generations of healing materials according to the healing material involved. (Mater horiz et al., 2020). The first generation of self-healing materials was based on extrinsic mechanisms and employed encapsulated external healing agents. This generation had the disadvantage of only supporting a single cycle of self-healing (bekas et al., 2016). To overcome this limitation, the second generation of self-healing polymeric materials emerged, based on intrinsic mechanisms, using the chemistry of reversible bonds; however, the self-

healing capability and mechanical performance of the materials were in compromise: the increase of one meant the decrease of the other. The intrinsic approach has been studied in all kinds of polymers, with special emphasis in the field of elastomers (Dahalke et al., 2018; Z wang et al., 2019). Later, further development of extrinsic systems was initiated through healing agents confined in vascular networks, giving way to the third generation of self-healing polymeric materials, with strong inspiration from nature. These systems have been extensively studied in thermosets, but their application in elastomers remains limited except for a few reports on silicones (M.W.Lee et al., 2018).

Finally, the fourth generation is currently growing fast and aims to overcome the different drawbacks of the previous generations. Hence, its objective is to develop a polymer with excellent mechanical properties, and high healing efficiency and resistance to multiple damage cycles through the combination of different healing mechanisms. However, the road to this point has been long and there are still some challenges to overcome.

2.2.2 Intrinsic self-healing system

Self healing can occur by reversible covalent bonds or by supra molecular interactions with in the system without intervention of any external agent. The self healing takes place based on its own rheological properties. This kind of system is mainly consists of thermoset materials.

In intrinsic systems, the material is inherently able to restore its integrity. While extrinsic approaches are generally autonomous, intrinsic systems often require an external trigger for the healing to take place (such as thermo-mechanical, electrical, photo-stimuli, etc.). It is possible to distinguish among 5 main intrinsic self-healing strategies. The first one is based on reversible reactions, and the most widely used reaction scheme is based on Diels-Alder (DA) and retro-Diels-Alder (rDA) reactions (Chen et al., 2002). Another strategy achieves the self-healing in thermoset matrices by incorporating meltable thermoplastic additives. A temperature trigger allows the redispertion of thermoplastic additives into cracks, giving rise to mechanical interlocking (Luo et al., 2009). Polymer interlocking based on dynamic supramolecular bonds or ionomers represent a third and fourth scheme. The involved supramolecular interactions and ionomeric clusters are generally reversible and act as reversible cross-links, thus can equip polymers with self-healing ability (kalistra et al., 2007;

yamaguchi et al., 2009) Finally, an alternative method for achieving intrinsic self-healing is based on molecular diffusion (yamaguchi et al., 2009).

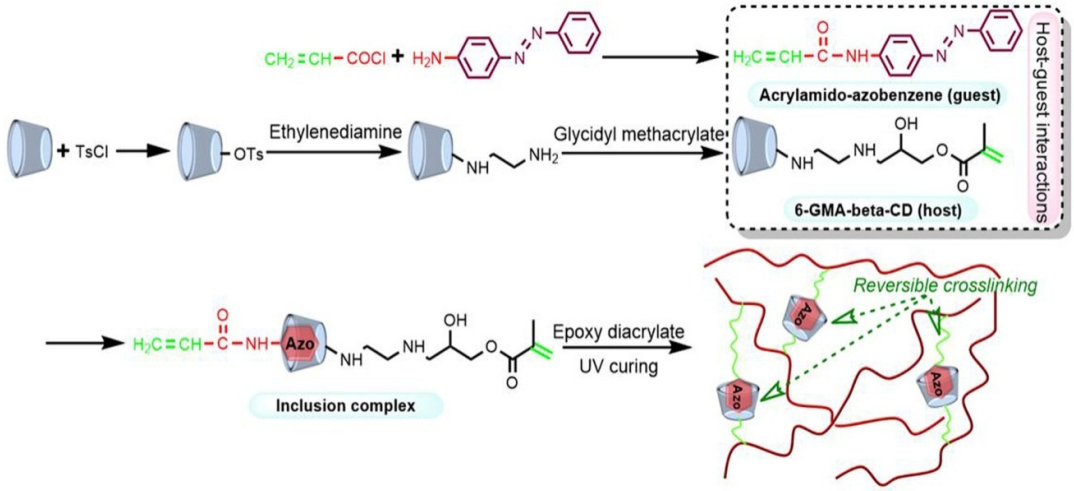

Figure 2. 3. Intrinsic self healing system.

Figure 2.3 illustrate intrinsic self healing system. host-guest chemistry is directly introduced into the cross linking structure of epoxy acrylate to endow the polymer with self-healing behaviors. Their host-guest chemistry is directly introduced into the cross linking structure of epoxy acrylateto endow the composite with self-healing behaviors. This was implemented by the above strategy, by designing and synthesized a β-CD/azobenzene inclusioncomplex (6-GMA-β-CD/AAAB) containing double C=C bonds. By facile ultraviolet (UV) curing process, the epoxy acrylate is cross linked by 6-GMA-β-CD/AAAB complex via free radical Co-polymerization. Benefited from the advantage of the reversible dynamic host-guest interactions, the obtained epoxy films exhibit excellent self-healing and mechanical properties. (Zen hu et al., 2019).

2.2.3 Extrinsic self-healing

A. Vascular-Based Self-Healing system

In Extrinsic self-healing the healing material is encapsulated with in any vascular shaped polymers or halloysite (especially hallow cylindrical shaped materials) and mixed or blended with in the system. Such that when an external damage occurs the healing material will flow out of the vascular chamber to the damaged area to provide self healing this could occur either by an external agent such as temperature UV light etc. Self healing effect occurs by exposure of damaged area to any UV light or external heat. (White et al. 2001; Yiamsawas et al. 2014)

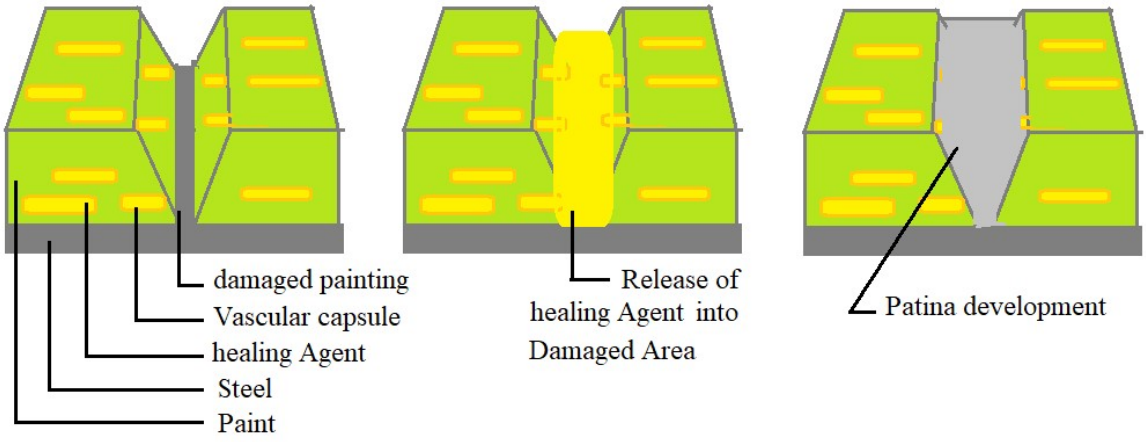

Figure 2.3: Vascular based self healing system.

Materials structures are like hallow cylindrical, tube; rod will come under this category. In particular for epoxy systems the uses of latent hardener with hallow cylinders will decrease the curing time. The importance of nano material in the epoxy system prefers the use of nano rods nano tubes rather micro based material since it increases the thickness with sedimentation problems. A typical representation of hallow cylindrical or vascular based self healing system is shown in the figure 2.3.

B. Microcapsules-Based Self-Healing system

Several encapsulation methods are available for encapsulating corrosion inhibitor. Corrosion inhibitor can be either natural polymer or synthetic inhibitor. (White et al. 2001; Yiamsawas et al. 2014)

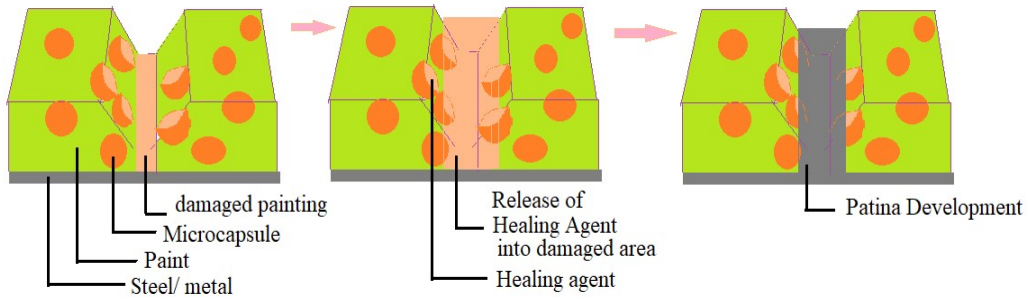

Figure 2. 4. Representation of Micro capsule based self healing system.

Encapsulation can be made by mixing different charged ionic solutions or materials such that opposite charged materials attract each other making one material encapsulated. Microcapsules or nano capsules containers are prepared with Single catalyst or multiple

catalysts for corrosion inhibition. A multilayer functionalized composite system will comes under this category. One of the most popular method for encapsulation of healing material is by using emulsions and then solidification. The selection of the healing material is such that one is polar and another is non polar with another solvent used for preparation of microcapsules. The non polar materials usually be oil, since all oil are non polar and having high unsaturated long chains which is a property of antioxidant. This combination (polar and non polar materials) can helps in formation of emulsion especially O/W oil in water. The wall formation and solidification can be done by mixing the O/W emulsion in urea formaldehyde solution. A typical representation of microcapsule self healing system is shown in the figure 2.4.

2.2.4 Survey on self-healing coatings for corrosion protection

In present era word epoxy has become entirely compatible with anti corrosion in theindustrial environment. Dr Castan and Dr Greenlee (Castan& Greenlee 1936), invented epoxy resin and in 1948, it was commercialized. Since then the emergence of potential approaches for epoxy resin could be seen every decade, maintaining epoxy on a continuous growth path for over half a century. Before 2001 the inventions mainly focused on treating slow-healing wounds, forming self-repairing flexible waterproof material, electrical cables with self-repairing protection, fluid self-healing seals, healing cracks in concrete to prevent leakage and preventing oxidation. Notable patents include the following:

- Self-repairing fiber reinforced matrix materials, including organic and inorganic matrices. This matrix composite material can repair micro cracks and release corrosion inhibitors or permeability modifiers in concrete and polymer-based shaped articles.
- The device and manufacturing method for electric cables with self-recovery protection.

During 2001 to 2005 period, the most work concentrated on self-repairing reinforced matrix materials, systems and methods of facilitating network diagnostics and self-healing, protection of parts made of composite materials with self-healing properties against oxidation and the method for applying self-repairing metallic materials to high-power diesel engines.

During 2006 to 2010 there was almost a 55% increase in patent filing between 2006 and 2010 compared to the previous period. Most patent applications were filed to mitigate the technical challenges posed by self-healing materials, including improvements to the anti-leakage properties of healing or solidifying material, the strength of the bond between a

healing agent and material matrix. Especially on the manufacturing method of self-healing polymers, composites, metal, alloys and other materials, and the method of encapsulation; and healing speed and the stability of healing materials.

After 2010 most of the work is on findings solutions to the previous problems, which include the following:

- Polymeric materials are used for, among other things, paint, upholstery, pipes and circuit boards. They can undergo degradation due to a number of factors, including heat, chemicals and mechanical forces.
- Conventional carbon fiber composite materials crack easily, the mechanical performance of the material is reduced and the material is difficult to repair.

The reasons for epoxy resin's popularity lie in the special mix of properties that epoxies possess most of the related patents have been filed in China, followed by the United States, Japan and Korea. After 2013 patent filings in China increased significantly. In 2016 there was almost a 50% increase in filings in areas such as, construction, automotive and aerospace, healthcare, electronics and semiconductors, industrial manufacturing, and packaging.

Summary:

Barrier Coatings is one of the easiest and cheapest ways to prevent corrosion therefore it is suggested to use barrier coatings like paint, plastic, or powder etc. Polymers and polymeric composite materials are widely disclosed in the patent filings in the field of self-healing materials, as they are cost effective and readily available. Significant advances have been made in recent years, but the field is still in its infancy. Many concerns – including environmental degradation, oxidation and the effects of temperature – are complex and must be analyzed from different areas such as material science and electrochemistry.

2.3 Lignin as a corrosion Inhibitor

Container based smart, green corrosion inhibition substances have pulled attraction in developing patina over a metal, in-order to decelerate corrosionreactions. Investigations are done with the corrosion inhibitors along with the combination of extractives of renewable resources to have synergetic effect on corrosion inhibition (Vijayan and AlMaadeed 2016).The first era of repairing device was mentioned more than a decade(White et al. 2001; Yiamsawas et al. 2014). Meanwhile, with the aid of this technology into coating industry container-based self-healing substances open up to important subject in smart coatings that can provide immediate remarks over a metal and repairs autonomously to considerably extend the life (Montemor 2014; Wei et al. 2014). Studies (Wypych 2017) reveals that active healing reagents are essential to be present in micro-capsules in order to prepare self-healing coatings. In self-healing mechanism the nested microcapsules concurrently rupture to release the recuperation reagents to the damaged part (Trask et al. 2007). Therefore, microcapsule is demanded to possess various features, which comprise high loading of corrosion inhibitor for fast responsiveness towards sudden damages as a result it plays an vital role in repairing using capsule-based smart materials.. The utilization of natural organic inhibitors is more efficient for corrosion inhibition than synthetic inhibitors. Biorefinery approach for the processes intensification of bio-fuel production has gained interests in the valorization of byproducts. One of the polymers that hurdles the bio-fuel production from lignocelluloses biomass is lignin. To remediate this polymer is used in several applications as fillers in slabs and paints, as a drug carrier, as a corrosion inhibitor, as a food packing polymer etc (Xie et al. 2016).

Some experiments were done on mild steel kept in hcl media for the investigating corrosion inhibition performance using garlic, onion, and bitter gourd (Yadav et al. 2016). Similarly quinine and caffeine were also tested on carbon steel in Hcl electrolyte solution (Awad 2006).Lignin acts as filler in paints(Rahman et al. 2018), different types of lignin (kraft and soda lignin)were used for comparison of organic corrosion inhibition performance of mild steel in 3.5 % Nacl electrolyte medium. However soda lignin gave good inhibition than Kraft lignin (Akbarzadeh et al. 2011). Recent studies reported that the use of nano lignin by encapsulating with different corrosion inhibitors(Isophorone diisocyanate (IPDI), Diphenyl Methane Diisocyanate (MDI)) by Pickering emulsion, and then subsequent polymerization using pre polymer solution by urea (Yi et al. 2015).

Husain has the modification of lignin by incorporation of aromatic scavengers (2-naphthol: AHN EOL and 1,8-dihydroxyanthraquinone: AHD EOL) during delignification process has improved the physical properties of the lignin fractions. Smaller fragments of lignin with high phenolic –OH content, increased solubility and antioxidant activity have led to improved inhibitive property of the modified lignin. The inhibition efficiency (84–93%) of both modified lignin (500 ppm) were observed to be better than unmodified organosolv lignin (EOL). It was deduced that the inhibition process was spontaneous and the inhibitors were mainly physically adsorbed onto the mild steel surface. (Hussian et al., 2015)

Apart from the natural polymers, natural oils extracted from plants and seeds have high linoleic acid content with long-chain unsaturated fatty acids that can form a polymer film when it is exposed to the natural environment or in presence of any external dryer (Halambek et al. 2010; Leal et al. 2018). Some plant/leaves oils such as neem oil that are water-soluble contain alkaloids, and a good amount of nitrogen, and sulphur contents which are responsible for formation of the protective layer(Bagale et al. 2018c).

The fluoro type silane used as a core material for encapsulation of corrosion inhibitor(Wei et al. 2014; Frankel 2016). Huan et al reported Multilayer nanocomposite for encapsulating the healing agent such as IPDI and lignin in melamine-formaldehyde using O/W pickering emulsion and byin-situ polymerization(Yi et al. 2015). Hussian (Hussin et al. 2015a) worked on different shell materials for encapsulation purpose, these being urea/phenol/melamine formaldehyde resin, using in situ polymerization approach.

Best degree of success or the optimum performance of the silanes on metal is observed with the single layered coating with combination of natural polymer and silane agents(Villa et al. 2016). These are high performance organic coatings, can be applied to materials that are under, or beneath the sea. The main advantages of High performance coatings, the major outcome of any organic paintings are having qualities such as high corrosion resistance in highly aggressive environments**.** It Can be applied in high relative humidity (more than 90%).These coatings has high thickness (DFT) can be achieved per coat**.** Provides resistance to weathering, especially UV light**.** These coatings also exhibit good mechanical properties such as high impact strength, abrasion resistance and hardness.

2.4 Cellulose as a corrosion Inhibitor:

Conversion of available natural/waste resources to useful products is a key to enhance ones national wealth. One of the renewable, sustainable and abundantly available raw materials is lignocellulosic biomass. This kind of biomasses consists of carbohydrate polymers (such as cellulose and hemicelluloses) and aromatic polymers (lignin) which can be easily converted to value added products(Division et al.). Since nano cellulose has hallow like structure it can accommodate any active chemicals which can be released whenever necessary and needed (Vijayan and AlMaadeed 2016; Zhao et al. 2017). Cellulose can be utilized for several applications such as nano containers to hold corrosion inhibitor fin paint industry(Selvaraj et al. 2010; Mohamed and Rehim 2015; He et al. 2019), as a drug releasing container(Huang et al. 2006; Almeida et al. 2014), and can be used as a super absorbent in farming to release fertilizers in addition to water(Zhong et al. 2012; Ramli 2019).

Corrosion generally occurs when steel or an alloy exposed to environment this could be due to the electrochemical reaction that takes place between the metal and environment (Montemor 2014). Synthetic Corrosion inhibitors are available such as nitrates Chromates are best example of corrosion inhibitor will generate toxic chemical compounds when it reacted with steel by forming a toxic corrosion product. chromates will generate chromium ions which will effects the living organism by causing cancer(Raja et al. 2016). Naturally available organic corrosion inhibitors have inherent properties like anti-oxidant, anti-inflammatory, anti-fungal, anti-cancer, anti-viral, and anti-microbial(Espinoza et al. 2016).Therefore natural organic corrosion inhibitors like lignin (Akbarzadeh et al. 2012; Yi et al. 2015) cellulose (G. and F. 2014) (that have high anti-oxidant properties), and oils that consists of highly unsaturated fatty acids are used as a self-healing materials for corrosion resistance (Suryanarayana et al. 2008).When these natural corrosion inhibitors are exposed to external environment (like temperature, pH, any precursor drier) or with some silane coupling agents (Wypych 2017) they form a polymerised film which acts as shielding agent against environment to avoid erosion of metal .

Several authors presented different mechanisms to prevent corrosion such as by creating polarized film on the metal by formulating coatings consist of opposite charged multilayer (layer by layer) nano composites (Yi et al. 2015), by encapsulation of corrosion inhibitors (Bagale et al. 2018c; Ogunleye et al. 2020), that are capable of formation of a polymerized film on the metal surface. Coating can be inhibited by applying epoxy and inhibitor based coatings, or with nano containers, or combinations of both. The use of

corrosion inhibitors in combination will have synergetic effect of corrosion inhibition thereby avoiding earlier deactivation, osmotic blistering, leaching of the coated paint etc(Patil and Radhakrishnan 2006; Padilla-Martinez et al. 2014). The combination of polyaniline and oxides such as ZnO, TiO_2, Fe_2O_3 have shown excellent corrosion resistance properties(Patil and Radhakrishnan 2006; Sathiyanarayanan et al. 2007a, b; Ramezanzadeh and Attar 2011; Ramezanzadeh et al. 2011; Olad and Nosrati 2013).

The controlled release of corrosion inhibitor on to the effected surface of metal depend up on the pH environment of the substrate and containers shape, size these are most important parameters that to be considered which in turn decides the amount of corrosion inhibitor that can be effectively loaded into nano fiber (Frankel 2016)

An active corrosion coatings were developed using hybrid sol-gel films (Silica-zirconia) that are formulated by introducing corrosion inhibitor 2-mercaptobenzothiazole containing halloysite nano container (having length 1-5 μm, diameter 10-150 nm). The self-healing behavior of coated AA2024-T3 aluminum alloy was studied by making markings on the coated alloy and by conducting immersion studies for 2 weeks using 3% of Nacl. The doped hybrid sol-gel coatings gave better performance when compared with conventional sol-gel coatings by stating that corrosion inhibition in hybrid coatings was triggered by controlled pH environment (i.e at pH 3), which enhances the supply of the corrosion inhibitor into corrosion pit (Shchukin et al. 2008).

The electro spun nano fibers were synthesized by dibutyltin dilaurate (DBTL) and Poly (vinyl alcohol) with a size range of 300–400 nm. Coatings were prepared along with the cross linking agent poly(diethoxy siloxane) (PDES) and a catalyst poly(dimethxy siloxane) (PDMS). The coatings were dried and scribed with coo cutter and then immersed in 5 % nacl solution for 48 hours. These have shown 88% corrosion inhibition (Subhedar and Gogate 2014)

Similarly nano fibers/tubes like Poly (acrylonitrile)(PAN) fiber with a size of 200–300 nm loaded with curing agent like dimethyl methyl hydrogen siloxane were investigated for shelf healing of the coatings by immersing marked coated stainless steel in 1M Nacl solution for 2 days [22].The self-healing ability of Mild steel in salt solution was studied using Poly(o-phenylene diamine) nano tube (150–200 nm) loaded with Poly(o-phenylene diamine)(Siva et al. 2013)

Natural cellulose nano fibers (100–500 nm) were used as a containers for self-healing material and corrosion inhibition of a carbon steel in brine solution with Oleic acid

(Yabuki et al. 2016), Calcium nitrite (Yabuki et al. 2014). Polyanile as a container for loading of Sulfonated polyaniline can be used as a corrosion inhibitor for self-healing of carbon steel in salt solution for the controlled release of corrosion inhibitor (Qiu et al. 2017). Halloysite nano containers can be effect used to check pH active corrosion inhibition (Shchukin et al. 2008; Bagale et al. 2018a).

Summary:

Based on the above findings it is proposed to study the Benzotriazole (BTA) loaded nano cellulose (NC) using sonochemical approach for evaluation of corrosion resistance of mild steel.

Micro or nano spheres in the paint formulations increase the solid content by reducing volatile organic compounds (VOCs), shrinkage and drying time and thereby to maintain the flow characteristics. Multi layered nano composite coatings having natural polymers as a healing material are encapsulated by Pickering emulsion and by in-situ polymerization techniques. The present study aims at synthesis of cellulose hallow nano fibers from naturally occurring lignocellulosic materials with hallow cylindrical shape to an hold more corrosion healing materials than spherical one (micro spheres). Encapsulation and polymerization method involves several steps like preparation O/W emulsion with healing agent and formation of shell wall around healing agent followed by solidification of shell wall by in-situ polymerizations. Where as in present study loading of corrosion inhibitor occurs by simply blending the NC with healing agent and vacuum filtered 3 times. The use of cellulose micro fibrils can overcome some issues that are faced by the micro spheres. Usually micro spheres are less denser and float on the surface of paint, or settling /sedimentation of micro spheres in the paint are some major issues. This can be overcome by 3D structure micro/ nano fibers that are dispersed evenly while coating to ensure the availability of the loaded healing agent everywhere.

The single layered high solid coating with combination of natural polymer and oil based corrosion inhibitor found to be the best corrosion inhibition epoxy system (M.G. Fontana et al., 1986). Hybrid coatings combination of organic an corrosion inhibitor gives better performance when compared to the two layer coatings that involves primer, and intermediate coatings (Chandrabhan et al., 2018). This reduces the steps in the coating preparation as it requires single coating. In view of the importance of natural material it is proposed to use natural biopolymer soda lignin and safflower oil as a self-healing agent along with dipodal or polymeric silane coupling agents such as (APTES) for corrosion inhibitors for mild steel.

Problem statement and Gaps:

Problem statement 1:

Several pretreatment process exists for delignification using lignocelluloses biomass. Every process has its own pros and cons. There is a need to intensify the pretreatment process especially delignification process in terms of high yield and quality with low energy input for smaller process volumes.

Gap Identification:

The acoustic cavitation processes is one of the leading pretreatment processes, which works on sonochemical principles for process intensification. So far several pretreatments process exists for lignocelluloses biomass using Ultrasonic horn and bath type reactors. But investigations on longitudinal horn a new configured ultrasonic equipment which works with the same principle of acoustic cavitation, but with larger volumes were not found.

Problem statement 2:

The synthetic corrosion inhibitors are toxic and carcinogenic to human health. There is a need to develop toxic free self healing sustainable coatings with low cost using renewable resources. The by-products obtained from bio-refinery were used for valorization by preparing self healing coatings.

Gap Identification:

Few authors have reported on natural corrosion inhibitors like lignin and cellulose. The combination of natural corrosion inhibitor synergetic effect of both lignin and safflower oil and further silanization of lignin nano capsules were not reported any where. Similarly the synergetic effect of cellulose nano fibers and benzotriazole was not reported.

Chapter 3

Materials and Methods

Chapter 3 Materials and Methods

3.1. Delignification

3.1.1 Materials

Main raw material required for the process i.e Tectona grandis (teak) sawdust was obtained from local saw mills in Warangal. Other required chemicals like Sodium carbonate (Na_2CO_3) and hydrogen peroxide (H_2O_2) were procured from S.D. Fine Chemicals, Mumbai. Deionized (DI) water was prepared from the DI water setup available in the laboratory. Soxhlet extractor having flask volume of 300 mL and thimble filter of size 130×45 mm was used in the study

3.1.2 Determination of Raw Material properties

A. Sample Preparation

The obtained sample was initially oven dried and sieved to -20/+40 mesh size (<0.841 to >0.45 mm) for further analysis and application of the sample.

B. Moisture content analysis of biomass

The moisture, of raw material teak saw dust was analyzed using a muffle furnace with a maximum temperature of 1000 $^{\circ}C$ with a thermocouple of chromel-alumel. The procedure is same like conventional Oven dried procedure to total solids content analysis in raw material in sample preparation section. The percent moisture can be calculated from equation 3.1

$$\% \text{ Moisture content} = \frac{1 - [\text{Weight dried sample plus dish} - \text{weight dish}] * 100}{\text{Weight sample as received}} \quad \text{(eq 3.2)}$$

Moisture content was 3.2 % in tectona grandis sawdust.

C. Composition analysis of lignocellulosic biomass

The compositional analysis was performed according to the NREL method. Pretreated biomass was washed with distilled water and oven dried at 105°C overnight. Removal of Extractives using soxhlet extractor having flask of volume of 300 mL (actual volume of processed liquid as 200 mL) and thimble filter of size 130×45 mm as shown in figure 3.1. Typically, 0.1 g of dried sawdust was added to 1 ml of 72 w/w% sulphuric acid solution and incubated at 30°C in a water bath by stirring with glass rod for 1 h. Further the concentration was reduced to 4 w/w% by adding 29 ml of distilled water and solution was then hydrolyzed

by autoclaving at 121°C for 1 h. Further, the hydrolyzed mixture was centrifuged to separate filtrate and residue. The filtrate was used to analyze Acid Soluble Lignin (ASL) and sugars.

$$Acid\ Soluble\ Lignin\ (ASL)\ \% = \left(\frac{UV\ abs * Volume\ of\ hydrolysis\ liquor * Dilution}{\epsilon * ODW\ sample\ (mg) * Path\ length} * 100\right) \quad (eq\ 3.2)$$

Where UV_{abs} is average UV-Absorbance of the sample

$$Dilution = \frac{V_{Sample} + V_{dilution\ solvent}}{V_{sample}} \quad (eq\ 3.3)$$

ODW is oven dry weight of sample, ϵ is absorbivity.

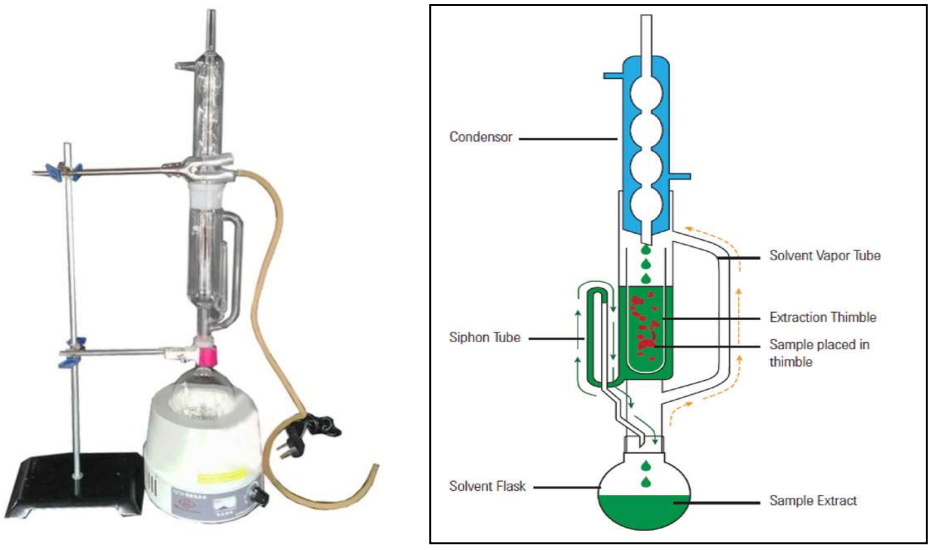

Figure 3. 1. Soxhlet extractor schematic diagram representing its parts.

The sample was separated by centrifugation, and then the supernatant was filtered using syringe driven filters of 0.22 micron. The glucose and xylose standards were prepared in order to determine cellulose and hemicellulose content using HPLC equipped with rezex RPM pb^{+2}(8%) phenomenex column with 300X 7.8 mm size and a refractive index detector. Matching the obtained data for the samples with the standards allowed determination of cellulose and hemicelluloses. The analytical column was run with HPLC grade water as a mobile phase. During the analysis, 0.5 µL of hydrolyzed sample was injected into HPLC column with 30 minutes of acquisition time, to elute all the monomers present in the column.

Acid Insoluble Lignin (AIL) is calculated according to the formula

$$(AIL)\ \% = \left(\frac{(ODW\ of\ the\ residue\ left\ after\ two\ step\ acid\ hydrolysis) - (wt\ \%\ of\ ash)}{ODW\ of\ sample}\right) \quad (eq\ 3.4)$$

The obtained residue, described as Acid Insoluble Residue (AIR) was kept in a muffle furnace at 575°C to determine ash content and difference of AIR, and ash content gave Acid Insoluble Lignin (AIL).

Total Lignin = Acid Soluble Lignin + Acid Insoluble Lignin. *(eq 3.5)*

The conversion factors for sugars are calculated according to the formula proposed by

Table 3. 1.Composition analysis of untreated sawdust

Component	Hydrolysis factor g of sugar / g of polymer	Untreated Sawdust (w/w %)
Glucan	1.11	35.7
Xylan	1.136	22.5
Arabinan	1.136	3.3
Mannan	1.11	2.8
Klason lignin	-	18.3
Acid soluble lignin	-	3.41
Extractives & Others	-	13.3

Composition of the tectona grandis sawdust composition is reported in Table 3.1. Typically the saw dust had around 35% cellulose, 28% hemicelluloses and 22% lignin.

3.1.3 Different Configurations of Ultrasonic Reactors:

A Longitudinal Horn

The recovery of lignin from sawdust has been investigated using different configurations of ultrasonic reactors such as longitudinal horn, conventional design of ultrasonic horn (vertical immersion type) and ultrasonic bath. Longitudinal horn is a kind of novel sonochemical reactor offering large transducer area and was procured from Roop Telsonic Ultrasonix Ltd, Mumbai, India. The horn has an operating frequency of 36 kHz and power dissipation of 150 W. The operational guidelines recommend that the transducer should be completely immersed in the liquid and to achieve this, the minimum volume required was 4 L. Additional stirrers were provided to ensure a proper mixing of the processed sludge. A separate provision for draining the processed fluids has been provided at the bottom of the reactor. Operating time cycle was set at 15 min followed by 10 min off to allow for cooling of the equipment. The schematic representation of the longitudinal horn used in the experiments has been shown in **Figure 3.2.**

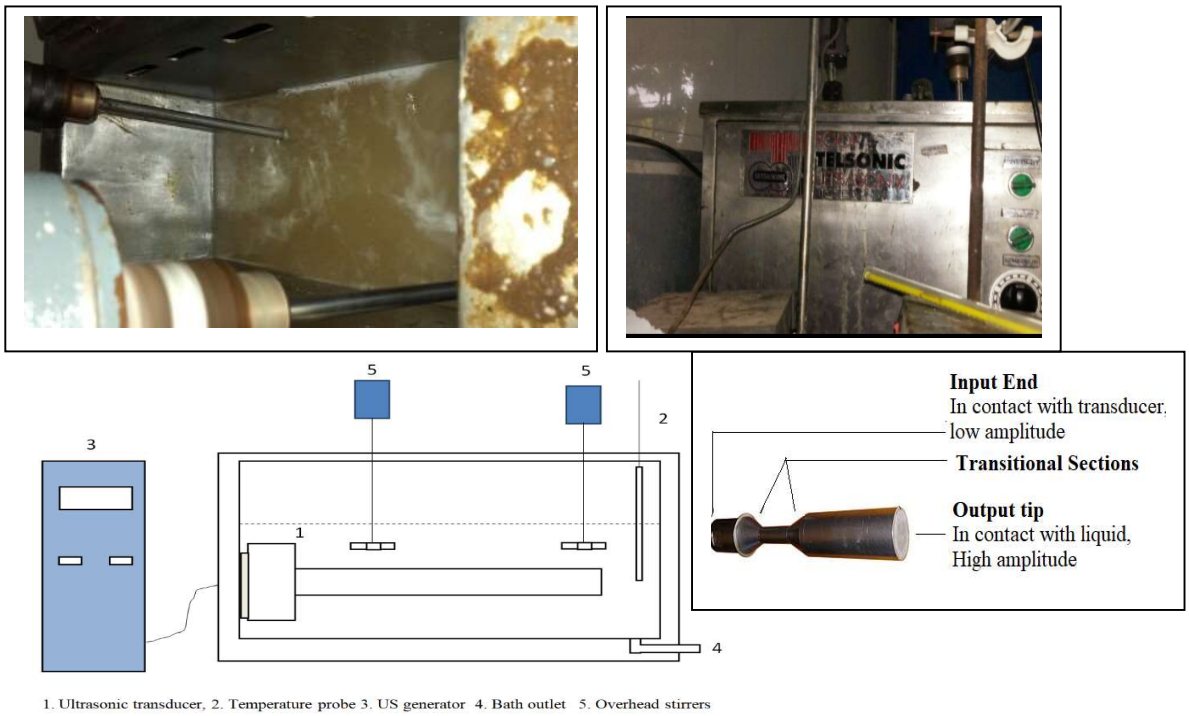

Figure 3. 2. Experimental setup of longitudinal horn and block diagram with its components.

The reactor works on irradiation using a single longitudinally vibrating transducer attached to one side at the bottom of the reactor. The reactor has dimensions of 15cm (W) × 33 cm (L) × 20 cm (H) with a maximum capacity of 8 L.

B. Ultrasonic Horn

Ultrasonic horn (vertical immersion type) used in the work had a rated power as 200 W and frequency of 24 kHz(UP200H.DC model) with a tip diameter of 10 mm. The horn has provision of varying the amplitude over the range of 10% to 90% and duty cycle over similar range. The schematic representation of the experimental setup for ultrasonic horn has been shown in **Figure 3.3**. During the operation, precautions were taken such that horn was dipped 0.5 cm into the solution. The glass vessel with a holding capacity of 100 mL was used as the reactor for the experiments.

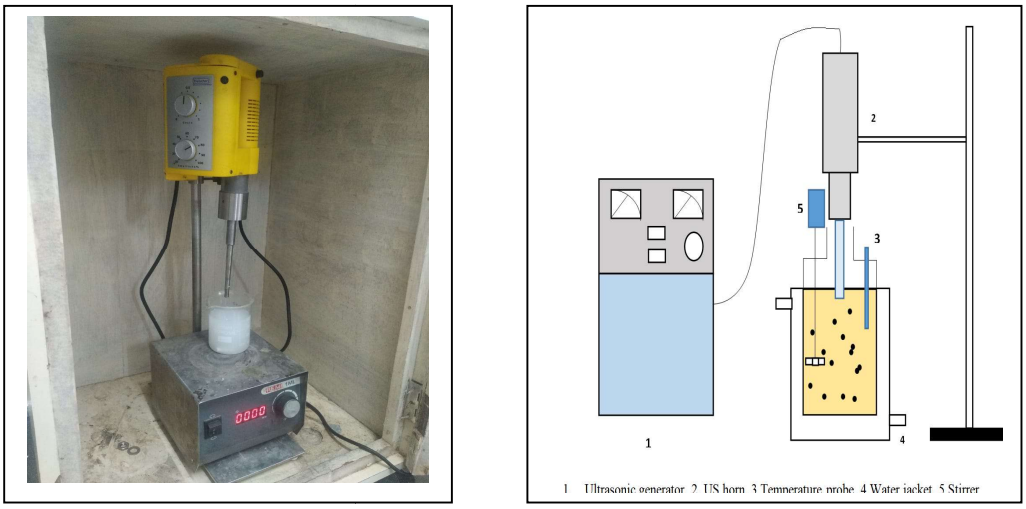

Figure 3. 3. Experimental setup of Ultrasonic vertical probe type horn and block diagram with its component

C. Ultrasonic bath

The ultrasonic bath purchased from M/s Dakshin, Mumbai is equipped with two transducers arranged at the bottom (under the plate and not in direct contact with the solution). The bath can be operated at two different frequencies as 22 kHz and 40 kHz. The power dissipation can also be varied up to a maximum of 150 W. The experimental setup for ultrasonic bath used in the study has been shown in **Figure 3.4**.

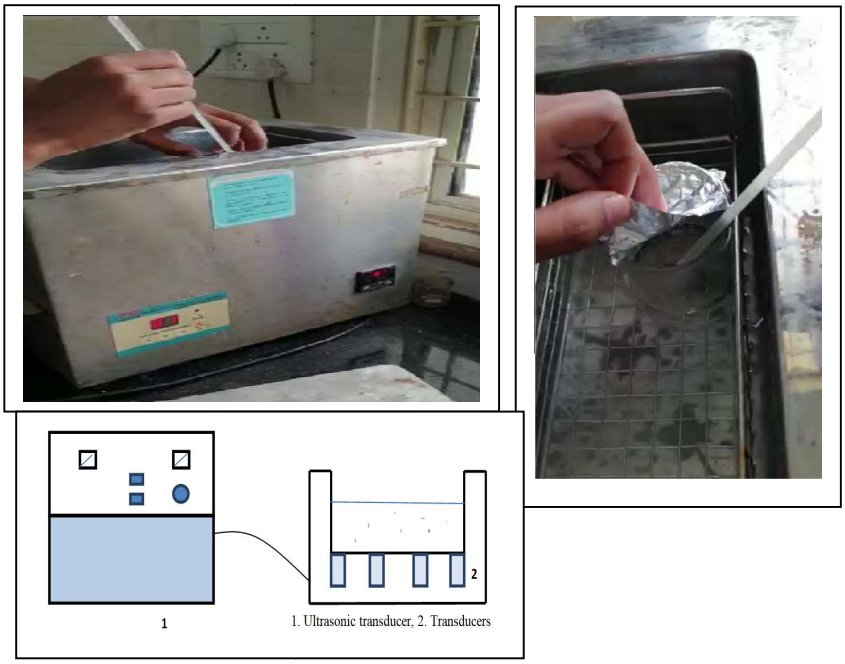

Figure 3. 4. Experimental setup of Ultrasonic bath and Schematic representation with its components.

The intensity and activity of cavitation in the different ultrasonic reactors depends on the locations and geometry of the transducers. In the case of longitudinal horn, it is expected that the cavitational effects are produced over a large region of the reactor since it is placed nearly in the middle of the reactor and has large dimensions. In the case of ultrasonic bath, the transducers are placed at the bottom of the reactor but not in direct contact with the reaction mixture, thus giving an indirect effect and hence lower intensity. In the case of ultrasonic horn, the effects are intense but localized mostly due to the lesser diameter of the transducer. Conventional approach for the delignification of sawdust was also applied using a 100 mL beaker as reactor placed on a heating mantle. The assembly also consisted of a thermocouple for measurement of temperature and a magnetic bead for stirring for uniform mixing of the processed solids in liquid.

3.2 Self healing coatings

3.2.1 Lignin as a corrosion Inhibition carrier

The required chemicals like formalin, urea, ammonium chloride, polyvinyl alcohol (PVA), 3-Aminopropyl triethoxy silane (3-APTES/APTES) KH550, Tri Ethanol Amine...etc were procured from sigma Aldrich were used in the study. Industrial Epoxy resin, hardener, and reactive diluents procured from Aditya Birla Ltd. Mumbai India. Epotec TW 5001 is an aqueous dispersion of liquid bisphenol A epoxy resin. Hardener as Epotec TH 7301 is a low viscosity, low colour modified cycloaliphatic polyamine curing agent for use with liquid epoxy resins. Safflower oil from Savita oil technologies Limited, Mumbai. For distilled water is used for electrolyte solution. Specification of epoxy resin and hardener given by manufacturer used in the coatings are given in table 3.1.

Table 3. 2. Specification of epoxy resin and hardener use in coating

Epoxy resin (TW-5001)

Properties	Specification
Appearance	White, semi solid.
Colour	0.5 G
Density	1.09 g/ml
EEW (Epoxy Equivalent wt based on solids)	195-220 g/eq
Viscosity @ 25°C (Brookfield, viscometer)	300-3500 cp
Non-volatile content	59-61%

b)Hardener. (TH 7301)

Properties	Specification
Appearance	Clear light yellow
Colour	1 G max
Viscosity (Brookfield, @ 25°C, CP)	270-380 cP
Non-volatiles	90%

3.2.2 Cellulose as a corrosion inhibition carrier:

The required chemicals like Sulphuric acid, and acetone and Benzotriazole (BTA were obtained from Sigma Aldrich. Epoxy resin, Polyamide, Adhesion promoter, wetting dispersant are obtained from M/s ADITYA Birla Ltd, Mumbai (India). Ultrasound 200Watt, 24kHz (UP-200H.DCmodel). Specification of epoxy resin and hardener given by manufacturer used in the coatings are given in table 3.2.

Table 3. 3. Specification of epoxy resin and hardener use in 2K epoxy polyamide coating

a) Epoxy resin

Properties	Result
Appearance	Clear, colorless
Colour (Gardner scale)	0.2 G
EEW(Epoxy Equivalent Weight)	187 g/eq
Viscosity@25°C (Brookfield Viscometer)	12,600 cP
Non-Volatiles	70%

b) Hardener. (Polyamide)

Properties	Result
Appearance	Pale yellow liquid
Colour	6 G
Viscosity@25°C(Brookfield Viscometer)	2000 cP
Non-volatiles	60 %

3.2.3Substrate Preparations for Coatings:

Substrate preparation is one of the significant stages in the coating. It creates the required surface for better coating and also improves adhesion characteristics. Mild steel (2 × 2 × 0.5 mm) was cleaned and further panels were smoothened with A394 emery paper and then electro coated water proof silicon carbide paper P320 emery paper.

3.3 Characterization

3.3.1 Fourier Transform Infrared Radiation spectroscopy (FTIR)

FTIR spectra is used to interpret the functional groups present in the nanocapsules and analyze them using FTIR analyzer (SHIMADZU FTIR-8400). Nanocapsules or benzotriazole loaded cellulose nano fibers are mixed with KBr in 1:3 ratio and thin circular pellets were prepared by homogenized and pressurized up to 2-3 kPa to make pellets and analyzed over mid-infrared region of 400-4000cm^{-1}. Nanocapsules residue were placed in oven for 10 minutes at 130ºC for drying and it is analyzed by FTIR for presence of urea formaldehyde functional groups in the nanocapsules shell.

3.2.2 Ultra Violet –Visible Spectrophotometer (UV-Visible Spectroscopy)

The lignin content after extraction of ASL was determined using the acetyl bromide method based on UV spectroscopy measurement. The Obtained lignin was mixed in a solution of 25 v/v% of acetyl bromide in acetic acid and placed in 50°C water bath for 30 min. The solution was cooled and 2.5 mL of glacial acetic acid, 0.5 ml of 0.5M hydroxylamine hydrochloric acid and 1.5 mL of 0.5M NaOH solutions were added. Subsequently the sample was subjected to spectroscopy analysis at 280 nm to determine the exact lignin yield.

The phenolic content is responsible for good corrosion inhibition characteristics. So total phenolic content in the lignin extract was determined by Folin-Ciocalteu method. By Lambda Perklin UV spectroscopy. In brief the lignin extract was diluted with methanol till the absorbance was fine until 0 or 0.5 A. To 0.5 ml of methanolic solution of lignin extract, 2.5 ml of 0.2N Folin phenol reagent (diluted 10 times with methanol) was added mixed well and left for 8 minutes. To this 2 ml of sodium carbonate solution (75 g /L) was added and mixed well. This is kept in a water bath of 50ºC for 1.5 hours and cooled to room temperature. The absorbance was measured by transferring 20 µl of solution to be determined into cuvette.

A Gallic acid calibration curve is made by preparing gallic acid stock solution (100-2000 mg/l). total phenolic content in the lignin extract was expressed as milli gram equivalent of gallic acid (GAE) per gram of lignin extract.

Benzotriazole controlled release studies under different pH environment were performed using UV-Vis spectrophotometer (SHIMADZU 160A model). The concentration of benzotriazole was measured at 262 nm and 273 nm for 1H benzotriazole (having two absorption peaks), and a single absorption peak of 273 nm for 2H benzotriazole.

3.3.3Scanning electron microscopy (SEM)

The micrographs of treated and untreated sawdust were obtained using the scanning electron microscopeTescanVega-3 MUT instrument (SEM) was used to evaluate the structure of cellulose nano fibers. During the analysis, samples were coated with gold powder and scanned under instrument operated at15 kV electron beam voltage with the aid of secondary electron detector.

3.3.4 Field emission scanning electron microscopy (FE-SEM)

The morphological structure of nano particles were analysed using Hitach S 4800 FESEM, model field emission scanning electron microscopy. Cressington sputter coater was used to coat platinum on the lignin nanoparticles for imaging purpose at 5-15 kV.

3.3.5 Transmission Electron Microscopy (TEM)

The high resolution TEM images of the ultrasound assisted synthesized lignin based nano capsules as well as benzotriazole loaded cellulose nano fibers were recorded using transmission electron microscopy TEM, PHILIPS, CM200 at 200 Kv accelerating voltage for electrons. The nanocapsules solution was placed on TEM grid coated with carbon to record micrographs.

3.3.6 X-Ray Diffraction (X-RD) analysis

X-Ray Diffraction (X-RD) analysis was performed using a powder X-ray diffractometer (PANalyticalX^{1}pert powder Model) under operating conditions of 45 mV and 30 mA. A step input spreading over 34.925 s, in step interval of 0.016 °was given for a 2θ range of 5-30°.

3.3.7 Gel permeation chromatography (GPC)

Gel permeation chromatography (GPC) was also used to establish the molecular weight of extracted lignin. During the analysis, extracted lignin sample (1 mg/mL as loading) was dissolved in tetrahydrofuran (THF) which acts as the mobile phase with flow rate set at 1 mL/min. 100 µL of sample was injected into the Waters RI2414 RI detector unit calibrated using mono-disperse polystyrene standards at a constant temperature of 35^{o}C.

3.3.8 Thermogravimetric analysis (TGA) analysis

Thermogravimetric analysis (TGA) analysis of the sample was performed using Thermax 700 Thermo Scientific TGA analyzer. TGA was applied to establish the thermal behavior of treated and untreated sawdust sample. A sample of 2 mg was used for analysis over a temperature range of 20-1000°C at a constant heating rate of 10°C in nitrogen (99.5% nitrogen) inert atmosphere.

3.3.9 Corrosion Inhibition Studies by CH Instrument.

Polarization and Impedance was measured by CH Instrument different weight percentages (i.e 0.5, 1, 1.5) of lignin were used for the experiments to modify water borne epoxy. The coatings were formulated with the composition (in parts by weight- pbw) of 0.3 titanium dioxide, 0.4 adhesion promoter, 35 hardener and 80 of epoxy-containing loaded nanocapsules. The modified lignin-based epoxy coatings were further coated on a mild steel with a thickness of approximately 50 µ by using paint brush. Curing was done at 40-50ºC for 1 hour in an oven. A manual scribe was made on the coatings and immersed in 3.5 wt% nacl aqueous solution for about five days.

After five days of immersion, marked coated mild steel panels were analyzed for EIS and potentio dynamic polarization studies using an electrochemical analyzer i.e CH Instrument model CH680, from the USA. Coated mild steel panels acted as working electrode, Platinum as counter electrode, and Saturated calomel as reference electrode in an electrolyte solution of 3.5 wt% of sodium chloride. Polarization measurements were made with a voltage range of -2V to +2V using a scan rate of 0.1667 mV/s.

3.3.10 Immersion or weight loss studies

Immersion studies were performed using 3.5 wt% of Sodium chloride solution which is equivalent to sea water concentration. Mild steel panels in five numbers were initially burred with emery paper as mentioned above for surface coatings. Both modified epoxies with benzotriazole loaded cellulose nano fiber and lignin nanocapsules are casted on mild steel panels and allowed it to cure for three hours in atmospheric environment or heating it in oven at 50ºC for 2 hours. After curing, a deep mark is made on the coatings with sharp edge knife, and weight loss measurement of the panel was done before immersion and after immersed in 3.5 wt % sodium chloride solution for 120 hours according to ASTM standard.

Chapter 4

Experimental Procedures

Chapter 4 Experimental Procedure

4.1 Delignification Process

The experimental work followed for delignification was explained in figure 4.1 as a graphical abstract and the step wise procedures in figure 4.2.

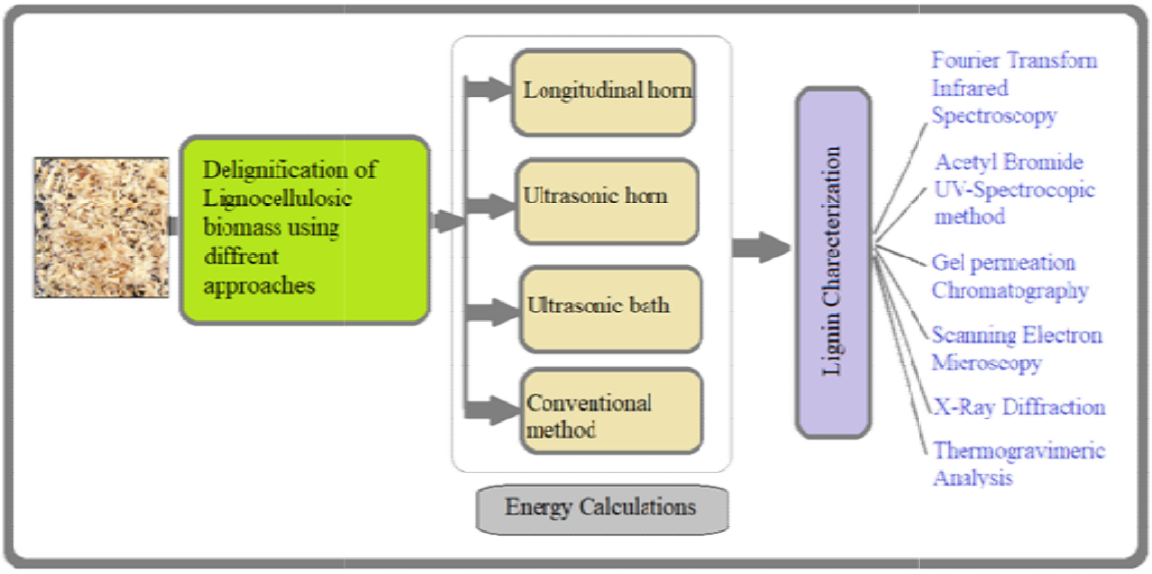

Figure 4. 1. A Graphical representation for delignification.

4.1.1 Procedure for Extractives Removal

Milled sawdust of -20/+40 mesh size (<0.841 to >0.45 mm) was subjected to extraction using toluene and ethanol (2:1 v/v %) for 60 minutes a soxhlet extractor to remove extractives. After extraction, the obtained residue of sawdust was used for compositional analysis and for further experiments of delignification using different approaches (three different ultrasonic reactors and conventional approach i.e. without using ultrasound)to know the effect on yield of lignin.

4.1.2 Delignification process

Initially in the case of conventional approach, the effect of concentration of alkali peroxide and the solid loading on the lignin yield was studied. Similar variations were further used in the experiments involving the use of ultrasonic reactors to study the effect of acoustic irradiation and the effect of ultrasonic parameters i.e. power and frequency for different type of reactor configurations. In the case of ultrasonic horn, the temperature was controlled with

help of water jacket while in the case of ultrasonic bath it was controlled with help of cooling coil that could be inserted into the bath.

For the case of longitudinal horn, since temperature could not be controlled using cooling water, cycles of operation (on and off) have been used. Operating time cycle was set at 15 min followed by off cycle for 10 min for cooling of the mixture. In initial run, the total treatment time was maintained constant at 80 min and lignin content was analyzed after sonication by increasing reaction time for 10 min. It was observed that the maximum removal was obtained at 70 min and there after the lignin removal only marginally changed at 80 min. Hence, constant treatment time as 70 min was considered for all experiments.

For the analysis, the solid residue was separated from the liquid using centrifugation at 3500 rpm subjected for 10. The filtrate was acidified to a pH of 5.5 with 6M Hcl and then 3 volumes of ethanol were added to precipitate hemicellulose. The pH of the filtrate was further reduced to 1.5-2 to precipitate dissolved lignin and termed as acid insoluble lignin (ASL). Figure 4.2 gives the step by step procedure for extraction of lignin. Lignin was analyzed quantitatively using the acetyl bromide method. Reproducibility of experimental results was confirmed by repetition of experiments two times and average values are reported in the figures/tables.

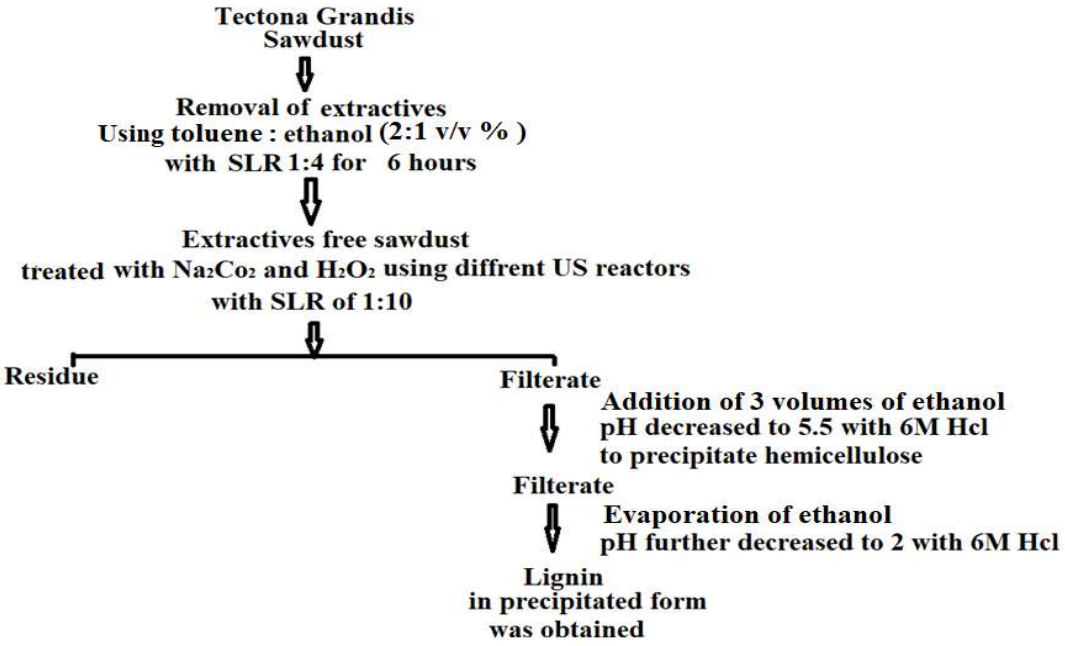

Figure 4. 2. Flow diagram of lignin extraction process

4.2 Ultrasound Assisted Synthesis of Lignin Nanocapsules

4.2.1 Synthesis of Lignin nano particles

Lignin is extracted from sawdust by a two-step process. Initially, sawdust is treated with 1:1 ethanol: toluene to remove water extractives. The separated residue (consists of cellulose, lignin, hemicelluloses) were further treated with sodium carbonate (0.2M) and hydrogen peroxide (1M), using ultrasonic horn with a fixed frequency of 24 kHz operated at a sonication power of 200 W, with an amplitude of 80 % and duty cycle of 0.5 for 70 minutes. Liquid to solid ratio was maintained at 10:1. The obtained solution after treatment of wood was separated by centrifugation at 4500 rpm for 5 minutes, and the pH of the filtrate was adjusted to 5-8 with Hcl. Hemicelluloses were precipitated, and separated by centrifugation, and the pH of the above filtrate solution was further reduced to 2 to precipitate residual lignin. The obtained lignin was then sonicated with probe type horn (200 Watts, 24 kHz, 10 minutes) and the particle size of lignin was measured and further investigated for its anti-corrosion properties and self-healing properties on mild steel.

4.2.2 Ultrasound-Assisted Synthesis of Silanized Lignin Nanocapsules

Synthesis of Lignin loaded Nanocapsules occurs in three steps. First step is preparation of O/W Pickering emulsion using Safflower oil and lignin by sonochemical method. Second step wall formation step (by in situ polymerization of urea and formaldehyde to form methylol urea). So urea formaldehyde pre-polymer solution was prepared by sonochemical method. Third step iswall solidification step (methylol urea further condenses to form polymeric shell). PVA surfactant solution was prepared and blended with pre-polymer solution by sonochemical approach. Drop wise slow addition of O/W pickering emulsion to the above surfactant and pre-polymer solution under sonication helps in better encapsulation of emulsion. Formed nanocapsules are functionalized through amino silane coupling agent under sonication.

I. O/W Pickering emulsion

Schematic representation for the fabrication of lignin based nanocapsules is given in figure 4.3(b**).** Initially, oil in water (O/W) Pickering emulsion was done using healing agents such as lignin and safflower. This was achieved by preparing 1g/15ml lignin-biopolymer

solution, and its pH was adjusted to 11-12 by ammonia to completely dissolve any traces of lignin and further its pH was adjusted to 2-3 by Hcl to precipitate the dissolved lignin in the mixture. 10 g of safflower oil is added to the lignin-biopolymer solution and the mixture is kept under sonication for 10 minutes until mixture forms emulsion.

II. Preparation of Urea Formaldehyde Pre-polymer solution

The required pre-polymer solution was prepared using 3 g of 37% of Formalin in a 250 ml beaker. To this1.5 g of urea monomer (CH_4N_2O), 0.15 g of ammonium chloride (NH_4Cl) initiator, and 0.15 g of resorcinol cross-linking agent, is added to it. The pH of the mixture was adjusted to 8-9 with TEA (Tri-Ethanol Amine). This acts as an emulsifier and maintains the ph to neutral. This alkalinization (especially with TEA) is performed to control corrosion of metal components. Sonication was done with the help of probe sonicator for 10 minutes, at the rate of 120 W power and 24 kHz frequency. Schematic representation of the procedure for preparation of urea-formaldehyde pre-polymer solution is given in figure 4.3 (a).

III. Fabrication of Lignin Nanocapsules

Preparation of surfactant solution was carried out by adding 0.01 g/mL of span 80 and 20 mL of 5% polyvinyl alcohol (PVA) solution followed by slow addition of pre-polymer solution i.e urea-formaldehyde to the surfactant. The whole process was done under sonication (200 W, 24 kHz, 10 minutes) with drop wise addition of a healing agent i.e. lignin-safflower oil emulsion to the surfactant and UF pre-polymer. The pH of the solution was brought down to 7 using Hcl and maintained in the same range for 10 minutes. The obtained solution was centrifuged for 15000 rpm and the formed nanocapsules were collected, washed and further centrifuged 3-4 times by the addition of 300 ml of distilled water. At the end washed with 50 ml acetone. The pellet was dried at 50˚C overnight.

IV. Functionalization of Lignin nano capsules by Amino Silanization

Surface modification of Lignin nanocapsules are done with APTES (3-Aminopropyl triethoxy silane). Functionalization Procedure as follows,1 v/v % (100 g) silane coupling agent in water solution is prepared to this 5 g of lignin nanocapsules are added. The ratio of KH550 : LNC are maintained as 1:5.Then, the pH of the solution was adjusted to 7.0 and sonicated for 15 minutes.

Sonication played an important and crucial role in producing nano materials by decreasing the processing time. It also helps in effective encapsulation of safflower oil and lignin through effective mixing.

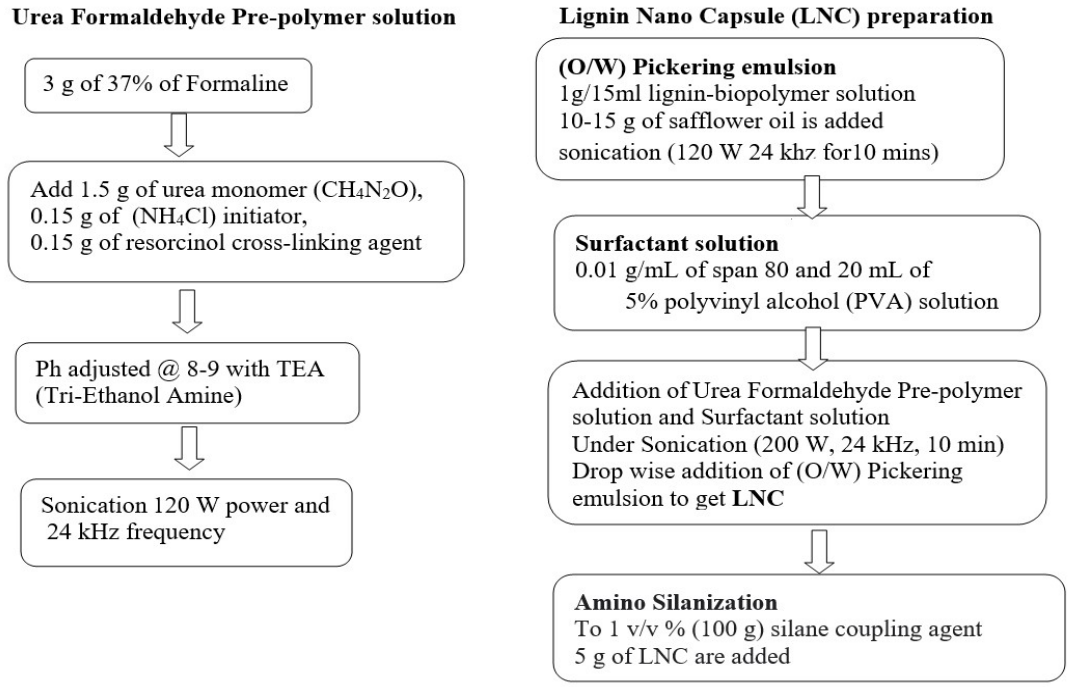

(a) (b)

Figure 4. 3. Flow diagram for preparation of a) UF Pre-polymer solution and b) Lignin nanocapsules.

4.2.1 Formulation of modified water bone epoxy by Lignin nano capsules

Water borne epoxy was modified by addition of Lignin nanocapsules to prepare high build solid epoxy organic coatings. The formulation of paint is similar to the two part epoxy coatings. First part consists of 80 Pbw water borne epoxy, 0.3 Pbw titanium dioxide, and 0.4 Pbw adhesion promoter, this is used as a standard epoxy to measure the performance of the modified epoxy. Part A(shown in Table 4.1) is modified by addition of 0.9 Pbw of lignin nano capsules. Where lignin quantity is in different measures such as 0.5, 1,1.5 Pbw.Second part is same for the standard as well as lignin based epoxy system that is polyamide hardner of 35 Pbw and xylene of 0.3 Pbw.

Table 4. 1. Formulation of Lignin Nano capsule based epoxy coating

	Material	Epoxy-amine coating (Pbw)	Encapsulated lignin nanocapsules based epoxy amine coating (Pbw)		
Part-A	Lignin	-	0.5	1	1.5
	Lignin Nanocapsules	-	0.9	0.9	0.9
	Epoxy resin	80	80	80	80
	TiO2	0.3	0.3	0.3	0.3
	Adhesion promoter	0.4	0.4	0.4	0.4
Part-B	Polyamide (Hardener)	35	35	35	35
	Xylene	0.3	0.3	0.3	0.3

4.3 Procedure for benzotriazole loaded cellulose nano fibers

A. Synthesis of Nano Cellulose

Teak saw dust (10 g) was treated with (1:2) ethanol: toluene in a soxhlet extractor for removal of extractives with solid to liquid ratio of 1:4. The extractives free residue was further bleached with Na_2Co_3 (0.2M) and H_2O_2(1M) in the presence of ultrasonic horn at 200 watt with 24 kHz frequency and with an amplitude of 80% for 70 minutes to remove lignin from the hydrolysate(Devadasu et al. 2019). The remaining residue is hydrolysed with 50 wt% sulphuric acid (1:10 solid to liquid ratio) kept in an ice bath while stirring frequently under sonication (200 watt, 24 kHz, for 0.5 duty cycle and 80% amplitude) for half an hour. Finally acid hydrolysis reaction was terminated by addition of double amount of distilled water, and further the pH of the reaction mixture was made neutral with 0.005 % aqueous sodium hydroxide solution. The nano cellulose can be collected by washing with fresh distilled water by centrifuging with 15000 rpm for 10-15 minutes and further the nano cellulose was washed with acetone and dehydrated, dried at 40-50˚C for an hour.

B. Encapsulation of Benzotriazole BTA in Nano cellulose (NC)

The procedure for the synthesis of cellulose nano fibers and benzotriazole loaded cellulose nano fibers were shown in figure 4.4. Acetone was utilized as a solvent for encapsulation of benzotriazole (BTA). Initially 2 g of nano cellulose (NC) were mixed with benzotriazole saturated solution of 0.1 wt% in 15 ml of acetone. The mixture was then sonicated at 200 watt, 24 kHz, for 0.5 duty cycle for 15 minutes followed by evacuation using vacuum pump in order to load benzotriazole in NC by removing any entrapped air in the hollow NCs. These experiments were repeated by differing the concentration of benzotriazole (2, 4, 6 wt %) to

check the effect of NC loaded benzotriazole on corrosion inhibition on mild steel. These benzotriazole encapsulated nano cellulose (NCB) were separated from acetone by centrifugation with 15000 rpm for 10-15 minutes and further it was dried for 50˚C.

A stopper was prepared in order to know the release rate of benzotriazole at varying PH. As reported in (Shchukin et al. 2008). NCB were soaked in copper ion solution (0.08M) for 2 – 3 minutes to form complex copper benzotriazole that acts as a stopper. When NCB exposed to different pH solution the benzotriazole release quantity is measured by UV Spectroscopy.

The dried NCB was then mixed with 2k epoxy polyamide, along with epoxy resin 80 wt% wetting and dispersant 0.2 wt % and adhesion promoter 0.4 wt% and, polyamide as 35 wt%, reactive diluents 0.3 wt% then coated on the mild steel with paint brush. The coatings without NCB are taken as standard STD.

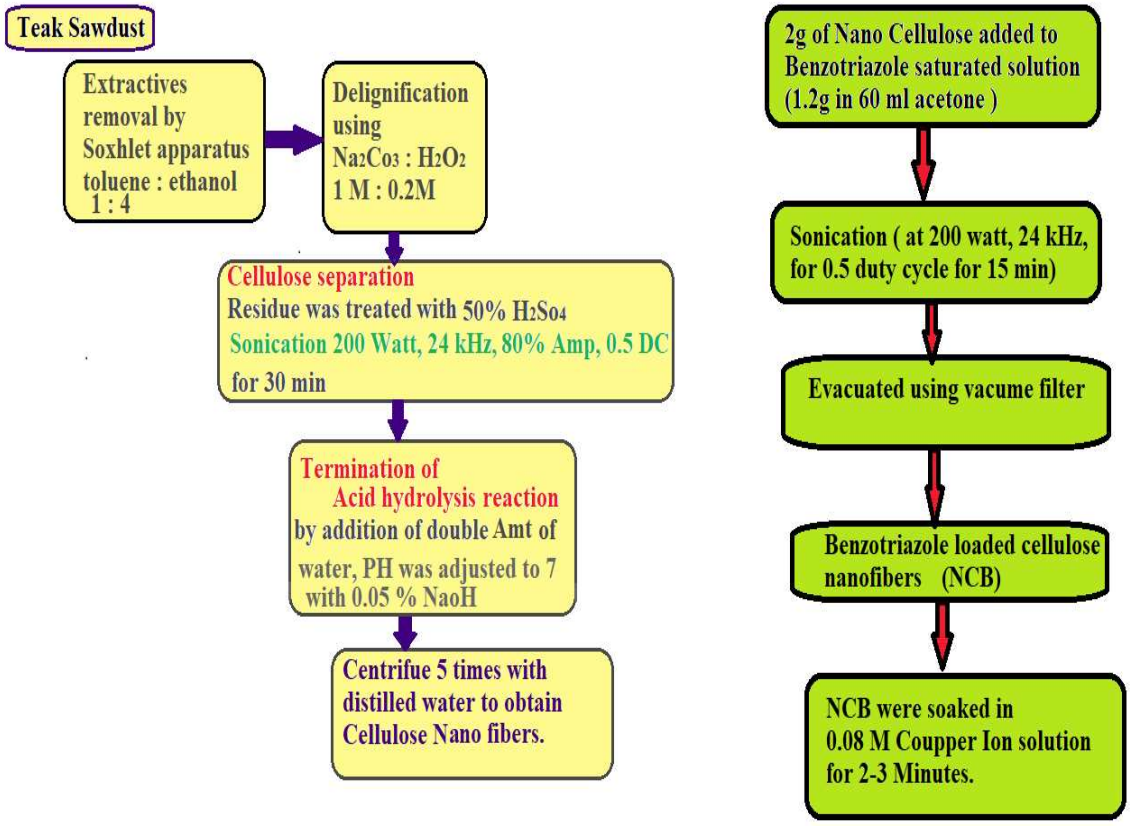

(a) (b)

Figure 4. 4. a) Procedure for cellulose preparation b) Procedure for benzotriazole loaded cellulose nano fibers.

H. PH controlled benzotriazole release studies

In order to know the behavior of NCB at different pH (acidic 3, normal 7, alkali 11 environments), 0.1 g/L NCB with and without stopper were kept in Sodium chloride solution (pH 11) and stirred with magnetic stirrer for 3 minutes and kept undisturbed and UV readings were measured at 2 hours interval for 24 hours. Similar experiments were conducted by varying the pH of the solution (using diluted hcl for pH 3 and aqueous solution as pH 7).

D. Formulation of modified epoxy

The formulations of benzotriazole encapsulated nano cellulose based on 2k epoxy polyamide system consists of part A and part B. Part A is blend of epoxy resin with 80 Pbw, adhesion promoter of 0.4Pbw, wetting and dispersant of 0.2 Pbw for standard epoxy. In addition to that 2, 4, 6 Pbw of benzotriazole loaded in 2 Pbw of cellulose was blended to get different concentration of corrosion inhibitor coatings. After thorough mixing of part A. Part B is added with polyamide 35 Pbw, and reactive diluents 0.3 Pbw.

Table 4. 2. Formulations of 2k epoxy polyamide benzotriazole loaded nano cellulose.

	Material	2k epoxy polyamide coating		Encapsulation of Benzotriazole in of NC, in 2k clear epoxy polyamide, Pbw		
		STD	NCB	2 NCB	4NCB	6NCB
Part-A	Benzotriazole	-	-	2	4	6
	NC	-	2	2	2	2
	Epoxy Resin	80	80	80	80	80
	Adhesion promoter	0.4	0.4	0.4	0.4	0.4
	Wetting and dispersant	0.2	0.2	0.2	0.2	0.2
Part-B	Polyamide	35	35	35	35	35
	Reactive diluents	0.3	0.3	0.3	0.3	0.3

Chapter 5

Results and Discussion

Chapter 5 Results and Discussion

5.1 Delignification Process

Alkali peroxide treatment is said to be one of the best treatment process for cleavage of β-0-4 linkages which are 80% of total linkages that binds structural carbohydrate and lignin(Neumann et al. 2014).Hence experiments were planned in such a way keeping one variable parameter constant and varying other parameters as shown in **table 5.1.**

Table 5. 1 Experimental runs for lignin yields using ultrasonic horn.

Sl.no	Na_2Co_3(M)	H_20_2(M)	Biomass loading (wt%)	Time (min)	C_f (wt%)	$k=\ln(C_o/C_f)\ t^{-1}$
1	0.1	0.2	8	70	62.42	0.013981
2	0.15	0.2	8	70	73.47	0.018956
3	**0.2**	**0.2**	**8**	70	**76.85**	**0.020903**
4	0.25	0.2	8	70	78.15	0.021728
5	**0.2**	0.4	8	70	78.91	0.022234
6	**0.2**	0.6	8	70	81.81	0.024347
7	**0.2**	0.8	8	70	84.12	0.026287
8	**0.2**	**1**	**8**	70	**84.14**	**0.026305**
9	**0.2**	**1**	2	70	76.38	0.020615
10	**0.2**	**1**	4	70	78.74	0.022119
11	**0.2**	**1**	6	70	82.94	0.025263
12	**0.2**	**1**	**10**	70	**85.14**	**0.027236**
13	**0.2**	**1**	**10**	80	87.12	0.025619
14	**0.2**	**1**	**10**	60	84.94	0.031552
15	**0.2**	**1**	**10**	50	82.15	0.034463
16	**0.2**	**1**	**10**	40	80.45	0.040805
17	Amplitude		50		72.24	0.018308
18			60		79.77	0.022829
19			70		82.67	0.025039
20			80		85.11	0.027207
21	Duty cycle		0.1		77.13	0.021076
22			0.2		78.46	0.021932
23			0.3		79.53	0.02266
24			0.4		81.32	0.023967
25			0.5		85.14	0.027236

The Lignin Yield (%) can be calculated as

$$\text{Lignin Yield \%} = \frac{w_f}{w} * 100 \qquad \textbf{(eq 5.1)}$$

'W_f' is Weight of dry lignin extracted, 'W' is Weight of total solid sample taken.

Rate constant was calculated from first order kinetics

$$ln\frac{C_f}{C_0} = -kt \qquad \text{(eq 5.2)}$$

'C_f' is final concentration of lignin extracted. 'Co' is initial concentration of lignin present. 'k' is rate constant, 't' is time in minutes.

5.1.1 Effect of Alkali and peroxide Concentration:

Alkali treatment can be classified as strong and weak alkali based treatment process. Using weaker acids helps in recovery of good quality lignin but might require higher temperatures and treatment times leading to higher costs.

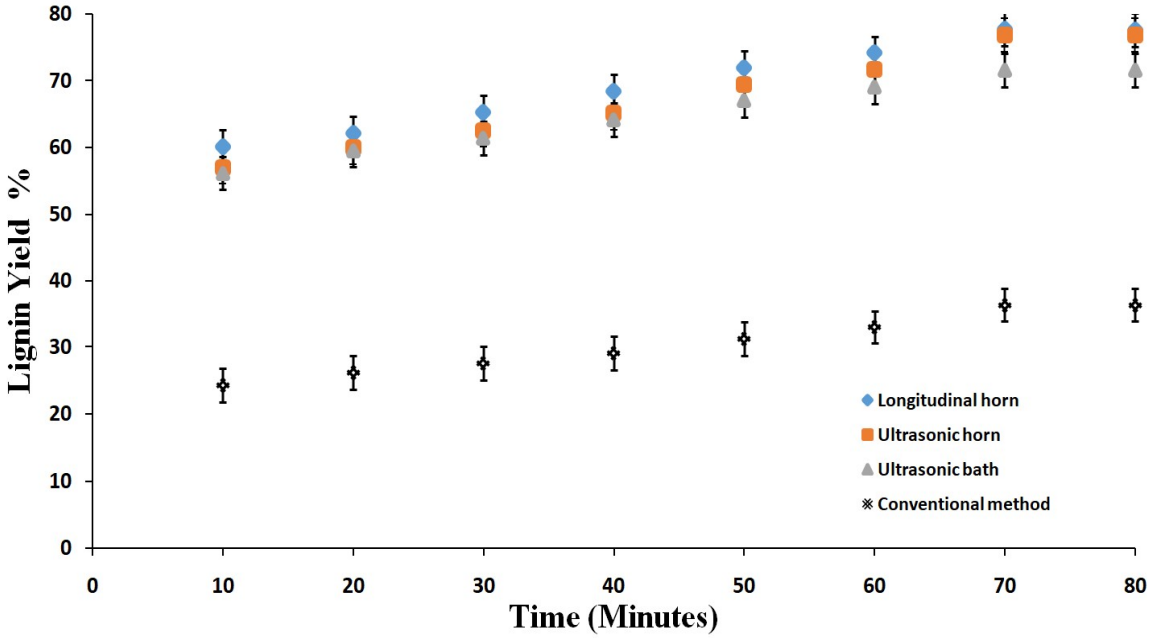

Figure 5. 1 Effect of different ultrasonic reactors on lignin yield under conditions of constant Na_2CO_3 loading as 0.2M, H_2O_2loading of 0.2M and biomass loading of 8wt%.

Sonication with hydrogen peroxide helps in improving the yield and purity of recovered lignin and can help in reducing the treatment temperatures (chhabra et al., 2017). Considering these aspects, experiments were conducted using the combination of sodium carbonate and hydrogen peroxide for lignin extraction from sawdust, first using conventional approach and then also in the case of ultrasound assisted approach. In the present work, for the conventional method, the effect of alkali and peroxide concentrations was studied by varying the sodium carbonate concentration over the range of 0.1 to 0.25M and hydrogen peroxide concentration over the range of 0.2 to 1 M. The obtained results depicted in **Figure 5.1;5.2;5.3** for different

approaches establish that 0.2 M as the sodium carbonate concentration, 1 M as the hydrogen peroxide concentration and 10% biomass loading gives best results for lignin extraction.

Table 5. 2. Effect of sodium carbonate loading (M) on lignin yield and kinetic rate constant

Na_2CO_3 (M)	Longitudinal horn		Ultrasonic horn		Ultrasonic bath		Conventional method	
	Lignin Yield (%)	Rate constant, k (h^{-1})	Lignin Yield (%)	Rate constant, k (h^{-1})	Lignin Yield (%)	Rate constant, k (h^{-1})	Lignin Yield (%)	Rate constant, k (h^{-1})
0.10	63.14	0.014258	62.42	0.013981	58.12	0.012434	21.62	0.00348
0.15	73.98	0.019233	73.47	0.018956	69.13	0.016791	32.62	0.00564
0.20	77.67	0.021418	76.85	0.020903	71.55	0.017957	36.35	0.006454
0.25	79.35	0.022535	78.15	0.021728	73.85	0.019162	36.05	0.006387

Use of higher alkali concentration helps in effective cleavage of ester, ether, and glycosidic linkages connecting the lignin and hemicellulose, finally giving higher lignin recovery. At lower concentrations of alkali (say 0.2 M), much lower removal of lignin is obtained as per the data shown in **Table 5.2**for the effect of sodium carbonate concentration. It is also important to note that beyond 0.2 M concentration, no improvement is observed in the case of conventional approach when the alkali concentration was increased to 0.25 M.

Table 5. 3. Effect of hydrogen peroxide loading on lignin yield and kinetic rate constant

H_2O_2 (M)	Longitudinal horn		Ultrasonic horn		Ultrasonic bath		Conventional method	
	Lignin yield (%)	Rate constant, k (h^{-1})	Lignin yield (%)	Rate constant, k (h^{-1})	Lignin yield (%)	Rate constant, k (h^{-1})	Lignin yield (%)	Rate constant, k (h^{-1})
0.2	77.67	0.021418	76.85	0.020903	71.55	0.017957	36.35	0.006454
0.4	79.41	0.022577	78.91	0.022234	75.6	0.020151	38.01	0.006831
0.6	82.91	0.025238	81.81	0.024347	79.5	0.022639	39.46	0.00717
0.8	84.21	0.026368	84.12	0.026287	79.82	0.022864	40.32	0.007374
1	86.12	0.02821	84.14	0.026305	80.52	0.023368	41.34	0.00762

Also for the ultrasound assisted approach, only marginal changes were observed and hence 0.2 M was established as the optimum alkali concentration. The trends with respect to hydrogen peroxide can be attributed to the enhanced formation of the hydroxyl radicals based on the dissociation reaction of hydrogen peroxide at higher strength, which act able to strongly cleave the carbohydrate lignin linkages. As seen in the **Table 5.3**, there is a stable increase in the extent of lignin removal for all the concentrations of hydrogen peroxide used in the present work for all the approaches and hence 1M can be established as the best hydrogen peroxide loading.

5.1.2 Effect of biomass loading

Biomass loading is an important parameter to be optimized in the pretreatment of biomass, as the structure, texture, and recalcitrant nature of the processed biomass are affected by the quantity of biomass. Typically, there must be enough exposure of biomass particles to the alkali with best conditions for mixing and mass transfer, which is dependent on the solid content in the reactor. The range of biomass loading studied in the work was from 2 to 10 wt% and the obtained results for the effect of loading are presented in figure 5.1b. It can be seen from the figure that as the biomass loading increases from 2 to 10 wt% by weight, the effectiveness of lignin extraction increases though only marginal effect is observed at higher loading i.e. 10 wt%. **Table 5.4**shows the actual data for the lignin yield as well as the kinetic rate constant. It can be also seen from the table that the kinetic rate constant also showed similar trends as the lignin yields. The obtained trends matched with the reported literature (yuan et al., 2018).

Table 5. 4. Effect of biomass loading on lignin yield and kinetic rate constant.

Biomass Loading (%)	Longitudinal horn		Ultrasonic horn		Ultrasonic bath		Conventional method	
	Lignin yield (%)	**Rate constant, k (h^{-1})**	**Lignin yield (%)**	**Rate constant, k (h^{-1})**	**Lignin yield (%)**	**Rate constant, k (h^{-1})**	**Lignin yield (%)**	**Rate constant, k (h^{-1})**
2	77.15	0.021089	76.38	0.020615	72.08	0.018226	30.58	0.005214
4	79.35	0.022535	78.74	0.022119	74.44	0.019488	33.94	0.005923
6	83.14	0.025432	82.94	0.025263	78.64	0.022052	40.14	0.007331
8	86.12	0.02821	84.14	0.026305	80.52	0.023368	41.34	0.00762
10	87.49	0.029695	85.14	0.027236	82.05	0.024537	42.14	0.007816

5.1.3 Effect of Frequency

Different frequencies were used for delignification using different ultrasonic reactors such as longitudinal horn operating at 36 kHz, vertical immersion/ probe type ultrasonic horn operating at 24 kHz and ultrasonic bath operating at 22 kHz. Longitudinal horn had maximum rated power as 150 W and hence in order to compare lignin yields at constant power, experiments were performed at power dissipation of ultrasonic horn (based on the adjustment in the amplitude) and similarly for ultrasonic bath as 150 W. **Figure 5.2**depicts the obtained results for the different ultrasonic reactors in terms of lignin yield at a constant power of 150 W, operating time of 80 min, 0.2M Na_2CO_3 and 1M H_2O_2 concentration with a biomass

loading of 10 wt%. It was observed that as the frequency of ultrasound increases, the lignin extraction increases to 85%. The effect of ultrasonic frequency is mainly on the cavitational intensity which in turn affects the production of hydroxyl radicals that act on ether linkages such as β-aryl, α-aryl, and α-alkyl. On increasing the frequency, cavitational intensity and hence the production of the hydroxyl radicals is favored due to enhanced hydrogen peroxide and water dissociation reactions. These radicals mainly act to depolymerize lignin giving rise to higher lignin separation. The effect of frequency is similar to that reported for extraction of various polyphenols and antioxidants from spinach (altemimeetal., 2015).

5.1.4 Effect of temperature on lignin yield using ultrasonic horn

The effect of temperature was investigated over the range of 323 to 363 K in the case of ultrasonic horn due to easiness of the experiments based on lower operating capacity. **Table 5.5**depicts the obtained results for the effect of temperature on lignin extraction using ultrasonic horn. It can be seen that as the temperature increases the lignin extraction also increases. Increasing temperature favors the deformation of lignin structure at higher kinetic rate thereby favoring the separation of lignin. The maximum lignin yield (84.12%) was observed at 343K with a rate constant of 0.03269 min^{-1}.

Table 5. 5. Effect of temperature on lignin yield and kinetic rate constant.

Temperature (K)	Lignin yield (%)	Rate constant k (h^{-1})	R^2
323	39.16	0.02786	0.98
333	67.78	0.02962	0.97
343	75.87	0.03210	0.99
353	81.64	0.03257	0.98
363	84.12	0.03269	0.98

Activation Energy for lignin extraction was also calculated using the Arrhenius equation 5.11. The linear form of equation can be represented as follows:

$$\ln(k) = \ln(k_0) - \frac{E_a}{RT} \qquad \text{(eq 5.3)}$$

A fitting of ln(k) against 1/T (K^{-1}) revealed the activation energy as 25 kJ/mole based on the calculations of slope ($-E_a/R$). The activation energy for the sawdust used in the work was lower as compared to activation energy for lignin extraction from wheat straw i.e.
29 kJ/mole(huang et al., 2006) confirming the suitability of sawdust for easier lignin removal.

5.1.5 Effect of amplitude and duty cycle on lignin yield using the ultrasonic horn

Amplitude and duty cycle are the crucial parameters for probe type ultrasonic reactors affecting the processing conditions and the net effects. Duty cycle means the time for which the sonication is on. Typically the duty cycle ranges from 10-100 % or can be represented as 0.1 to 1. If the duty cycle is said as 60% (or 0.6), then it implies that sonication is on for 6 seconds and off for the next 4 seconds. Power delivered to the system is affected by the amplitude. Amplitude can be explained as the intensity with which the ultrasonic waves are delivered. For the ultrasonic horn used in the work, the actual range of amplitude is 10-90 %, and in the present work, it was varied from 50 to 80%. Table 5.6 depicts the obtained results for the effect of amplitude and duty cycle on lignin yield for the case of ultrasonic horn. It can be seen from the table that as the duty cycle and amplitude increases, the extent of lignin extraction also increases. Quantitatively speaking, when the duty cycle was increased from 0.1 to 0.5, lignin yield increased from about 77% to 85% with a corresponding increase in the rate constant from 0.0210 min^{-1} to 0.02723 min^{-1}.

Table 5. 6. Effect of amplitude and duty cycle lignin yield and kinetic rate constant in the case of ultrasonic horn.

Ultrasonic horn operating parameters	**Lignin yield (%)**	**Rate Constant k (min^{-1})**	**R^2**
Amplitude (%)			
50	72.24	0.018308	0. 98
60	79.77	0.022829	0. 98
70	82.67	0.025039	0. 99
80	85.11	0.027207	0.99
Duty cycle (%)			
0.1	77.13	0.021076	0.99
0.2	*78.46*	0.021932	0.98
0.3	79.53	0.02266	0.99
0.4	81.32	0.023967	0.98
0.5	85.14	0.027236	0.99

Similarly, an increase in the amplitude from 50 to 80% resulted in an increase in the extraction of lignin from 72.24% to 85.1%. Increase in both duty cycle and amplitude gives a more intense cavitation giving better interaction of biomass with sonication waves and production of higher quantities of oxidizing agents as hydroxyl radicals and hydronium ions which are capable of removing the lignin to a higher extent. The study presented here allows

establishing the best conditions for amplitude and duty cycle that can give better efficacy as well as better durability for the equipment.

5.1.6 Comparing different ultrasonic reactors

The results for comparison of the different ultrasonic reactors are also represented in **Figure 5.1 a to c**. It can be seen from the figures that longitudinal horn typically gives higher lignin yield as compared to all the other approaches. Quantitatively, higher lignin yield as 87.4% was observed in the longitudinal horn when operated at input power of 150 W, as compared to ultrasonic horn (lignin yield of 85.1 %) and ultrasonic bath (lignin yield of 82 %) and same power dissipation. In the case of longitudinal horn, the cavitation spreads over the entire region of the equipment, with the aid of large transducer that is connected horizontally to one end, giving maximum intensification**.** Two stirrers rotating at equal speed of 1000 rpm were also arranged at two ends inside the vessel. These stirrers are required considering the volume being treated in this reactor.

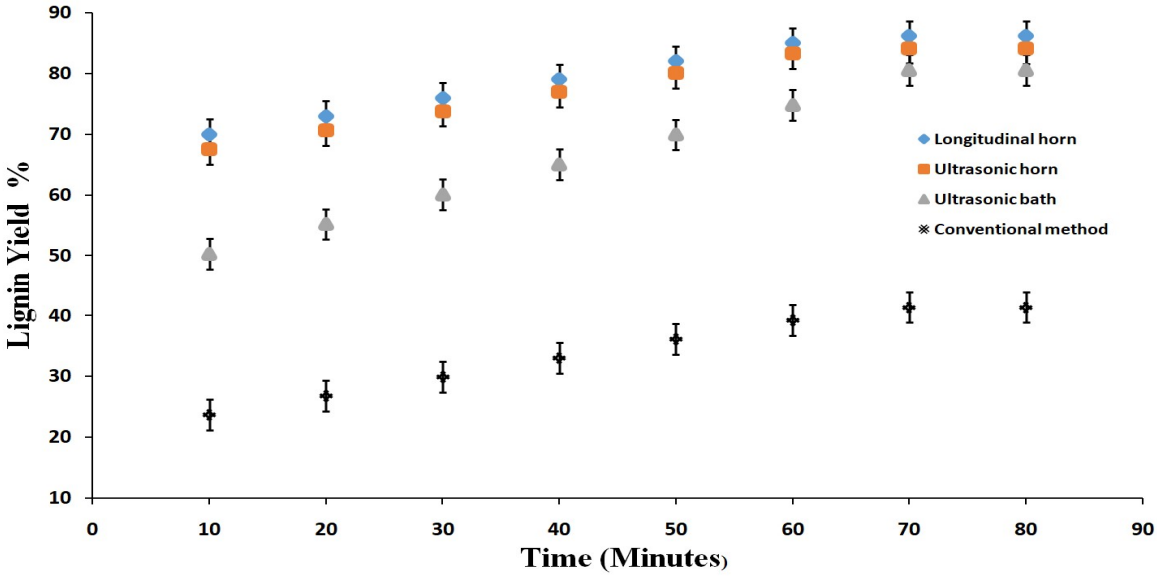

Figure 5. 2.Effect of different ultrasonic reactors on lignin yield under conditions of constant Na_2CO_3 loading as 0.2M, H_2O_2 loading of 1M and biomass loading of 8wt%.

Stirrers help in generating bulk liquid flow and continuous renewal of substrate at the cavitational zone finally contributing to the higher efficacy for lignin yield. In the case of ultrasonic horn, stirring was not required due to the lower volumes of operation and the geometry of the vessel was selected such that there are no formation of vortices inside the vessel having smaller diameter and longer length.

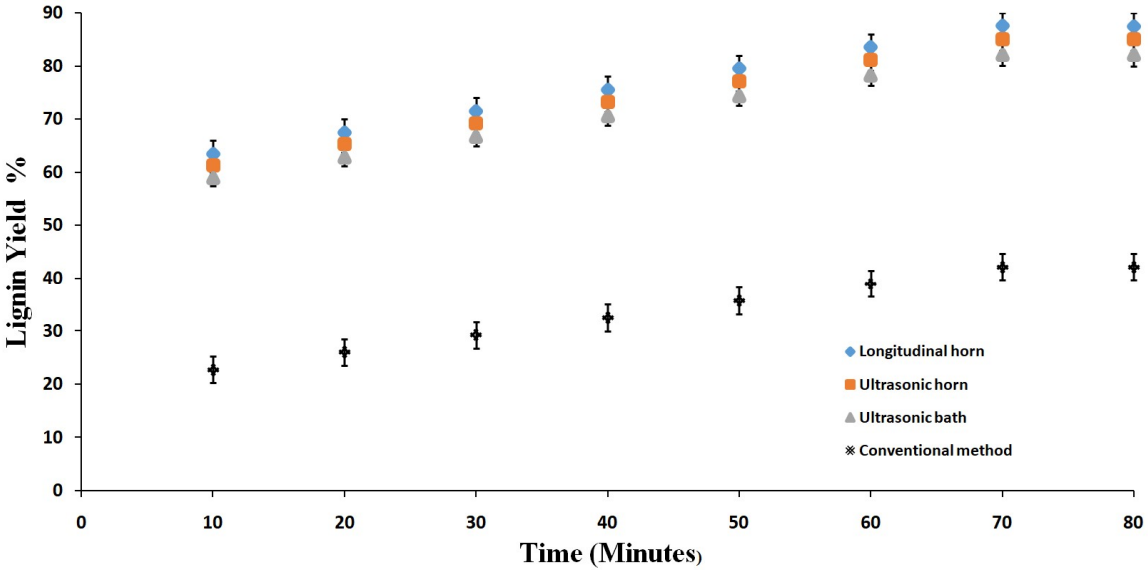

Figure 5. 3. Effect of different ultrasonic reactors on lignin yield under conditions of 0.2M Na_2CO_3, 1M H_2O_2 and biomass loading of 10 wt%.

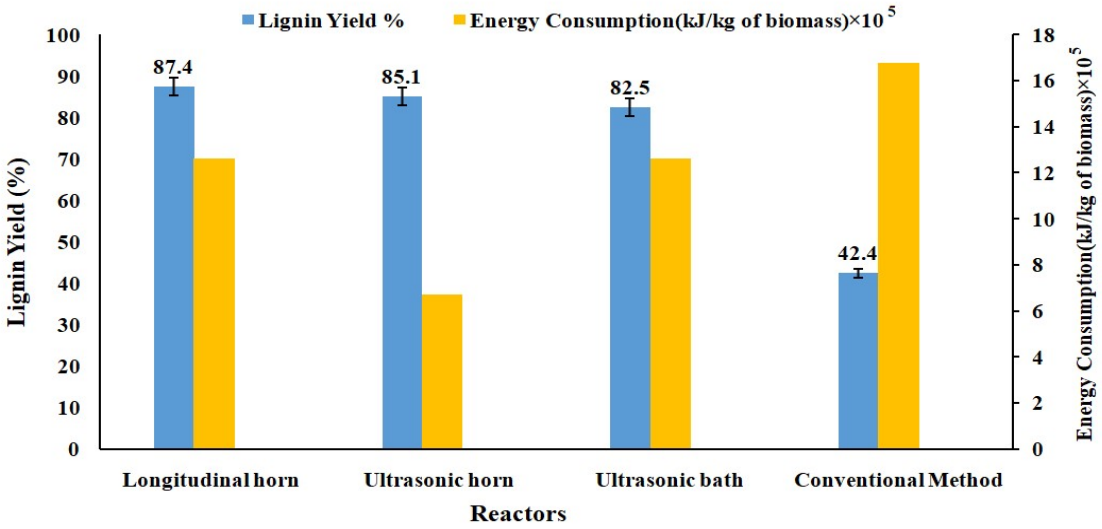

Figure 5. 4. Comparison of Lignin yield with different ultrasonic reactors under conditions of constant treatment time of 60 min, 0.2M Na_2CO_3 loading, 1M H_2O_2 loading and power of 150 Watts.

In the case of large reactor volumes, for good efficacy of sonication, additional mechanical stirring is recommended as the flow generated due to ultrasound is limited (dominant turbulence and local micro mixing is generated).It was also observed from the work that the direct contact type configurations as longitudinal horn and ultrasonic horn (vertical immersion) gives higher cavitational activity as compared to the ultrasonic bath with indirect contact that result in lower extents of lignin.

The data in (Figure 5.1 a, b, c) also establishes that all the ultrasonic reactors resulted in higher lignin removal as compared to the conventional approach (without ultrasound and only stirring).In the case of ultrasonic irradiations, the biomass is subjected to the mechano-acoustic (physical) and sonochemical effects (chemical) driving the depolymerization, and condensation reactions to a higher extent also giving the improved yield of lignin by cleavage of lignin-carbohydrate linkages of biomass.

5.1.7 Characterizations

A. FTIR Analysis

Pretreated and dried saw dust was mixed with spectroscopic grade potassium bromide (KBr) powder in 1:3 ratio and pelletized in thin 1mm circular disk dimensions. The pellet was kept in a pellet slot for FTIR analysis under mid-range from 4000 to 400 cm^{-1}. The obtained results were in terms of graph between wavelength and absorption as depicted in **Figure 5.3** for the lignin obtained from longitudinal horn, ultrasonic bath and ultrasonic horn.

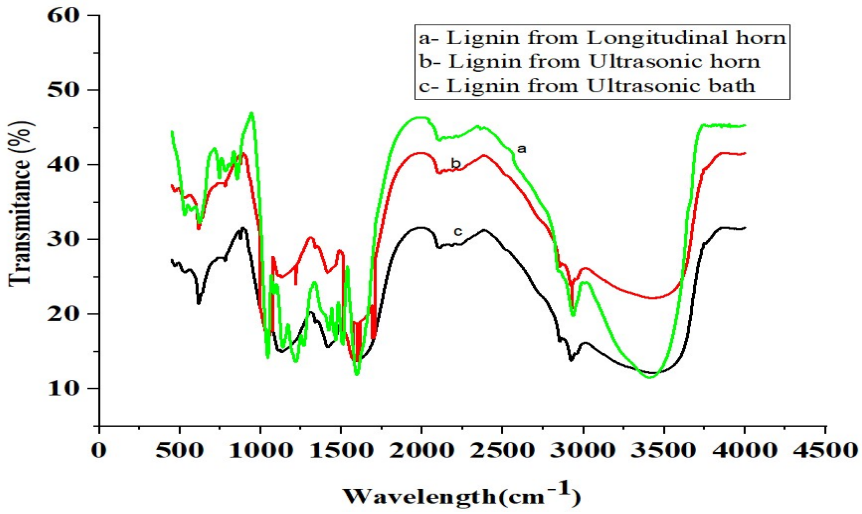

Figure 5. 5.FTIR spectra of lignin extracted using ultrasonic horn, longitudinal horn and ultrasonic bath

The variation in the intensity of each peak corresponds to the presence or absence of a chemical structure of a component. The observed peaks at 1745 and 1606 cm^{-1}were assigned to carbonyl (C=O) stretching in the side chain and aromatic ring stretching respectively, which are characteristic of lignin [29].

It can be also seen from the figure the dominant peak was obtained at 1599 cm^{-1}confirming the presence of lignin as this is attributed to the C=C stretching of aromatic ring in lignin. Similarly the observed peaks at 1219cm^{-1} relates to C-C, C-O, and C=O stretching

of guaiacyl unit. The presence of peaks from 1123-1110cm^{-1}, indicates aromatic C-H deformation of the syringyl unit, and peak at 874.68 cm^{-1}is assigned to C-H bending of syringyl units and aromatic ring in lignin (adapa et al., 20011).The intensities of lignin peaks were observed to be different for different acoustic cavitational reactors. Maximum lignin peak intensities were obtained for longitudinal horn which implies maximum amount of functional groups present indirectly corresponding to maximum lignin content. These lignin peak intensities were lower for lignin extracted from ultrasonic horn and bath as compared to longitudinal horn which indicates presence of lesser amount of lignin in the case of other two types of reactors.

B Morphological Analysis

The scanning electron microscopy analysis gives information about the morphological changes of any material. In particular to the biomaterials, SEM and XRD offer as important techniques to establish the variation in the structural changes of treated biomass as compared to the untreated biomass. **Figure 5.4** depicts the micrographs obtained for untreated sawdust, treated sawdust with conventional approach and using ultrasonic horn, longitudinal horn, and ultrasonic bath.

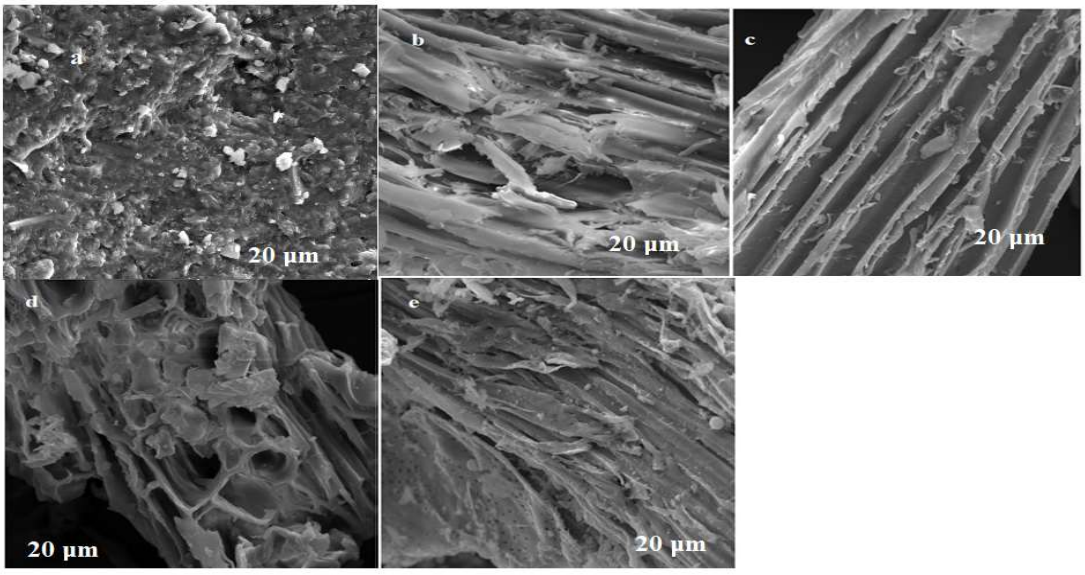

Figure 5. 6 SEM images of (a) untreated sawdust and treated sawdust using (b) conventional method (c) ultrasonic horn (d) longitudinal horn (e) ultrasonic bath

The existence of pores and appearance of cellulose micro-fibrils on treated sawdust confirmed structural changes in outer layer of the biomass which in turn reflects to lignin removal (Dhabhai et al., 2013).The presence of groves in the treated sawdust using the probe

type and presence of voids in the treated sawdust using the longitudinal horn type also confirms the lignin removal to a higher extent. For the ultrasonic bath, treated sawdust shows clear micro fibrils only at some places indicating that the effect of bath is only seen at some places whereas the other regions didn't show much sign of effective lignin removal. The observations confirmed that ultrasonic bath offers limited efficacy compared to ultrasonic horn or the longitudinal horn.

C. X-Ray Diffraction analysis of biomass after ultrasound treatment

X-Ray Diffraction analysis can be used for calculating the crystalline index (CrI) of a material, which is defined as the percentage of crystalline content in the material. The crystallinity index is one of the important parameters especially in pretreatment of lignocellulosic biomass as it reveals the degree of recalcitrant nature of treated biomass. **Figure 5.5** represents obtained results for the crystallinity index of pretreated sawdust with different ultrasonic reactors. .

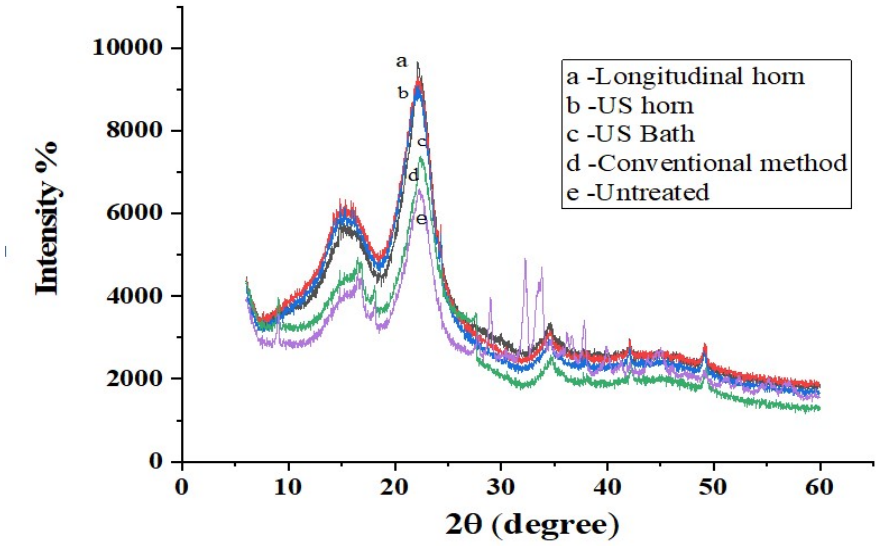

Figure 5. 7 XRD results for sawdust treated with (a) longitudinal horn (b) ultrasonic horn (c) ultrasonic bath (d) conventional method and (e) untreated sawdust

The important distinguishing features are the peak intensities observed at 2θ angles of 23° and 19°.The amorphous region is typically observed at 19°and at 23° both amorphous and crystalline regions exist. As the recalcitrant nature of biomass decreases, crystallinity should increase (Mawhood et al., 2016). The crystallinity index was calculated using the peak intensity at specific (2θ) angle based on the following equation 5.4.

$$CrI\ (\%) = \frac{(I_{002} - I_{am})}{I_{002}} * 100 \qquad (eq\ 5.4)$$

where I_{002} is the maximum intensity of 002 peaks at $2\theta = 23^{o}$ and I_{am} is the intensity at $2\theta = 19^{o}$. The presented results in **Table 5.7**confirmed an increase in the crystallinity based on the treatment with 20.7%, 14.5 %, 10.8 % and 6.6 % as the increase for longitudinal horn, ultrasonic horn, ultrasonic bath and conventional approach respectively. The observed increase can be attributed to the fact that lignin which is considered as an amorphous component having linkages between cellulose and hemicelluloses is removed during the treatment. Highest increase in the case of longitudinal reactor confirms better efficacy of the cavitational effects in this type of configuration.

Table 5. 7. Crystallinity index for processed material using different treatment approaches

Treatment approaches	Crystallinity index
Longitudinal horn	56.6
Ultrasonic horn	53.7
Ultrasonic bath	52
Conventional method	50
Untreated saw dust	46.89

D. Gel permeation chromatography analysis

Gel permeation chromatography (GPC) is basically size exclusion chromatography (SEC) that separates analytes on the basis of size. The technique is often used for the analysis of polymers. The molecular weight of different types of lignin varies according to the type of extraction conditions and due to the presence of mono lignin units after extraction. The molecular weight-average M_w, molecular-number average M_n and Polydispersity $[M_w/M_n]$ of the extracted lignin obtained using ultrasound assisted approach under best treatment conditions were observed to be 2907 Da, 2779 Da and 1.04 respectively. The observed results are attributed to the fact that alkali combined with peroxide and ultrasound not only cleaves the bonds of carbohydrate-lignin linkages but also separates lignin to a maximum extent.

The presence of guaiacyl units in lignin has a higher molecular weight as compared to the syringyl units (Hua et al., 2016). From the results presented in **Figure 5.6,** it was clearly demonstrated that extracted lignin using ultrasound shows peaks between 1123-1110, and 874.68-817 which indicates the presence of syringyl units and C–H out-of-plane vibrations in position 2, 5 and 6 of guaiacyl units. Generally the presence of these S,G-units more occurs in secondary wall of sawdust, and less in middle lamella lignin. The observation confirms the breakage of secondary wall based on the cavitational intensity.

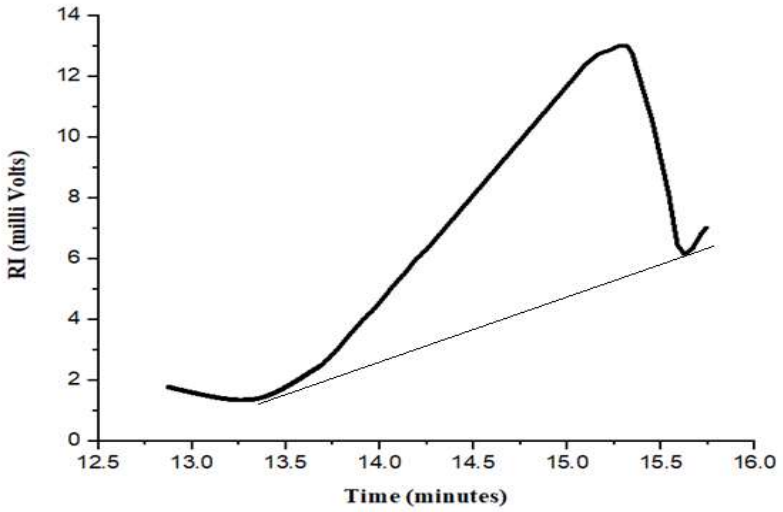

Figure 5. 8. Molecular distribution of extracted lignin.

E. Thermogravimetric analysis of biomass

TGA analysis measures the weight change as a function of increasing temperature in an atmosphere of nitrogen as an inert environment. The thermal behavior of the treated and untreated sawdust was analyzed using TGA analysis performed at the ramp rate of 5˚C/ min. The results for the TGA analysis are shown in **Figure 5.7** for the untreated and ultrasound assisted alkali peroxide treated sawdust. It was observed that the weight loss occurred in three stages. In the first stage from 50 to 210 °C, there is no significant loss of weight and the stage is mainly considered a drying period for the removal of moisture. Subsequently, at 200°C, degradation of hemicellulose starts. In the second stage of 200 to 350°C, devolatilization starts, and decomposition of hemicelluloses occurs at a very fast rate, and degradation of cellulose and some part of lignin also occurs at a faster rate compared to other stages. The TGA graphs showed a steep slope in this range, indicating a drastic loss of weight with an increase in temperature, affected by the significant thermo chemical changes, devoltalization. At this stage, it was observed that there is a 50-53% weight loss for the untreated sawdust and about 63-65% weight loss for the sample of ultrasound-assisted pretreated sawdust. The observed trends can be attributed to the fact that 80% of biomass is formed from volatile matter, and the remaining consists of solid carbonaceous material (altimimi et al., 2015). Finally, in the third stage, from 310 to 500°C, about 20% weight loss was obtained for the untreated sawdust and 9wt% weight loss for the ultrasound-assisted alkali treated sawdust which can be attributed to the stability of the ultrasound treated sawdust as compared to

untreated sawdust. Beyond 600°C, there was no noticeable weight loss both in untreated and ultrasound–alkali treated sawdust.

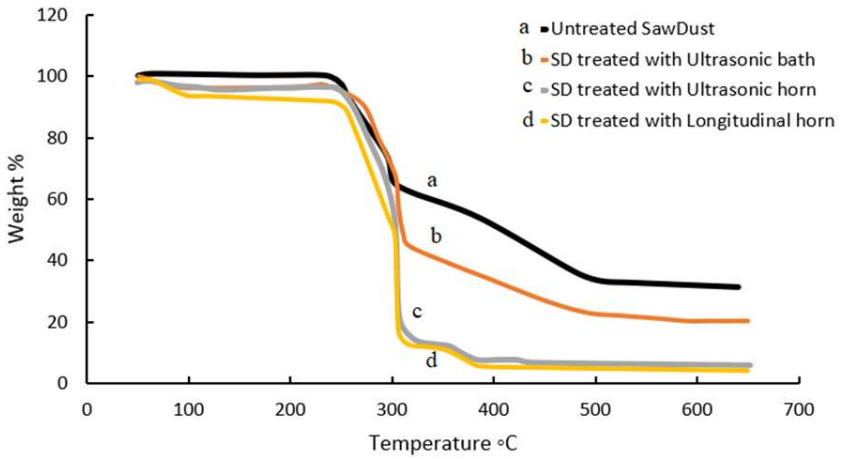

Figure 5. 9. TGA graphs of untreated sawdust (a) and treated sawdust using various ultrasonic reactors (b) ultrasonic bath (c) ultrasonic horn (d) longitudinal horn.

Composition

The Composition analysis of untreated and treated sawdust was performed according to NREL method as mention in the materials and method section. Table 5.8 tells about the composition analysis of untreated sawdust and treated sawdust using different configured ultrasonic reactors under optimized conditions (0.2M Na_2CO_3, 1M H_2O_2, 10 wt% biomass loading, 70 minutes treatment time). The decrease in the lignin content in the treated sawdust implies removal of lignin content during the pretreatment. The Glucan and manna polymers represent cellulose composition, and xylan and Arabinan represent hemicellulose composition. The extractives and others (may include ashes) are reported.

Table 5.8: Composition analysis of untreated and treated sawdust

Component	Untreated Sawdust (w/w %)	Longitudinal Horn (w/w %)	Ultrasonic horn (w/w %)	Ultrasonic bath (w/w %)	Conventional Method (w/w %)
Glucan	35.7	29.9	29.2	27.8	13.5
Xylan	22.5	19.6	18.3	14.2	11.4
Arabinan	3.3	3.1	3.0	2.5	2
Mannan	2.8	2.3	2.1	1.7	1.2
Klason lignin	18.3	7.32	15	15.5	15.9
Acid soluble lignin	3.41	0.68	0.72	0.9	1.21
Extractives & Others	13.3	ND	ND	ND	ND
	ND – Not Determined				

5.1.8 Energy requirement for different ultrasonic reactors

Lignin removal was performed using different ultrasonic equipment configurations such as longitudinal horn, vertical horn, and an ultrasonic bath. The obtained lignin yields have been compared in **Table 5.8** also showing the comparison with the conventional approach. It is clearly observed that there is a 2-3 fold increase in lignin extraction using sonication when compared with the conventional approach, which can be attributed to the cavitational effects.

The energy requirement for the delignification was calculated for all the ultrasonic reactors using the following equation(Pinjari and Pandit 2010):

$$E_{(dissipated)} = P \times I_t \times \eta \times A \qquad (eq\ 5.5)$$

Where $E_{(dissipated)}$is actual energy dissipated, P is actual power of horn(W), I_t is irradiation time of the ultrasonic horn(s)and η is efficiency of the equipment, A is amplitude.

Specific energy in this contest can be defined as the energy required for delignification of biomass per unit mass of biomass(Thesis 2012)

$$S.E = E_{(dissipated)} / B \times V. \qquad (eq\ 5.6)$$

S.E is the Specific Energy (kJ/kg), B is Biomass concentration (kg/L) and Volume, (L).

Energy density which is the actual amount of energy dissipated per unit volume was determined as per the following equation (Thesis 2012).

$$E_{(density)} = E_{(dissipated)} / V. \qquad (eq\ 5.7)$$

Where $E_{(density)}$is Ultrasonic Energy density (kJ) and V is volume (L).

The energy required for stirring can be found from (Pinjari and Pandit 2010):

$$E_{(Stirring)} = P \times T \times N \qquad (eq\ 5.8)$$

Where $E_{(Stirring)}$is energy for stirring, P is power required for stirring (W), T is operating time (s) and N is number of stirrers.

The energy requirement analysis for stirring and ultrasonic irradiation established that minimum power consumption is required for operation of ultrasonic horn when compared with longitudinal horn and ultrasonic bath. Energy densities for different ultrasonic devices were calculated for the specific volume of operation in ultrasonic horn (6.72×10^6 kJ/m^3) which is less when compared to longitudinal horn (12.6×10^6 kJ/m^3) and ultrasonic bath (12.6×10^6 kJ/m^3). The energy required for longitudinal horn stirring is more as it requires two stirrers on extreme ends of the reactor for better mixing, which is also the case in ultrasonic

bath. The problem was compensated in the ultrasonic horn, by using a small diameter vessel which has provision for one stirrer.

Table 5. 8. Comparison of different ultrasonic reactors in terms of energy requirements, lignin yield and overall efficacy.

Treatment approaches	Specific Energy consumption (kJ/kg of biomass)	Energy density (kJ/ m^3)	Energy required for stirring (J/s)	Lignin yield (%)	Remarks
Longitudinal horn (150 Watts, 36 kHz)	12.6×10^7	12.6×10^6	8.64×10^5	87.4	Decrease in recalcitrant nature of the material and increase in crystallinity because of sonochemical effects and continuous stirring
Ultrasonic horn (150 Watts, 24 kHz)	6.72×10^7	6.72×10^6	4.32×10^5	85.1	Operates better for lower volume processing up to 2-3 L, and sonication is efficient for vessels of smaller diameter to length ratios
Ultrasonic bath (150 Watts, 22 kHz)	12.6×10^7	12.6×10^6	4.32×10^5	82	Cavitation occurs unevenly, with low intensity as compared to horn-type sonication
Conventional method	16.74×10^7	NA	17.28×10^5	42	High energy is needed as compared to sonication. 4-8 h processing is required for better lignin yield, which is much higher than ultrasound.

It is important to note that though the energy consumption is higher the effects obtained in longitudinal horn were better as confirmed by the lignin yields. It was thought desirable to compare in terms of the specific energy requirements for lignin removal. The results shown in Table 8 confirm that the specific energy for the case of longitudinal horn was similar to ultrasonic bath but lower as compared to the conventional approach. Thus the efficacy of longitudinal horn is clearly established as it is able to process much larger volume with higher yields though at marginally higher energy consumption compared to the vertical immersion type horn.

Summary:

The proposed work clearly established that lignin extraction from sawdust using different ultrasonic reactors was more effective as compared to the conventional approach with about 2 – 3 times more lignin yields. The lignin yields established for different acoustic devices were in the order of longitudinal horn (87.4%), immersion type vertical ultrasonic horn (85.1%), and the ultrasonic bath (82%). FTIR analysis showed that the absorbance peaks

are obtained at 1595 and 1700 cm^{-1} revealing the existence of lignin. It was also observed that maximum peak intensity is observed for the sample processed using a longitudinal ultrasonic horn. Crystallinity index of treated sawdust was maximum in the case of longitudinal horn (56.6%) followed by ultrasonic horn (53.7%) and ultrasonic bath (52%). SEM images of ultrasound-assisted treated biomass, confirmed lower size as compared to the conventional method, which can be attributed to the strong cavitation effects. Energy consumption was observed to be less for ultrasonic horn compared to longitudinal horn and ultrasonic bath and was the maximum for the conventional method. The energy requirement for the longitudinal horn was higher, as it required more energy for stirring as compared to ultrasonic horn, though this is justified on the basis of much larger volumes being handled. The work has clearly established an effective lignin extraction approach based on the combination of sodium carbonate and hydrogen peroxide intensified using the ultrasonic reactors.

5.2 Performance Evaluation of Lignin nanocapsules based epoxy Coatings

In spite of the presence of several types of corrosion inhibitors, such as synthetic chemicals, crude oils, synthetic polymers and hydrogel. We opted for lignin because it is a sustainable natural biopolymer which contains more phenolic compounds. For experiments teak sawdust was chosen to extract lignin which is obtained from nearby local mills at Warangal. Lignin extraction is done with an ultrasonic horn which is a sonochemical approach. Since extracted lignin is obtained when sawdust is treated with alkali peroxide (0.2 M Na_2Co_3 and 1 M H_2O_2), the lignin that is precipitated is acid insoluble lignin (ASL). ASL is a polar component (soluble in water) which is a good characteristic for corrosion inhibitor.

Generally, a natural polymer can act as a corrosion inhibitor with self-healing characteristics (G. and F. 2014). However, lignin also acts as a stabilizer to get the required particle size that is acceptable to hold a critical concentration of the healing agent. Initially, lignin is just used as a filler in the curing material (epoxy resin). Another interesting characteristic of lignin is its self-healing capabilities, as it has methoxyl and hydroxyl and phenyl groups which are responsible for generating a passive layer on the mild steel for self-repairing and corrosion inhibition (Frankel 2016). It has good antioxidant properties with the presence of phenol and hydroxyl groups. Phenol groups decrease or chelate with the divalent metal ions that are responsible for further accelerating corrosion reactions. A thin passive

layer formation takes place while chelation of lignin occurs with metal ions. This sign of self-repairing characteristics was observed by the generation of a passive layer on a metal surface with lignin can be termed as self-healing for corrosion resistance.

Natural oils consisting of more unsaturated fatty acids act as antioxidant. Safflower oil consists of highly unsaturated fatty acids of linolenic acid, which is responsible for better antioxidants. A way for self-healing was proposed with natural oil containing long chain of unsaturated fatty acids, which can form a polymerized film on reaction with oxygen in the presence of dryer near the cracked area on a steel (Nesterova et al. 2012). Safflower oil along with a small amount of dry cobalt helps in drying the oil once the oil is exposed to the environment (by oxidation) due to the rupture of nanocapsules.

Sonochemical approach was adopted for mixing processes instead of using conventional isotropic machines. Sonication helps in producing controlled sized nanoparticles. It also reduces the time for mixing by manipulating the time and power required for sonication along with the lignin loading and liquid to oil ratios to achieve the required size. The extracted lignin nano particles are shown in TEM image having an average particle size of 106 nm.

Nanocapsules can be synthesized using three steps(Frankel 2016; Wypych 2017).

1) Emulsification step, 2) Urea Formaldehyde UF Wall formation and 3) Wall solidification. Emulsification step generates O/W Pickering emulsion, since alkali lignin is insoluble in water and can be easily adsorbed on the oil surface.

In hybrid layered nanocapsules preparation, the second step is UF wall formation. This can be achieved by sonication of UF resin with PVA surfactant. UF is a thermoset polymer, used as an additive in paints and boards. Drop wise addition of lignin safflower oil emulsion into the UF surfactant solution was done under sonication. The rate of addition of lignin decides the size of the nanocapsules. As the sonication time reached10-15 minutes a thin layer was observed covering the lignin and oil emulsion droplets. This layer is Urea Formaldehyde wall formation step, occurred due to cross-linking of water molecules with urea-formaldehyde.

As sonication progresses the formation of thick layer appears by deposition of more UF on the capsule till there is saturation of covalent bond between water and UF. Lignin was perfectly encapsulated for lower loadings (i.e. for 0.5,1 and 1.5 wt %) it can be confirmed from the observations as there is no change in color. A graphical abstract showing procedure for encapsulation of lignin and development of patina formation on damaged coatings of mild steel is shown in the figure 5.10.

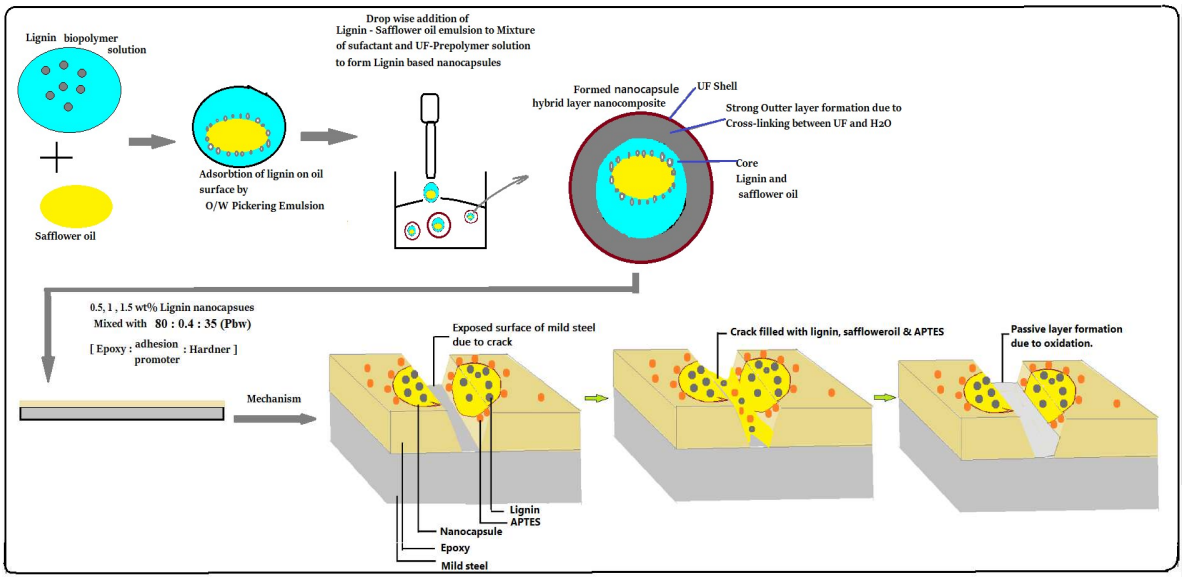

Figure 5. 10. Graphical abstract showing patina formation on damaged coatings of mild steel.

There exits some literatures where lignin of different ppm mixed in electrolyte solution itself to check the corrosion inhibition of lignin on mild steel (Akbarzadeh et al. 2011). But themotto of the present work is to develop a sustainable, eco-friendly, cheap corrosion inhibitor system with better performance with lower concentrations of corrosion inhibitor. The synergistic effect of safflower oil and lignin was checked to know the inhibition performance of the corrosion for lower concentrations of corrosion inhibitor.

Final step is to functionalize lignin nanocapsules by addition of 3-Aminopropyl tri-ethoxy silane coupling agent is meant to bind the nanocapsules to epoxy resin. The role of a coupling agent is to form a functionalized surface which is capable of forming a bond with a steel surface that is chemically inert, anti-fouling, scratch resistant, and to create super hydrophobic surface when it is coated along with epoxy.

Here lignin safflower oil and APTES will act as a coupling agents, lignin will chelate with metal by sharing its lone pair of electrons. Safflower oil has shown good anti oxidant properties with its long chain unsaturated fatty acids. Tri Ethanol Amine will also contribute in decelerating the corrosion performance during alkalization of UF prepolymer. APTES will bind the lignin nano capsule with the epoxy. We have observed synergetic effect of all these gives better corrosion resistance performance when coated along with the water borne epoxy resin.

5.2.1 Characterization

A. Fourier Transform Infrared Radiation spectroscopy of Nanocapsules

Figure 5.11 gives the FTIR spectra of lignin-safflower oil-based nanocapsules, lignin extracted, and safflower oil. The peaks at 1707-1691 and 1591 cm^{-1} represent unconjugated carbonyl stretching of aldehyde/ketone group, which represents all the three monomers of lignin. Peaks at 1123-1110 cm^{-1} represent aromatic C-H deformation of syringe unit. FTIR analysis of lignin that is extracted from the sawdust has similar peaks with the pure lignin peaks at 1222, 1603, 1652 cm^{-1}. The broad absorption peak of OH is obtained at 3538–3310 cm^{-1} are similar for lignin and nanocapsules (Akbarzadeh et al. 2011, 2012).The IR spectra of the polymeric urea-formaldehyde shell materials (UF Shell), peaks at1747, 1652.75 cm^{-1} represent C=O stretching vibration are observed and matched with the reported characteristics peaks for UF resin by suryanarayana (Suryanarayana et al. 2008).

The stretching vibration peaks at 1631-1652, and 1463 cm^{-1} are attributed to the C = Stretching, and C–H bonding, respectively in UF spectra. Also the carbonyl stretching observed at an absorption band of 1720 cm^{-1}(Suryanarayana et al. 2008). Similar peaks are also observed in lignin nanocapsules but with slight change in peak position confirming the presence of urea-formaldehyde as shown in Figure 5.11.

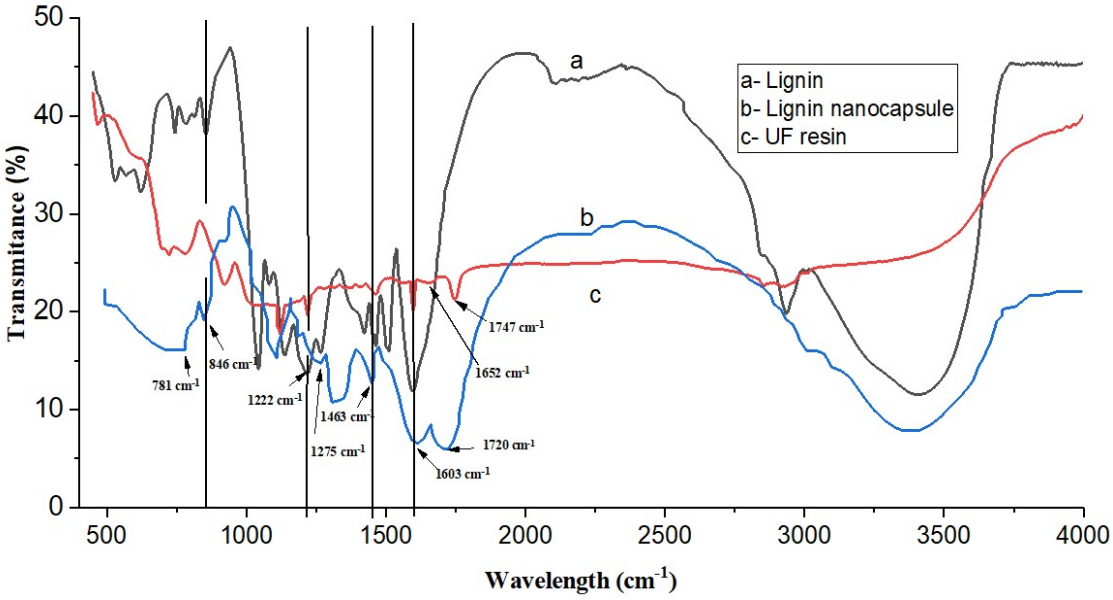

Figure 5. 11. FTIR graphs of a: lignin b: lignin nanocapsules and c: urea-formaldehyde resin.

Safflower oil has prominent peaks at 1465 cm^{-1} corresponds to CH_2 bending for edible oil and peaks from 1440-1470 cm^{-1}used to determine the total unsaturated fatty acid (Wypych 2017). 1275 cm^{-1} belongs to $SiCH_3$ group, and 781 cm^{-1} for CH_2 rocking. These kinds of peaks are observed in nanocapsules at 1465, 1279, 781 cm^{-1} which implies the presence of safflower oil in nanocapsules. Peaks of UF shell, lignin and safflower oil in the lignin nanocapsules spectra confirm the clear encapsulation of lignin and safflower oil in UF shell.

B. Determination of Total phenolic Content

The phenolic compound in lignin indirectly corresponds to the anti oxidant properties. Generally phenolic contents are resistant to chemicals, alkali, and shows good corrosion resistance properties. This procedure is same as mentioned by Mounguengui 2016, Faustino 2010(Faustino et al. 2010; Mounguengui et al. 2016).

Absorbance of the sample was measured at 765 nm against blank, i.e., distilled water. Similar procedure was adopted to prepare test sample of lignin extract, and absorbance of the sample was measured at 765 nm using UV/VIS spectrophotometer nm against blank, i.e., distilled water. Quantification was done on the basis of a standard curve of gallic acid. A standard curve of extinction against gallic acid concentration was prepared. A 0.5 g of lignin extract was and it was diluted for 9 times in distilled water, a final volume of 5 ml of sample is used to measure absorbance at 765nm to calculate total phenolic content.

The total phenolic content were expressed as percentage w/w and calculated using following formula,

$$\textit{Total phenolic content (\% w/w)} = GAE \times V \times D \times 10^{-6} \times 100/W, \qquad \textit{(eq 5.9)}$$

GAE - Gallic acid equivalent (µg/ml), V - Total volume of sample (ml), D - Dilution factor, W - Sample weight (g).

GAE (µg/ml) = 936 (µg/ml) ; Total phenolic content (w/w %) = 86 (w/w %).

C Field Emission Scanning Electron Microscopy (FE-SEM)

Figure 5.12 show FE-SEM images and its corresponding histogram of particle size distribution for lignin nano capsules. Imaging was done at a scale of 500 nm. The morphological structure of lignin nano capsules shows the rough surface around the each encapsulated nano particle corresponds to the urea formaldehyde shell. The average size of lignin nano capsules is having 146 nm.

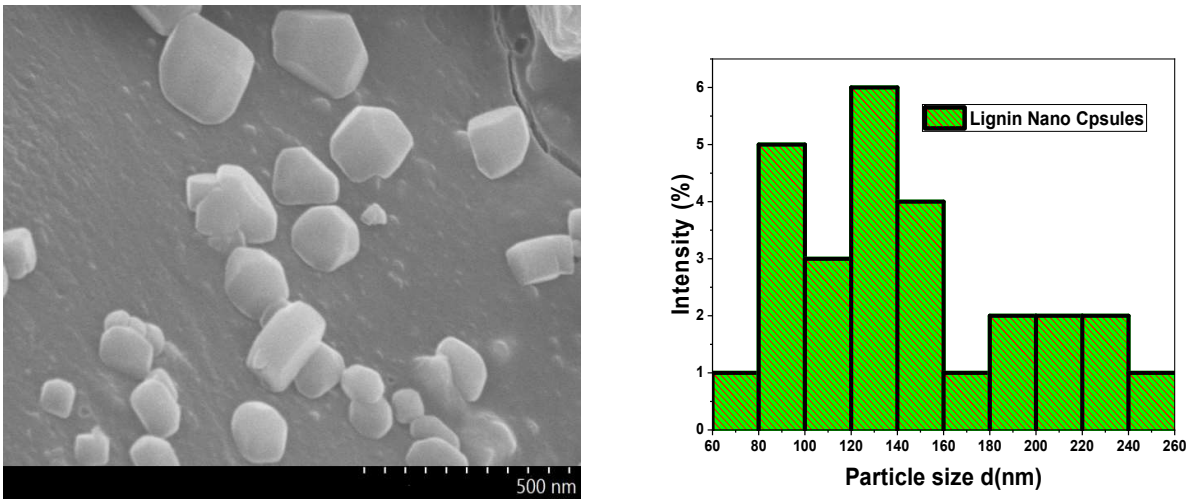

Figure 5. 12. FE-SEM images (scale500nm) and particle size distribution of Lignin nano capsules.

D Transmission Electron Microscopy (TEM)

The TEM Images as shown figure 5.13 represents the structure of the lignin nano particles. The histogram shows the average size of nano particles are given adjacent to TEM image with a average 106 nm.

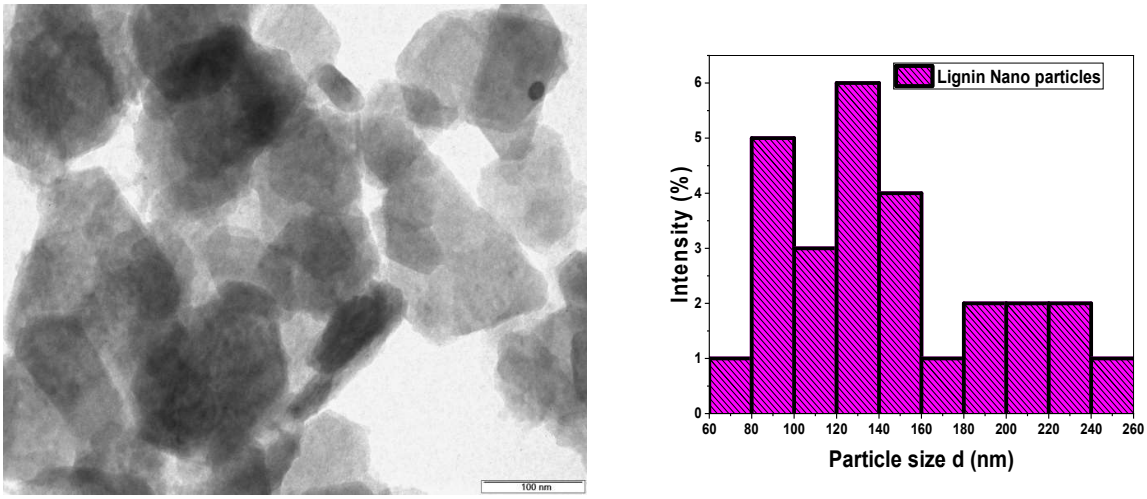

Figure 5. 13. TEM image (scale 100 nm) particle size distribution of Lignin based nanoparticles.

5.2.2 Corrosion Inhibition Studies

(I) Polarization Studies by Tafel plot

From **Figure 5.14**, the Tafel plot shows the change of current density with the potential for different concentrations of lignin in an epoxy coating. From the Tafel plot it can be seen that the corrosion current density on mild steel decreased with the increase in the lignin loading. In the physical sense the flow of electrons into the metal was decreased (may be due to the formed oxide layer is strong enough to slow down the flow of electrons). The corrosion current I_{corr} values for bare 1.0423E-5 A/cm^2, and this was decreased to 1.662E-6 A/cm^2 for standard, and its value further decreased to 2.409E-8, 3.139E-7, and3.703E-8 A/cm^2 for 0.5, 1 and 1.5 wt% LNC respectively.

These I_{corr} values are in similar trend with reported literature values. That is for 1.5 wt% lignin loadings I_{corr} value that decreases to 2 fold with respect to the standard epoxy which is better value as reported by rahman et al (Rahman et al. 2018) (I_{corr} for epoxy 1.90E-06 A/cm^2, and epoxy with 1 wt% [ethylene Glycol] lignin loadings 4.16E-08 A/cm^2). Similar trend was observed for (Kasaeian et al. 2018), a 4 fold decrease in I_{corr} value is observed when graphene oxide (GO) nano sheets were non-covalently functionalized with 1H-Benzimidazole (corrosion inhibitor) was used to modify epoxy to develop corrosion resistant coating for mild steel in 3.5 wt% chloride solution after 24 hours of immersion (water borne epoxy based I_{corr} value 8.75 µA/cm^2, at Ph 1 , and for modified epoxy I_{corr} value 4.59 µA/cm^2). (Hussin et al. 2015b) has used 500 ppm of different lignin (Soda, Kraft, Ethanol) in 0.5M Hcl solution for corrosion resistance of mild steel, and has shown I_{corr} value for Standard >kraft lignin >ethanol lignin >soda lignin.

However, it has also been observed that, as the lignin loading increases, the corrosion potential E_{corr} also moved from negative values towards positive potential values. This confirmed that there is an increase in corrosion potential as lignin loading percentage increases in the coating of mild steel. This values of E_{corr} for bare mild steel, standard epoxy coating, 0.5, 1, 1.5% of nanocapsules coating, are -0.59, -0.47, -0.488, -0.319, -0.292 V, respectively. This shift in the potential value is attributed to the fact that lignin forms a protective layer on the surface of mild steel which acts as a corrosion-resistant layer. This trend is similar to previously reported one (Sonawane et al. 2008; Adsul et al. 2018; Bagale et al. 2018b).

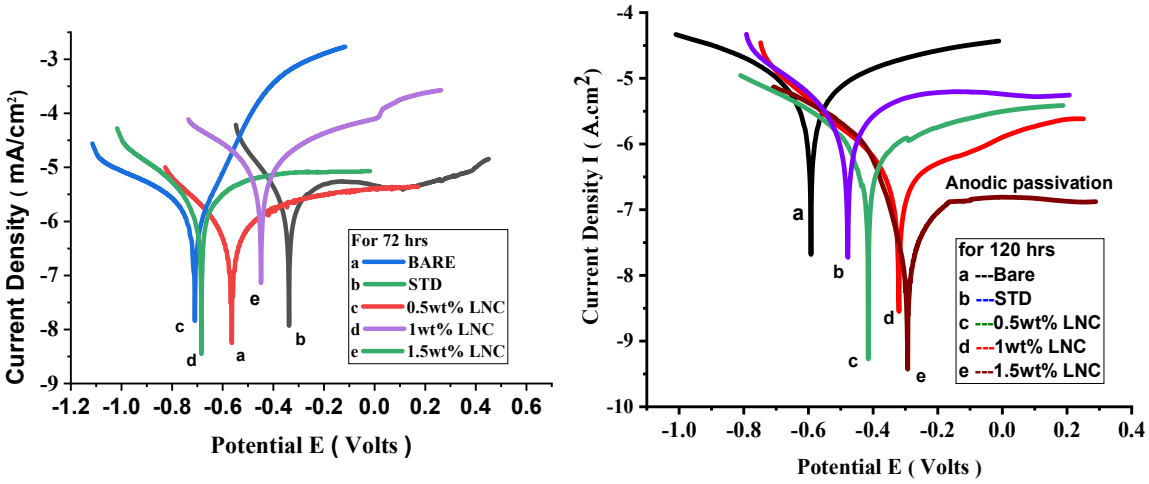

Figure 5. 14. Tafel plot for mild steel strips coated with different percentage of lignin nanocapsules (LNC) after A) 72 B) 120 hrs immersion in 3.5 wt% nacl Solution (a: Bare metal; b: Standard epoxy coating; c: 0.5% of LNC; d: 1% of LNC (lignin nanocapsules) in the epoxy coating.

(II) Impedance Studies

Electrochemical impedance spectroscopic (EIS) measurements were performed at room temperature of 25˚C to investigate the behavior of coating containing lignin-safflower oil as a healing agent for corrosion inhibitor. Bare mild steel, standard epoxy, and nanocapsules (with different lignin loadings i.e 0.5, 1, 1.5 wt%) coated mild steel panels were immersed in 3.5 wt% Nacl solution for about five days to measure EIS data over a frequency range of 1MHz to 0.01 Hz with a AC sinusoidal voltage signal 10 mV applied to the system.

BODE PLOT:

Bode plots for water-borne epoxy coating with different weight percentages of lignin in nanocapsules are given in **figure 5.15** from the graph that, as the weight percent of lignin in nanocapsules increases, the impedance |z| value also increased when compared to standard epoxy coating. It can see that from epoxy coating without lignin shows less impendence value and gets corroded easily with increase in frequency.

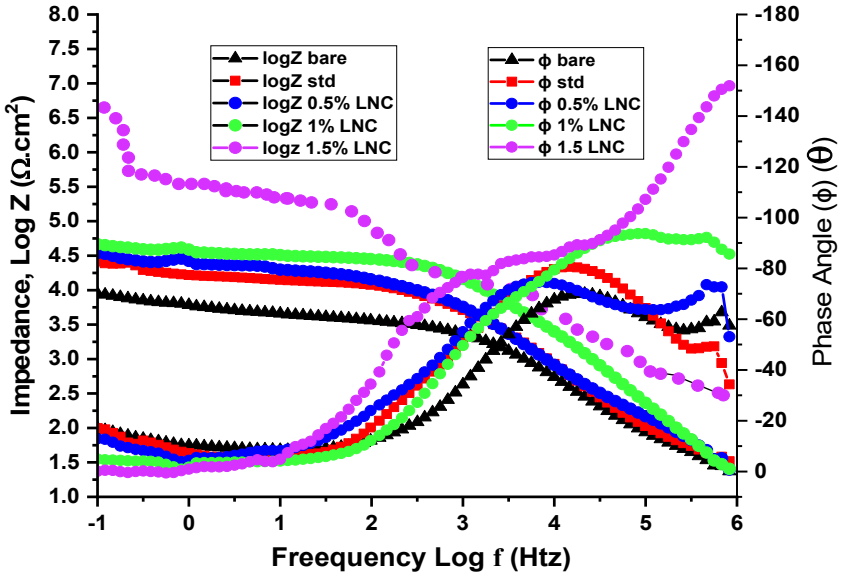

Figure 5. 15. Bode plot for mild steel strips(bare), Standard epoxy coating (STD), 0.5, 1, 1.5 wt% of LNC (lignin nanocapsules) in the epoxy coating after immersed in 3.5wt% nacl Solution for 120 hours.

Impedance at high frequency represents total resistance that is solution resistance plus polarization resistance 6.44E6 Ω.cm^2. The Solution resistance shows R_s 318.5 Ω.cm^2, and the Polarization resistance is Rp 6.44E6 Ω.cm^2. Lignin with epoxy coatings shows very high impendence magnitude due to the presence of phenolic groups, that present in alkali lignin adsorbs on the steel surface forming a barrier between steel and the corrosive environment. The impedance values of various experiments as reported by rahman et al as 10k Ω.cm^2, hussain et al 158 Ω.cm^2 , mojtab et al 2659 Ω.cm^2 , Devadasu et 5E+6 Ω.cm^2.

From the graph, two phase maxima was present, one is at mid frequencies another at higher frequency, these represent the developed double layer on the surface of the mild steel. The occurrence of two-time constants in the Bode plot shows that the electrochemical process is taking place between the metal and the coating. The value of the phase angle ranges between -120 to -60° reveals that the coating behaves as a capacitor. At low frequency, the nanocapsules based polymeric coating shows more resistance to corrosion with lower phase angle compared to standard epoxy coating. rahman et al(Rahman et al. 2018) as has shown lag in phase angle with one time constant at lower frequency. Mojtab (Kasaeian et al. 2018) reported lag in phase angle in around 60-70º at lower frequency. A suitable equivalent electric circuit was fitted by software according to the data obtained during potentio dynamic and EIS measurements in **figure 5.15**.

NYQUIST PLOT

Figure 5.16 represents the Nyquist plot for mild steel strips coated with different percentage of nanocapsules coatings after immersed in 3.5wt% nacl Solution for 120 hrs. It shows the relation between the magnitude of impedance in real and imaginary phases.

From the graph, the increase in impedance takes place with increase of lignin % in the nanocapsules of water borne epoxy amine coating.

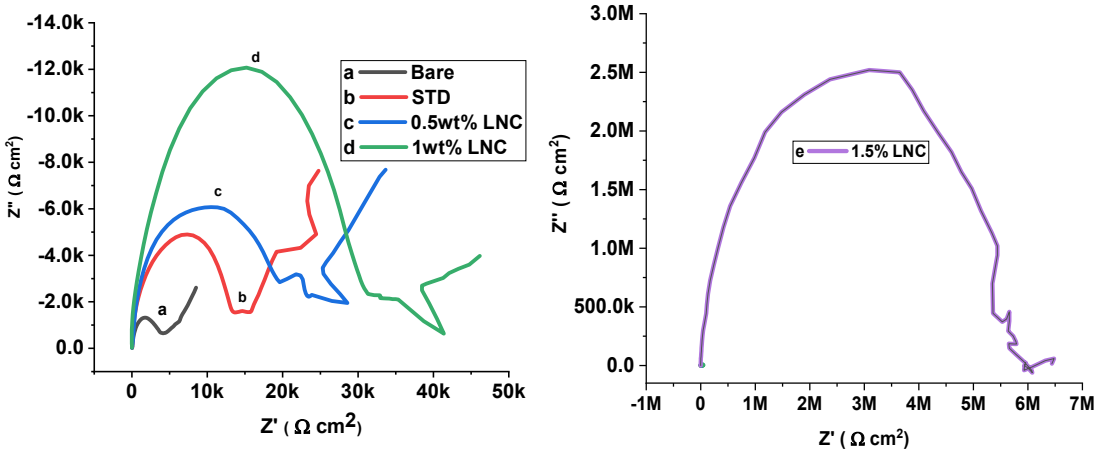

Figure 5. 16.Nyquist plot for mild steel strips (bare), Standard epoxy coating (STD), 0.5, 1, 1.5 wt% of LNC (lignin nanocapsules) in the epoxy coating after immersed in 3.5wt% nacl Solution for 120 hours

The impedance value is observed to be 8.4E3, 2.6E4, 3.6E4, 4.5E4, 6.2E6 ΩCm^2 for bare, standard epoxy amine coating and (0.5, 1, 1.5 %) lignin-based nanocapsules incorporated epoxy coatings.

The high impedance value implies that resistance to flow of current increases representing there is no/low passage of electrons to and from the surface of the mild steel. Therefore there is an increase in corrosion inhibition by the incorporation of lignin nanocapsules in waterborne epoxy amine. This effect is attributed to the presence of phenolic and other functional groups in lignin material. The surface properties of the newly formed protective layer on the surface of the mild steel and the epoxy coating are not the same, but the development of the patina over the surface can increase the life of coating in terms of corrosion. From the literature (Rahman et al., 2018, kasaeian et al., 2018, Hussian et al., 2015b) higher loadings of corrosion inhibitor containing epoxy has larger diameter as compared to standard coatings.

Coating and Electric Double layer Capacitance:

Coating Capacitance and electric double layer capacitance is calculated by fitting nyquist plot from Z sim win soft ware. Each fit has an error of approximately 8.09 $\pm$ 0.12% and a chi square of (0.0081E 6)$\pm$ 1.3.

Electric double layer Capacitance

Capacitance of Electric double layer C_{edl} is a basically measure of electric charge by conducting ions that stored in an electrode, formed due to polarized charged ions between electrolyte and electrode by forming a double layer. These two layers consist of oppositely charged ions. They are insulated by a thin layer that sticks to the electrode's surface. C_{edl} value indirectly corresponds to the stored energy in the developed patina. C_{edl} value at low frequency 0.01 htz was obtained for 0.0379, 0.0211, 0.0137, 0.727, 0.2142 for bare, std epoxy, 0.5, 1, 1.5 % LNC nF.cm^{-2}. The increase in this electric double layer capacitance C_{edl} value shows coatings with 1% LNC acts as a pseudo capacitor. C_{edl} value nearly equal and a bit less than our results that are obtained by Rahman et al as mentioned in the above has reported C_{edl} value for Epoxy-4.700E-6, 1E-LNP-5.140E-7, 1.5E-LNP-6.036E-5 F.cm^{-2} (Rahman et al. 2018).

This C_{edl} value got increase to the Akbardaz et al C_{edl} value for soda lignin with different concentrations to modify epoxy was reported to have 50 ppm-720, 100 ppm-816, 200 ppm 922, 400 ppm 1045, 800 ppm 1432 F.cm^{-2} (Akbarzadeh et al. 2011).

Hussian et al has modification of lignin by incorporation of aromatic scavengers (2-naphthol: AHN EOL and 1,8-dihydroxyanthraquinone: AHD EOL) during delignification process has lead to have higher phenolic content improved the physical properties of the lignin fractions. 0.5 HCL~28E-6, 500ppm – AHN ~ 48E-6, 500 ppm –AHD ~ 44E-6 F.cm^{-2} (Hussin et al. 2015a).

Coating capacitance:

Similarly the coating capacitance C_c are calculated at the mid frequency region for bare, STD, 0.5, 1, 1.5% LNC as 0.012264, 0.412, 0.343, 0.236, 0.191µF.cm^{-2}. These values represents some amount of charge (in micro faraday per square centimeter) is stored in the developed oxide layer. Indirectly oxide layer stops the flow of electrons into the metal, thus exhibiting protectiveness of the mild steel. This trend of coating capacitance C_c values are similar for (rahman et al 2018). Epoxy-5.542E-8, E-LNP-1 as 4.878E-9, E-LNP-1.5 as 4.878E-9 F.cm^{-2}. (Zang et al., 2015), shown value for 46% PVC 3.25E-9 F.cm^{-2}.

(ii) Equivalent electric circuit:

The equivalent electric circuit represents similar to the disturbed/ damaged by cross mark coatings. Illustration of the equivalent electric circuit is represented in the figure 5.17. This circuit represents intermediate immersion of damaged coatings, because the electrolyte diffusion occurs in the gaps among the fillers. Each component in equivalent electrical circuit has a similarity with the coating elements, such as R_s represent solution resistance, R_c coating resistance, C_c coating capacitance, W Warburg diffusion, R_{pol} polarization resistance, C_{edl} electric double layer capacitance.

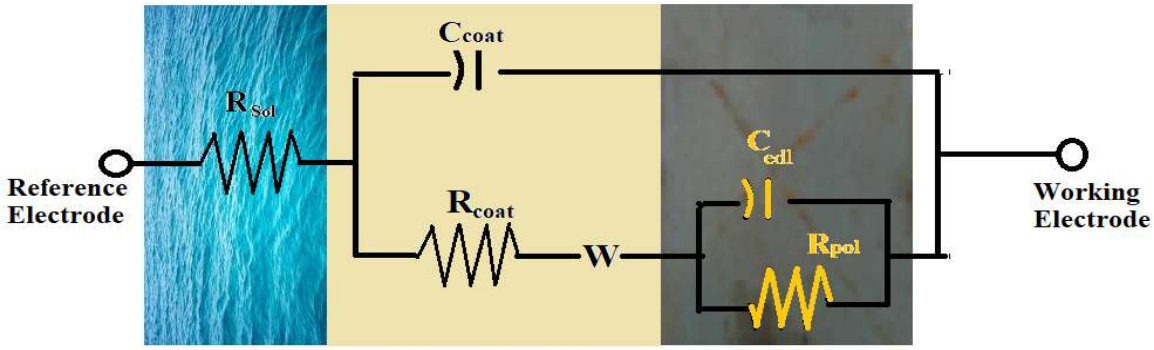

Figure 5. 17. Equivalent circuit model for lignin-based epoxy coating on mild steel.

(III) Immersion Studies:

The self-healing ability of nanocapsules was evaluated using the immersion technique with mild steel (coated with modified epoxy containing nanocapsules) in 3.5 w/v% of Nacl solution for five days. During the period the photographs of the mild steel were collected at zero, 24, 48, 72 and after120 hours as shown in figure 5.18.

The weight loss of the marked coated panels was recorded after 72 hours and 120 hours of immersion in 3.5 wt% nacl solution. The corresponding corrosion rate with respect to the weight loss studies are calculated according to the formula

$$Corrosion\ rate = \frac{87.6 * w}{t * A * \rho} \quad (eq\ 5.10)$$

Where corrosion rate is expressed as mm/yr, t is exposure time in hours (hr), w is weight loss in grams (g), A is exposed area in cm^2, and is the density of the mild steel in g/cm^3.

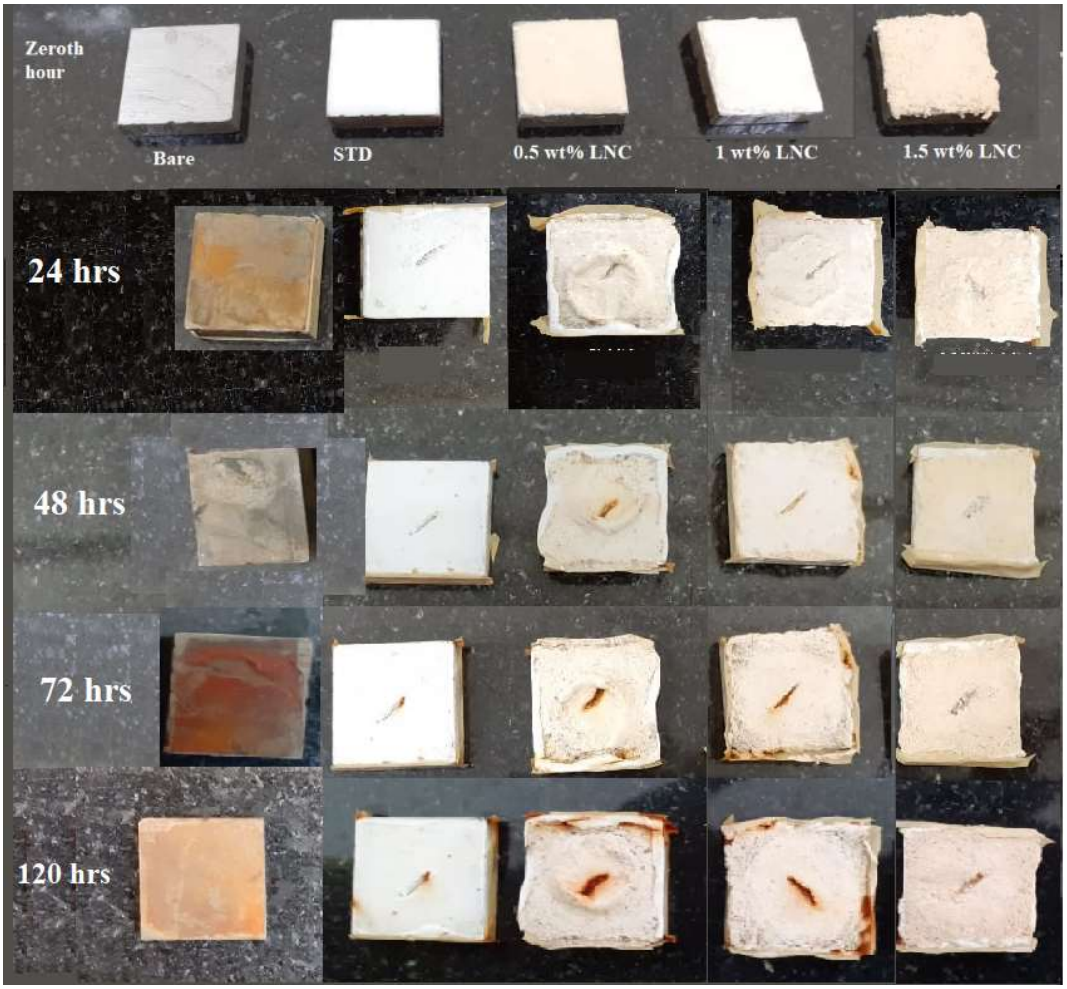

Figure 5. 18. Immersion studies (using 3.5 wt% nacl solution) of mild steel, with STD, and organic coatings (0.5, 1, 1.5 wt% lignin nanocapsules) for 120 hours.

From weight loss studies, the corrosion rate was found to be 46.868±1.2 , 8.276±1.1, 3.626±0.8, 1.394±0.9, 0.1022±0.4 mm/year for bare, standard, 0.5, 1 wt% lignin loadings is shown in figure 5.19. These corrosion rate values were much better than the results when lignin is used in electrolyte solution instead of in epoxy coatings as reported by akbardaz et al 2011. Gravimetric studies for others as reported by (hussain et al 2013, rahman et al, 2018) reveals corrosion rate is almost similar to the present work weight loss studies.

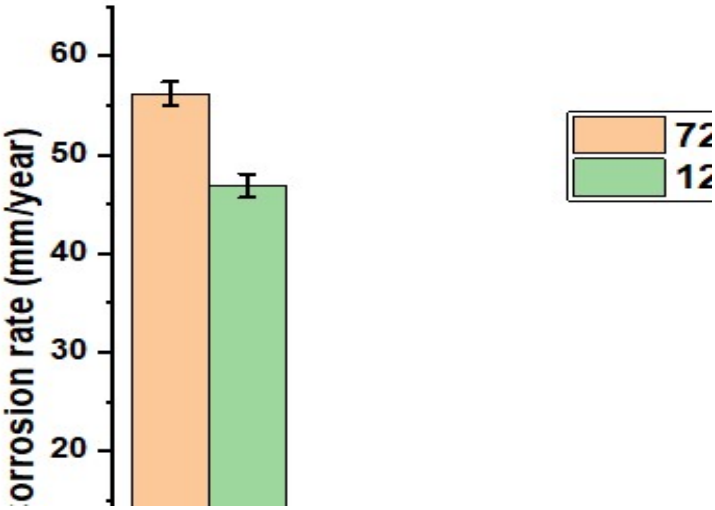

Figure 5. 19. Corrosion rate of bare, STD, and (0.5, 1, 1.5 wt%) nanocapsules blended coatings on mild steel after 120 hours of immersion in3.5 wt% nacl solution as determined by Weight loss studies.

Summary:

The proposed work explores the application of natural corrosion inhibitors for self-healing and corrosion resistance of mild steel. Safflower oil and extracted lignin were used as corrosion inhibitor as well as the self-healing agent. Potentio dynamic polarization studies, and EIS studies were performed for water-borne epoxy coating (with, and without nanocapsules) for 120 hour of 3.5 wt % nacl immersion. I_{corr} values for bare is 1.0423E-5 A/cm^2, and this was decreased to 1.662E-6 A/cm^2 for standard, and its value further got decreased to 2.409E-8, 3.139E-7,3.703E-8A/cm^2 as weight of lignin increases from 0.5, 1, 1.5wt % in nano-capsules. Impedance values are higher for LNC coatings compared to bare, and standard coatings. The impedance value was observed to be 2.4 x10^4 ΩCm^2 for standard epoxy amine coating and increased to 5.8x10^6 ΩCm^2 with the incorporation of lignin-based nanocapsules in the epoxy coatings. Corrosion rate from weight loss studies for bare steel, standard epoxy, (0.5, 1, 1.5 wt %) lignin loadings are 46.868±1.2, 8.276±1.1, 3.626±0.8, 1.394±0.9, 0.1022±0.4 mm/year respectively, which confirms the better corrosion rate with the increase in lignin loadings. Better self-healing behavior was observed from EIS analysis and immersion studies.

5.3 Performance evaluation of benzotriazole loaded cellulose as a corrosion inhibitor coatings

5.3.1 Characterizations

A Fourier Transform Infrared Radiation spectroscopy (FTIR) Analysis

FTIR spectrum of benzotriazole, cellulose nano fibers CNF and benzotriazole encapsulated cellulose nano fibers CNB is given in **figure 5.2**0. O–H and C–H bands in the cellulose are assigned to 3419 cm^{-1} and 2905 cm^{-1} peaks (Zang et al.,2017). 1640 cm^{-1} is apt for the absorbed water. The peak at 1380 cm^{-1} represents C-H bending vibration. Peaks at 1280 cm^{-1} in cellulose spectrum represent C-H bending of crystalline cellulose by ensuring the synthesized cellulose is crystalline in nature. The low peak intensity of cellulose crystallinity peak confirms the extracted cellulose is having some extent of crystalline nature. That in turn represents presence of voids or gaps on the surface of cellulose nano fibers.1166 cm^{-1} represent anti symmetric stretching in ester or C–O–C bond in the cellulose. A small sharp peak at 897 cm^{-1} ensures the presence of β–glycosidic linkage which relates to glycosidic C_1-H deformation having ring vibration contribution. 990 cm^{-1} peaks represents C-O valence vibration of cellulose (yue et al., 2012).

Absorption bands (C=C, C=N and N=N) are found at 1620–1380 cm^{-1} (weak and medium) and 1380–1090 (strong) cm^{-1} regions [9]. A peak corresponds to 1208 cm^{-1}represents C-H in plane bending of benzene ring.892, 775, 745, 739 cm^{-1} tells C-H bending benzene moiety ring in benzotriazole (borin et al., 2003)

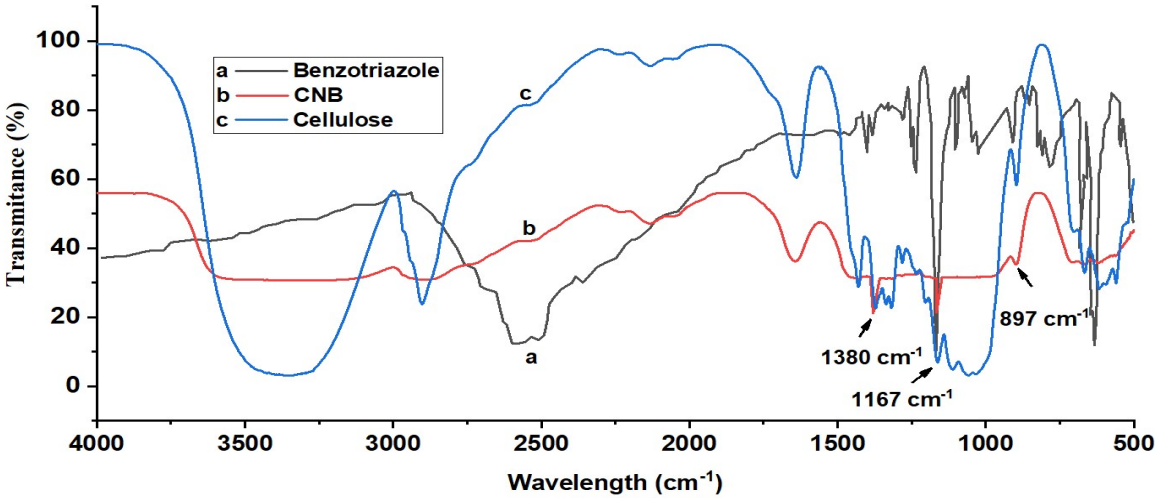

Figure 5. 20. FTIR Spectra of (a) Benzotriazole (b) Benzotriazole loaded Cellulose nano fibers CNB (c) Cellulose.

Benzotriazole loaded cellulose nano fibers (CNB) has peaks at 1380, 1167, 897, cm^{-1} which are main peaks of cellulose corresponding to (C-H bending, C-O-C bond, C_1-H with ring vibration) explained above, this ascertain the presence of cellulose in CNB.CNB Spectrum with 1380 cm^{-1} peak may be relates to strong bands of C=C, C=N and N=N bonds. The presence of another peak 772 cm^{-1} corresponds to C-H bending of benzene ring in benzotriazole.

B Transmission Electron microscopy (TEM).

TEM images of synthesized nano cellulose and benzotriazole loaded nano fiber are shown in figure 5.21a at different scales. The TEM image clearly shows hollow nature of the synthesized nano cellulose and CNB. The hallow structure can accommodate more amount of benzotriazole as compare to encapsulation of benzotriazole. The TEM figures concludes that it consists of an average lumen of diameter 23 nm and average length of 176 nm.

C Scanning Electron Microscopy (SEM)

SEM images of synthesized nano cellulose are shown in figure 5.21b at1 µ in scales. The SEM image clearly shows hollow nature of the synthesized nano cellulose and CN as well as benzotriazole loaded cellulose nano fiber. The Proper sonication resulted in almost equal sized and shaped cellulose nano fiber as shown in figure 5.21 b.

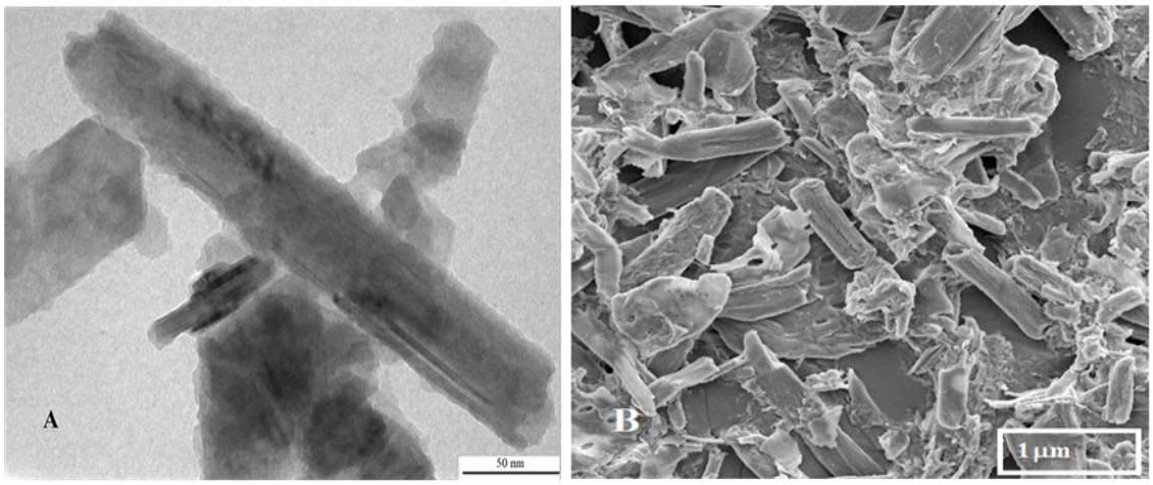

Figure 5. 21 (a) TEM image of cellulose nano fibers(b) SEM images of benzotriazole loaded cellulose nano fibers and CNB.

The SEM **figures 5.21(b)** concludes that it consists of an average lumen of diameter 23 nm and average length of 176 nm. Since the cellulose nano fibers were synthesized by two

step sulphuric acid hydrolysis, the outer structure consists of sulphate and ester groups which are negatively charged are responsible for replacing the anions that are leaving the mild steel. The hallow structure can accommodate more amount of benzotriazole as compare to encapsulation of benzotriazole.

D Benzotriazole controlled release studies at different PH.

Benzotriazole has two molecular configurations that are 1H benzotriazole, and 2H benzotriazole as mention by borin et al.2003. The concentration of benzotriazole was measured at 262 nm and 273 nm for 1H benzotriazole (having two absorption peaks), and a single absorption peak of 273 nm for 2H benzotriazole. From the **figure 5.22(a)** it can be ascertain that initially the benzotriazole release rate was high for NCB without stopper when compared with stoppers. The conversion of 1H benzotriazole to 2H benzotriazole can occur at an alkali environment at a pH of 11, and for the acidic and normal environments benzotriazole is having two peaks conforming 1H benzotriazole. As time progresses benzotriazole controlled release rate was slow for CNB with stopper as compared to NCB without stoppers. The benzotriazole release rate with respect to time (for 24 hours) is shown in **figure 5.22(b)** and its rate was higher for pH 2 than pH 11 while the minimum was observed at pH 7.

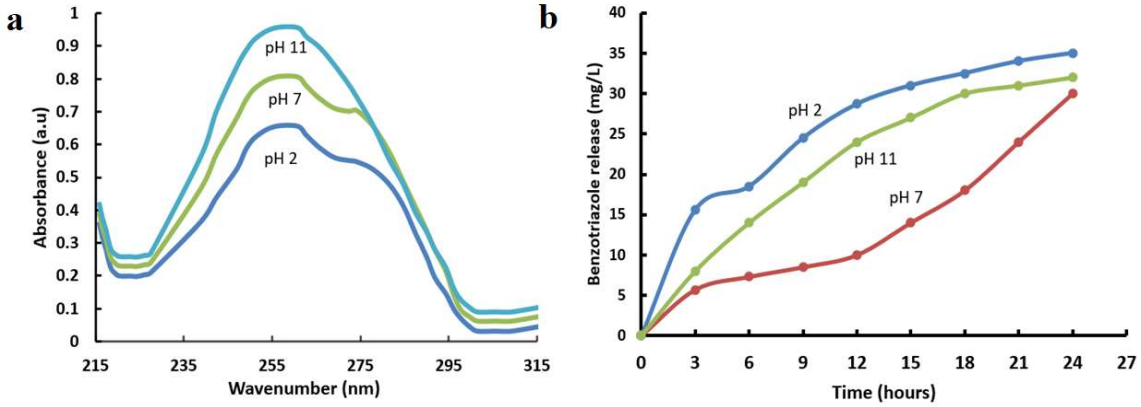

Figure 5. 22(a): Benzotriazole release rate with respect to time at 2, 7, 11 pH environment.(b) Benzotriazole release absorption curves for different pH (2,7,11) after 24 hours of immersion in 3.5 wt% nacl solution

5.3.1 Corrosion Inhibition studies

I Polarization Studies

A general electro chemical kinetics was analyzed by Tafel plot. The (I_{corr}) values can be estimated using Tafel plot which represents the flow of electrons from the mild steel to the surrounding solution. Figure 5.23 represents the Tafel plot for bare metal, 2K epoxy polyamide coating alone as a standard (STD) and 2K epoxy polyamide coating with cellulose nano fibers loaded with benzotriazole of different weight percent (2, 4, 6 wt %) for 72 and 120 hours of immersion in 3.5 wt% nacl solution. From the Figure 5.23, it can be observed that the corrosion current density decreases with increasing in concentration of benzotriazole loadings in cellulose nano fibers. It can be found that I_{corr} value is $8.243x10^{-4}A/cm^2$ for bare and further the value decreases to $1.482\ x10^{-6}A/cm^2$ (for 2K Epoxy-polyamide coating) and its value is further decreased to $1.304\ x10^{-6}$, $2.472\ x10^{-8}$, $2.688\ x10^{-8}\ A/cm^2$, for coatings consist different benzotriazole loadings of 2, 4, 6 wt% in cellulose nano fibers. The potential value got shifted towards positive value that is -1.425, -0.826,-0.682, -0.498, -0.475 Volts for bare, standard, and 2, 4, 6 wt% of CNB Coatings respective

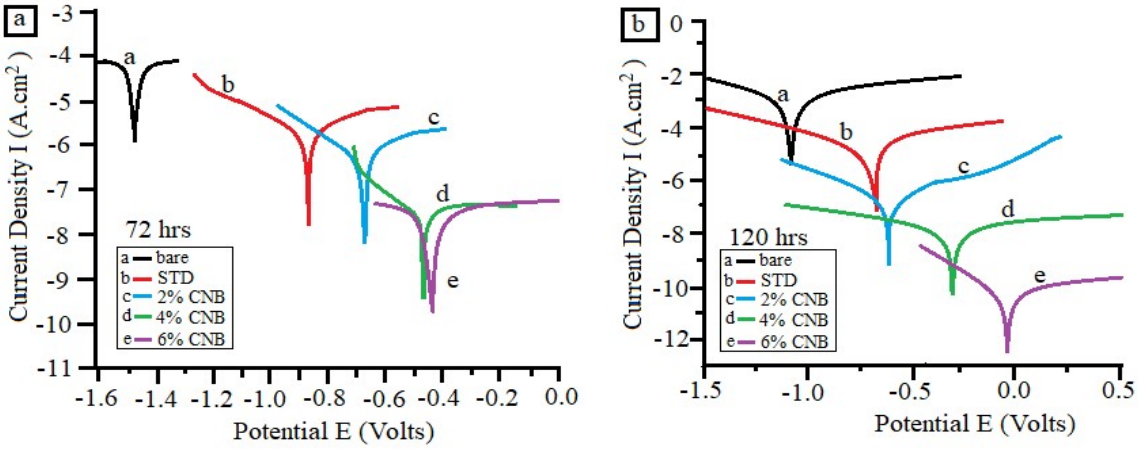

Figure 5. 23. Tafel plot for bare mild steel, standard, STD, NCB 2, NCB 4, NCB 6 after (a) 72 (b) 120 hours of immersion in 3.5 wt% nacl solution.

Similar trend was observed in current density (I_{corr}) and in corrosion potential (E_{corr}) after 120 hour as shown in figure 5.23b. The (I_{corr}) values decreased to a minimum of 5.726E-10 A/cm^2 with the increase in CNB loading coatings the (I_{corr}) are as follows for bare, standard, 2, 4, 6 wt% of CNB loading coatings are 6.037E-4, 3.206E-5, 8.779E-7, 4.8174E-8, 5.726E-10 A/cm^2 respectively. The corrosion potential E_{corr} values got shifted towards positive values

from -0.972, -0.584, -0.518, -0.347, -0.002 Volts for the corresponding bare metal, standard coatings, 2, 4, 6 wt% of CNB loading coatings respectively.

II Impedance studies

Bode Plot

Bode plot also gives the impedance of the coating system. The total resistance, solution resistance, and coating resistance can be found from the bode plot. The **figure 5.24** represents the bode plot for bare, standard, 2, 4, 6 wt% CNB benzotriazole loaded cellulose nano fibers coatings in 3.5 wt% Nacl solution after 120 hrs. The corresponding table gives the impedance value, and coating and electric double layer capacitance. At low frequency the total impedance corresponds to $|Z|_{0.01}$ value for 6wt% CNB is 1.258E7 Ω.cm^2. This value got reduced to 4.677E6, 1.995E6, 1.584E5, 1.0E4 for 2, 4 wt% CNB, standard, and bare.

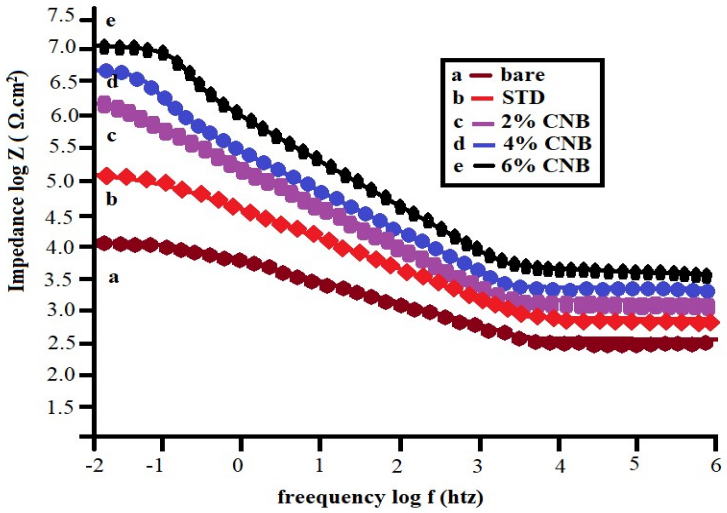

Figure 5. 24. Bode plot for bare, standard, 2, 4, 6 % CNB coatings epoxy in 3.5 wt% Nacl solution after 120 hrs of immersion.

This decrease in impedance value is due to the removal of formed rust in turn causing pitting on the damaged surface of the coating. All the graph values are moved the left most corner of the bode plot which represents the better coating characteristics of the coating. As the prepared coating system is just acts as a pseudo capacitor, the impedance value is not zero, but has some stored charge in the real system. This was represented as capacitance of electric double layer C_{edl}. The value of C_{edl} are more are less having similar capacitance values for the different coatings. These C_{edl} values are 0.355E-06, 0.316E-07, 0.588E-07, 0.251E-06, 0.155E-04 for bare, standard, 2, 4, 6 wt % CNB coatings.

Similarly the coating capacitance also having similar trend that are 0.794E-06, 0.251E-04, 0.398E-04, 0.1E-03, 0.251E-03 for bare, standard, 2% , 4%, 6 wt% CNB. The coating capacitance corresponds to the coating impedance at angular frequency of log ω zero.

B. Nyquist Plot

The coatings impedance can be found from the nyquist plot. The maximum impedance of up to 2.25E+6 can be observed from the figure 5.25a for 72 hours of immersed mild steel with coatings of 6 wt% CNB. This impedance value may further decreases to 1.3E+6 for 2 wt% CNB and its value got reduces for standard 2k polyamide epoxy coatings as shown in figure 5.25a. This may be due to the formation of passive layer on the damaged region. The results clearly shows that coatings with 2, 4, 6 wt % CNB gives better impedance value when compared to the standard coatings.

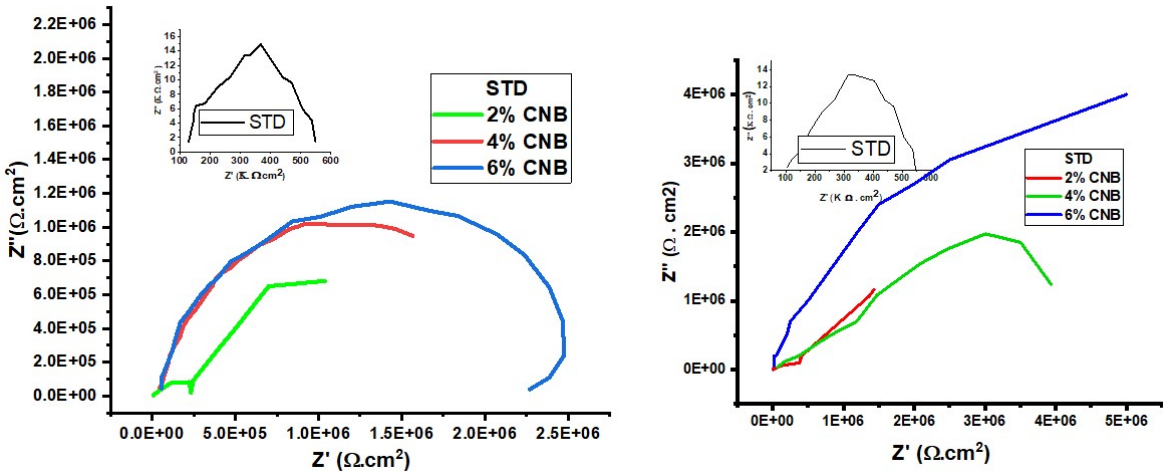

Figure 5. 25. Nyquist plot for bare mild steel, standard, STD, 2%NCB, 4% NCB, 6% NCB after a) 72 hours b) 120 hours of immersion in 3.5 wt% nacl solution.

However impedance values at 72 hours is much lower than that at 120 hours this can be confirmed by comparing figure 5.24 (a) and (b). The impedance values in figure 5.24 (b) of standard and coatings has followed similar trend as in figure 5.24 (a). 2 wt % CNB coatings have shown less inhibition to corrosion than 4 and 6 wt % CNB coatings. In spite of that 2 wt% CNB has shown higher impedance than standard coatings. The impedance value after 120 hours of immersion for 6 wt% CNB has greater than 5E+6 that is higher than that of 6 wt% CNB coatings i.e 2.2E+6 for 72 hours.

(i) Coating and Electric Double layer Capacitance

Capacitance and electric double layer capacitance is calculated by fitting nyquist plot from Z sim win soft ware. Each fit has an error of approximately 1.303± 0.12% and a chi square of 1.69-4. The Electric Double layer Capacitance C_{edl} represents the energy storage between the coatings and the polymerized film. C_{edl} values are 0.355E-06, 0.316E-07, 0.588E-07, 0.251E-06, 0.155E-04 for Bare Epoxy, 2, 4, 6% CNB. The increase in the C_{edl} values for 6 % CNB blended epoxy coatings compared to 4, 2 % CNB represent increase in the CNB loadings increases the electric Double layer Capacitance values. The Coating Capacitance Cc represents total capacitance of the 2K Polyamide CNB epoxy coating system. Cc values are 0.794E-06, 0.251E-04, 0.398E-04, 0.1E-03, 0.251E-03for Bare Epoxy, 2, 4, 6% CNB. The increase in the C_c values for 6 % CNB blended epoxy coatings compared to 4, 2 % CNB represent increase in the CNB loadings increases the coating capacitance values. These are in similar trend with respect to the C_{edl} values.

Electric double layer and coating capacitance values increases as CNB% increases in 2k polyamide epoxy coatings increases. A maximum of 0.251E-03, 0.155E-04 $F.cm^{-2}$ for electric double layer and coating capacitance was observed. These values tell the modified coatings acts as a pseudo capacitor.

(ii) Equivalent Electric Circuit

An equivalent electric circuit was fitted from nyquist plot using "***Z sim win***" soft ware. The equivalent electric circuit represents similar to the disturbed/ damaged by cross mark coatings. The circuit in the figure 5.26 represents intermediate immersion of damaged coatings, since the electrolyte diffusion occurs in the gaps among the fillers. Each component in equivalent electrical circuit has a similarity with the coating elements, such as R_s represent solution resistance, R_c coating resistance, C_c coating capacitance, W Warburg diffusion, R_{pol} polarization resistance, C_{edl} electric double layer capacitance.

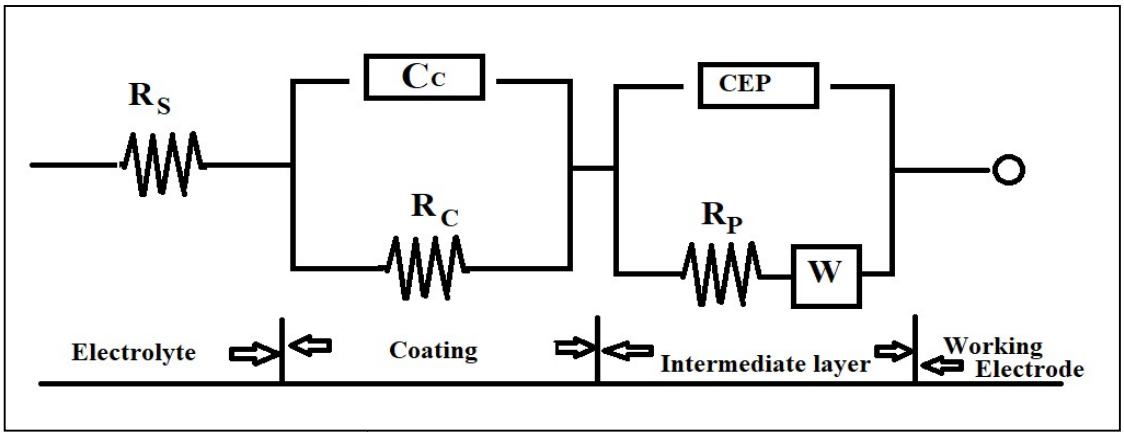

Figure 5. 26. Equivalent circuit model for 2K Polyamide CNB epoxy coating on mild steel.

III Immersion studies and weight loss studies

Figure 5.27 shows corrosion rate of mild steel after marking the coated plates with knife and immersed in 3.5 wt% Sodium chloride solution for 120 hours. 2k polyamide epoxy coatings are less viscous when compared to epoxy based cellulose nano fibers, this may be due to presence of cellulose nano fibers. The surface of the material coated with cellulose nano fibers is harder and behaves like hydrophobic when compared with standard 2k polyamide coatings.

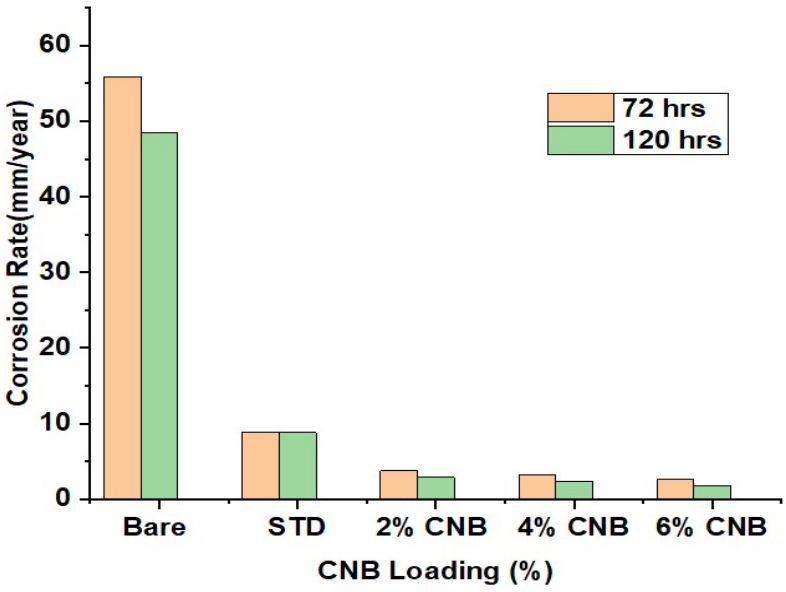

Figure 5. 27. Corrosion rate for bare standard 2, 4, 6% CNB after 120 hrs of immersion in 3.5 wt% Nacl solution.

Bare mild steel shows high corrosion rate as compared to standard 2k polyamide coating and with Benzotriazole loaded cellulose nano fibers as shown in **figure 5.27**. Gravimetrically the corrosion rate was calculated by the following formula.

$$Corrosion\ rate = \frac{8.76 * w * 10^4}{t * A * \rho} \qquad (eq\ 5.11)$$

Where t is exposure time in hours (hr), w is weight loss in grams (g), A is exposed area in cm^2, and is the density of the mild steel in g/cm^3.

Summary:

A modified 2k epoxy polyamide was prepared using cellulose nano fibers and encapsulated benzotriazole to evaluate corrosion resistance of mild steel. The importance of sonication to have uniform sized particles in preparation of cellulose nano fibers were confirmed with SEM image. TEM and SEM images also prove the hallow structure of nano cellulose. As benzotriazole is active in acidic environment, immersion studies were done with 3.5 wt% Sodium chloride solution with different concentrations of benzotriazole loadings in cellulose nano fiber using sonication in presence of acetone polar solvent. FTIR results revealed that CNB has similar peaks as that of benzotriazole and Cellulose Nano fiber ensuring the loading of benzotriazole. All the corrosion rate, polarization, impedance values were noted at different interval that is after 72 and 120 hours with immersion of mild steel (bare and coated after marking) in 3.5 wt% Sodium chloride. Potentio dynamic polarization studies have shown decreased in current density values from 6.037E-4, 3.206E-5, 8.779E-7, 4.8174E-8, 5.726E-10 A/cm^2 for corrosion potential of E_{corr} are -0.972, -0.584, -0.518, -0.347, -0.002 Volts respectively for bare, standard, 2% CNB, 4%CNB, 6% CNB after 120 hr.

The impedance value after 120 hours of immersion for 6 wt% CNB has maximum value up to 5E+6. Corrosion rate from weight loss studies has also proved corrosion rate is higher for 2, 4, 6 wt% CNB as compared to bare and standard after 120 hr.

5.4 Comparing the Performance of self healing epoxy coatings

The natural polymers extracted from sawdust were explored for self healing corrosion inhibition applications. Good number of authors published the application cellulose and lignin as a corrosion inhibitors base on 3 layer (base layer: usually primmer; middle/Intermediate layer ; final layer) mechanism, however very few were focused on single layer high solid build, solvent less coatings for marine application. Therefore present work focused on the high performance high build solid hybrid coatings with natural polymers such as lignin and cellulose.

The high-performance coatings can be applied in different situations in which like splash zone of off shore structures, underwater in sea and rivers, on damp surfaces, in highly acidic and alkaline environments such as pickling units, in the battery chamber of a ship or submarine, in sewage disposal units, seawater transport through jetties, etc. Present study aims at two different structured corrosion inhibitor carriers which are made up of natural polymers like lignin and cellulose for epoxy modification.

Case 1 Multi layered nano composite coatings with lignin as a healing material encapsulated by Pickering emulsion by in-situ polymerization techniques.

Case 2 Benzotriazole loaded cellulose nano fibers as a healing material for development of hybrid coatings.

This comparison study aims to compare these two case studies with the other published articles. In case 1 Lignin acts as a corrosion inhibitor by chelating, It also acts as a stabilizer during the preparation of nano capsules. Encapsulation and polymerization method involves steps like preparation O/W emulsion with healing agent and formation of shell wall around healing agent followed by solidification of shell wall by in-situ polymerizations. While in case 2 study loading of corrosion inhibitor occurs by simply blending the NC with healing agent and vacuum filtered 3 times.

Corrosion is an accelerating reaction therefore the metal will be corroded very fast by corrosion products if the formed product loosely binds with the metal causing pitting. The lignin and cellulose consists of anions that combine with the Fe^{+2} or Fe^{+3} ions and forms a corrosion product rust during oxidation (losing of electrons) of mild steel. If this corrosion product rust binds strongly to the metal forming a new polymerized layer which is inert there by reducing accelerating corrosion reactions. Since lignin and cellulose are potent of free radical scavengers like hydroxyl OH^-, carboxyl $COOH^-$, methoxy OCH_3^-, sulphate SO_4^{-2},

groups, therefore they can act as sacrificial anode by sharing its lone pair of electron with free d-electrons of metal ions by chelating.

5.4.1 Structural Comparison of lignin and cellulose as a corrosion inhibition carrier.

Micro or nano spheres/hollow rods/tubes in the paint formulations increase the solid content by reducing volatile organic compounds (VOCs), it also decreases shrinkage and drying time and thereby to maintain the flow characteristics.

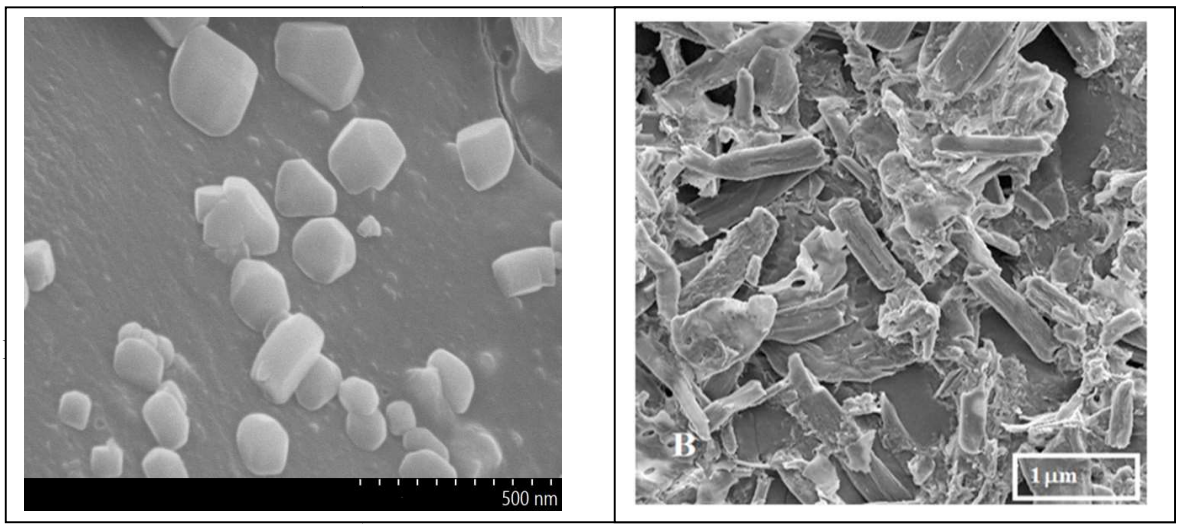

Figure 5. 28. a) FE-SEM image of lignin nanocapsules and b) SEM image of cellulose nanofibers.

The use of cellulose micro/nano fibrils can overcome some issues that are faced by the micro spheres. Usually micro spheres are less denser and float on the surface of paint, or settling /sedimentation of micro spheres in the paint are some major issues. This can be overcome by 3D structure micro/ nano fibers that are dispersed evenly while coating to ensure the availability of the loaded healing agent everywhere.

In the case 1 using amino silanized lignin nanocapsules in water borne epoxy the coating impedance was little lesser than in case 2. These results can be interpreted in two important points. Firstly cellulose due to its hollow cylindrical structure can hold more benzotriazole up to 6wt%, and also due to its surface charge contribute a coating impedance of $10^7 \Omega cm^2$. Secondly lignin is rich in phenolic ions which are spherical microcapsules of size 40-117µm richly loaded with healing reagent (Isophorone diisocyanate, IPDI) epoxy coatings has shown self healing coatings with an impedance of $\geq 10^5 < 10^6$ (Yi et al. 2015). Nano Lignin of size 15-20 nm is used as a filler in epoxy and found coating resistance as a $\geq 10^5$(rahman et al., 2017).

5.4.2 Epoxies and Curing Agent characteristics

Epoxies

For the proposed work semi solid epoxy were chosen for both lignin and cellulose coatings but with different viscosities. In detail water borne epoxy-amine coatings was used in lignin based coatings. It is in white colour semi solid epoxy having high solid content epoxy. Their characteristic such as equivalent weight based on solids was reported as 195-220 g/eq and its viscosity as 300-3500 cp with a non-volatile content of 59-61% epoxy.

The characteristic of epoxy resin used in cellulose based coatings are having an equivalent weight based on solids was reported as 187 g/eq and its viscosity as 12,600 cp with a non-volatile content of 70% epoxy.

Curing Agent

A curing agent provides polymerization reaction by consuming itself. For the proposed work two different characteristics of curing agents were chosen for development of high build solid hybrid coatings. One polyamide with high viscosity and less drying time (good corrosion resistant that is used especially for solid coatings). Another curing agent is cycloaliphatic polyamine with less viscosity and long drying time. Different characteristics of epoxies and curing agent were chosen to show how effectively solid organic paintings with less viscous, less drying time epoxy system compete with the high viscous and high drying time epoxy system.

The impedance value is different for two standard epoxy systems that is due to its viscosity and its drying time difference especially when mixed with water borne epoxy and polyamine which is having less viscosity and high drying time when compared to epoxy with polyamide. For standard coatings of 2k polyamide (with high viscosity 2000 cp) is greater than standard cycloaliphatic polyamine curing agent (with low viscosity 230 cp).

5.4.3 Comparing the Polarization studies for coatings with LNC and CNB.

Corrosion generally occurs at an rate determined step by an equilibrium between two opposing electrochemical reactions (ECR). Those are one is anodic, another one is cathodic reaction, when these two reactions are in equilibrium, and there is no net flow of electrons, at this point corrosion current density and corrosion potential can be measured. This can be represented in a tafel plot. Tafel plot gives a correlation between electrochemical kinetics relating the rate of an electrochemical reaction to the over potential. The Tafel equation was

first deduced experimentally and was later shown to have a theoretical justification. The equation is named after Swiss chemist Julius Tafel. Horizontal axis is potential, vertical axis is the current density. The curved lines represent anodic and cathodic currents. The slopes represent the theoretical current for anodic and cathodic branches.

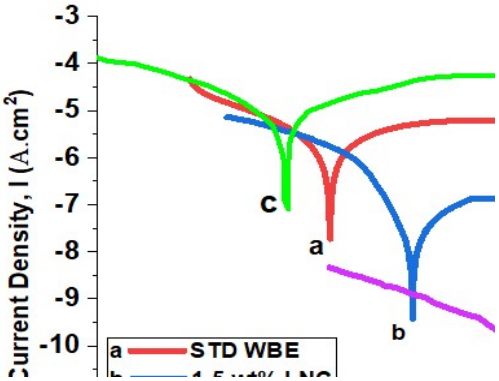

Figure 5. 29. Tafel plotfor a) bare, b) standard for waterborne epoxy (STD WBE), c) Lignin nanocapsules 1.5 wt% LNC, d) standard 2k polyamide (STD-2KP) e) Benzotriazole loaded Cellulose nano fibers 6 wt% CNB.

Anodizing of the metal surface in a electrochemical cell is done by applying accelerating current to working electrode. Working electrode is a damaged / marked high thick solid coatings on the mild steel surface containing more anions ions. The produced rust will enhance the anodizing layer to more thick, free of porous, with high adhesive and inert nature that will not allow further corrosion to occur. These coatings will increase the potential to corrosion potential with corrosion current density or passive current or even to a limiting current density to the place where polarization occurs. Anodic or cathodic passivation depends upon limiting current of anodic curve or cathodic curve.

The current density I_{cor} for standard water borne epoxy STD WBE 1.662E-6, and 1.5% LNC 3.703E-8 for a corrosion potential of E_{cor} -0.47, -0.292 respectively. similarly for benzotriazole loaded cellulose nano fibers 2k polyamide system standard has a current density Icor of 3.206E-5, and 6% CNB is 5.726E-10, for a corrosion potential of E_{cor} of -0.584,-0.002 respectively. The proposed work has shown decrease in the current density, with respect to 6% CNB coatings compared to the 1.5% LNC coatings. The difference in I_{cor} values may be due to the difference in viscosities of epoxy system as explained above. Lowest I_{cor} value for CNB coatings when compared to the LNC coatings says CNB coatings are better than LNC coatings.

A 4 fold decrease in I_{corr} value was observed when graphene oxide (GO) nano sheets were non-covalently functionalized with 1H-Benzimidazole (corrosion inhibitor) was used to

modify epoxy to develop corrosion resistant coating for mild steel in 3.5 wt% chloride solution after 24 hours of immersion(water borne epoxy based I_{corr} value 8.75 µA/cm^2, at Ph 1 , and for modified epoxy I_{corr} value 4.59 µA/cm^2) (Kasaeian et al. 2018).

5.4.4 Comparing Impedance from Bode plot for coatings with LNC and CNB

Bode plot for modified solid epoxy coatings with lignin and cellulose are shown in the **figure 5.29**.In the bode plot at low frequency of voltage the flow of current into metal is less that represents high impedance (total resistance/ coating resistance). Vice versa at high frequency of voltage the current flow into the metal is high that represents low impedance (only solution resistance exists).

Synthetic corrosion inhibitors gives best performance when compared to the organic coatings alone. But from proposed experiments the high solid organic, solvent free single layer hybrid coatings also provides competition with the synthetic corrosion inhibitor such as benzotriazole coatings.

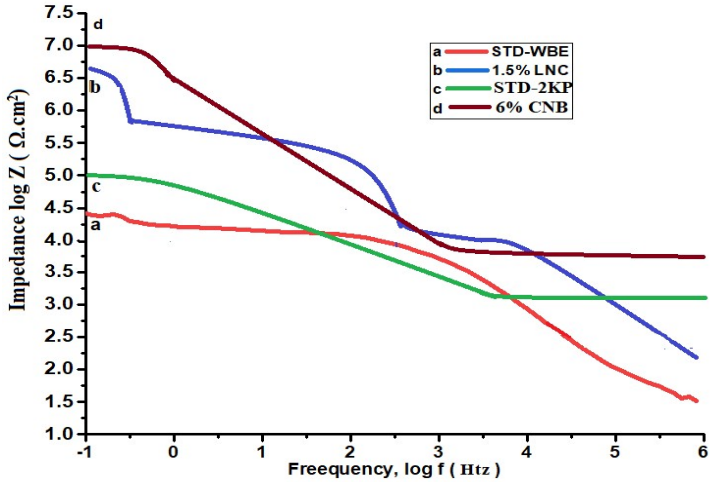

Figure 5. 30. Bode plot for a) Standard for waterborne epoxy (STD WBE), b) Lignin nanocapsules 1.5 wt% LNC, c) standard 2k polyamide (STD-2KP) d) Benzotriazole loaded Cellulose nano fibers 6 wt% CNB.

From the figure the impedance value at low frequency of voltage, for cellulose based 2k poly amide coatings is 1.578E5, and for standard 2k polyamide coatings alone is 2.42E4. The coating resistance of CNB coatings is 1.258E7 which is higher when compared to the LNC coatings that is 6.444E6 in an overall the both CNB as well as LNC coatings can be represented as better corrosion inhibition coatings.

From the literature pH-controlled self-healing polymer coatings with cellulose nano fibers (CNF) have reported an effective release of corrosion inhibitor OA (Oxalic Acid). The coatings are of three layered; the first layer consists of primer coat. Second layer is middle coat epoxy resin mixed with CNF and OA @ pH 8.4, this layer was coated by adjusting it with different pH 10.4, 10.9, 11.4, 11.9, 12.2, 12.8. The top coat is epoxy resin alone. The dried damaged coatings were immersed in 0.05 wt% sodium chloride solution for 24 hours. The Impedance values of plain coatings are reported as 40k, and for CNF+OA at (Ph 8.1)~80k , and at different Ph 11.4, 11.9, 12.8 as 400k, 200k, 80k (Yabuki et al. 2016). Finally it concludes at CNF+OA of ph 11.4 coatings gives higher impedance 400k with self healing.

5.4.5 Comparing Impedance from Nyquist plot for coatings with LNC & CNB

Nyquist plot from **figure 5.31** also gives about the system impedance and capacitance. The coatings with 6wt% CNB gives graph almost nearly a line with impedance greater than 10^6 Ω.cm^2. Generally a pure capacitor will have a straight line parallel to imaginary impedance (Z``**)** with a zero impedance (He et al., 2011). But CNB coating system acts as an pseudo capacitor having a capacitance of 0.155E-4F.cm^{-2}. Similarly coatings with 1.5 wt% LNC gives impedance 10^6 Ω.cm^2 with a pseudo coating capacitance of 0.214E-9 F.cm^{-2}.

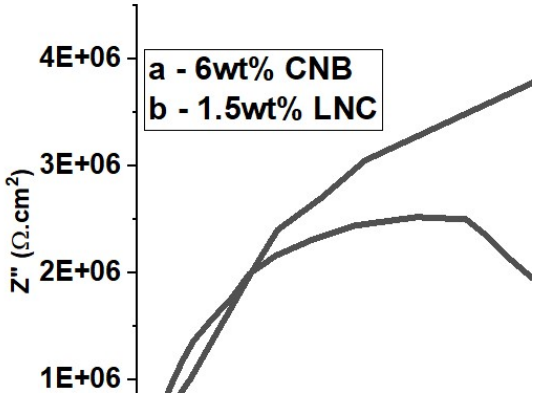

Figure 5. 31. Nyquist plot showing 6 wt% CNB and 1.5 wt% LNC after immersion in 3.5wt% nacl for 120 hrs.

The Electric double layer capacitance C_{edl} is attributing to the newly formed polymerized layer (self healing) that is able to stores some energy. The C_{edl} value of CNB coatings is 0.251E-3 F.cm^{-2} is higher than 0.1917E-6 F.cm^{-2} for LNC coatings. Obviously the increase in C_{edl} value for the hybrid (CNF+ benzotriazole) CNB coatings reveals high amount of energy

is stored when compared to the LNC coatings. Therefore the overall coating capacitance also got increased.

Table 5.9 gives values related to polarization (I_{cor}, E_{cor}) impedance (Solution, polarization and coating), and capacitance parameters and corrosion rate of modified epoxies with CNB and LNC coatings of different concentrations. All the parameter values have shown a better performance when compared to the other literature (Yi et al., 2015: Rahman et al., 2017). The proposed coatings have also shown self healing ability, along with corrosion inhibition.

Therefore the prepared coatings are high performance high solid and thick coatings which are capable of self healing and chemical resistant. Therefore concluding that the silanized lignin nanocapsules along with safflower oil have shown a better corrosion inhibition values along with self healing and is able to compete with the CNB based hybrid coatings.

Table 5. 9. Comparison of polarization, Impedance, and corrosion rate data for lignin and cellulose as a corrosion inhibition carrier.

Slno	**Tafel Plot**		**Capacitance($F.cm^{-2}$)**		**Impedance ($\Omega.Cm^2$)**			**Corrosion rate**
	I_{corr} (A/cm^2)	**Ecor**	**C_{edl} Electric Double layer**	**C_c Coating Capacitance**	**R_s Solution Resistance**	**R_p Polarization Resistance**	**R_c Coating Resistance**	**W.r.t Weight loss (mm/year)**
Bare	1.04E-5	0.592	0.0379E-9	0.0126E-6	23.7684	8726	7.816E3	46.868±1.2
Epoxy	1.66e-6	-0.47	0.0211E-9	0.412E-6	23.173	2.5153E4	2.4227E4	8.276±1.1
0.5% Lnc	2.40e-8	-0.488	0.0137E-9	0.343E-6	25.538	3.4801E4	2.915E4	3.626±0.8
1% Lnc	3.13E-7	-0.319	0.7347E-9	0.236 E-6	25.538	4.4745E4	4.22E4	1.394±0.9
1.5% Lnc	3.70E-8	-0.292	0.2142E-9	0.1917E-6	318.5004	6.443E6	6.444E6	0.1022±0.4
Bare	6.03E-4	-0.972	0.355E-06	0.794E-06	316.2278	9.683E3	1.0E4	48.449±1.3
Epoxy	3.20E-5	-0.584	0.316E-07	0.251E-04	630.957	1.578E6	1.584E5	8.834±1.4
2% CNB	8.77E-7	-0.518	0.588E-07	0.398E-04	1000	1.994E7	1.995E6	2.882± 0.9
4% CNB	4.87E-8	-0.347	0.251E-06	0.1E-03	2511.886	4.674E6	4.677E6	2.324±1.1
6% CNB	5.2E-10	-0.002	0.155E-04	0.251E-03	3162.278	1.258E7	1.258E7	1.766± 0.6

5.4.6 Comparing corrosion rate for coatings with lignin and cellulose as a Corrosion inhibitor carrier.

Gravimetric analyses were performed to evaluate the performance of modified epoxy systems with lignin and cellulose. Immersion studies using 3.5wt% nacl solution was used and weight loss studies for average of three different experiments were taken.

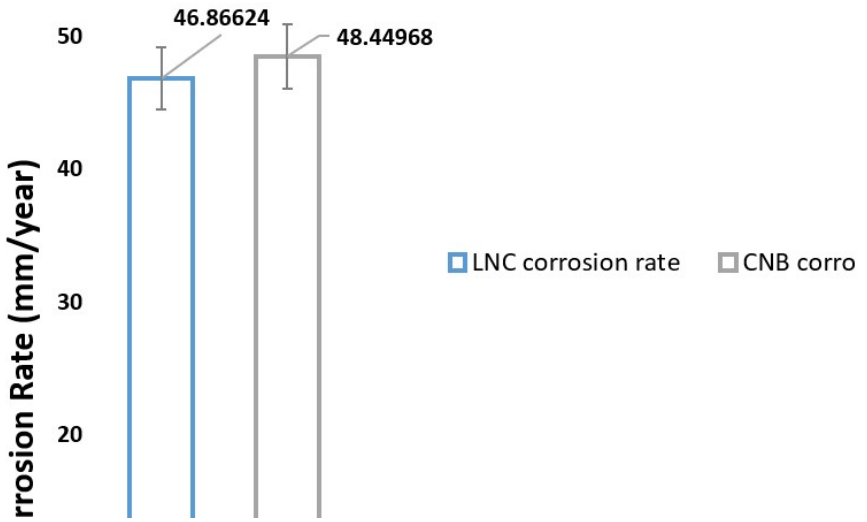

Figure 5. 32. Corrosion rate for different concentrations of organic corrosion inhibitor after 120 hrs of immersion in 3.5 wt% Nacl solution.

From the **figure 5.32** weight loss studies gave nearly equal corrosion rates for the lignin bases coatings when compared with the cellulose based coatings.

From this we can tell lignin based coatings without any synthetic corrosion inhibitor but with little amount of coupling agent is able to compete with the coatings benzotriazole loaded cellulose nano fibers. This reduces the number of layers (primer, intermediate, top). High thick single layer coatings with good corrosion resistance can be done.

Summary:

The performance of two materials were compared by choosing different characteristic epoxies and curing agents In case one 2k water borne epoxy-amine coatings were modified with 0.5, 1, 1.5% lignin nanocapsules. In second case 2k polyamide epoxy was modified by 2, 4, 6% benzotriazole loaded cellulose nano fibers CNB. The gravimetric analysis by weight loss studies proved the corrosion rate is nearly equal to high loadings of both coating system that is for 1.5% LNC is 0.1022$\pm$0.4 and for 6% CNB is 1.76$\pm$0.6 mm/year. The impedance value from bode and nyquist plot reveals for the modified epoxy coating systems as 6.444E6,

1.258E7for 1.5% LNC and 6% CNB coatings respectively. Apart from impedance two coatings also acts as pseudo capacitor with a coating capacitance of0.155E-06, 0.155E-04 $F.cm^{-2}$ for 1.5% LNC and 6% CNB coatings respectively.

Chapter 6

Conclusion

Chapter 6 Conclusion

6.1 Conclusion

The salient conclusion drawn from the present investigation are summarized below

Conclusion on Process Intensification for delignification of tectona grandis saw dust as sustainable biomass using different configured acoustic cavitational devices

- The Lignin extraction from sawdust using different ultrasonic reactors was more effective as compared to the conventional approach with about 2 – 3 times more lignin yields.
- The lignin yields established for different acoustic devices were in the order of longitudinal horn (87.4%), immersion type vertical ultrasonic horn (85.1%), and the ultrasonic bath (82%).
- FTIR analysis reveals that the absorbance peaks were obtained at 1595 and 1700 cm^{-1} revealing the existence of lignin. It was also observed that maximum peak intensity is observed for the sample processed using a longitudinal ultrasonic horn.
- Crystallinity index of treated sawdust was maximum in the case of longitudinal horn (56.6%) followed by ultrasonic horn (53.7%) and ultrasonic bath (52%).
- SEM images of ultrasound-assisted treated biomass, confirmed lower size as compared to the conventional method, which can be attributed to the strong cavitation effects.
- Energy consumption was observed to be less for ultrasonic horn when compared to longitudinal horn and ultrasonic bath type and was the maximum for the conventional method.
- The energy requirement for the longitudinal horn was higher, as it required more energy for stirring as compared to ultrasonic horn, though this is justified on the basis of much larger volumes being handled.

- The work has clearly established an effective lignin extraction approach based on the combination of sodium carbonate and hydrogen peroxide intensified using the ultrasonic reactors.

Conclusion drawn on self healing coatings based on amino silanized encapsulated lignin nanocapsules through sonochemical approach

- Safflower oil and extracted lignin were used as corrosion inhibitor as well as the self-healing agent.
- The FTIR spectra of lignin nanocapsules analysis confirms that the presence of lignin structural groups and safflower oil peaks and UFresin peaks this ensure that LNC are made up of all three (lignin, safflower oil, UF resin).
- Potentio dynamic polarization studies, EIS studies were performed for water-borne epoxy coating (with, and without nanocapsules) for a time period of 120 hour in 3.5 wt % nacl solution.
- I_{corr} values for bare is 1.0423E-5 A/cm^2, and this was decreased to 1.662E-6 A/cm^2 for standard, and its value further got decreased to 2.409E-8, 3.139E-7,3.703E-8A/cm^{2}as weight of lignin increases from 0.5, 1, 1.5wt % in nano-capsules for the modifed epoxy coatings.
- The corrosion potential value got increased showing the thermodynamic state of the anodized metal. E_{cor} values are -0.592, -0.47, -0.488, -0.319, -0.292 for bare standard, 0.5, 1, 1.5wt % lignin nano-capsules.
- Impedance values are higher for LNC coatings compared to bare, and standard coatings. the impedance value was observed to be 2.4 x10^4 Ω cm^{2}for standard epoxy amine coating and increased to 5.8x10^6 ωcm^{2}with the incorporation of lignin-based nanocapsules in the epoxy coatings.
- Electric double layer and coating capacitance values increases as LNC% increases in water borne epoxy coatings increases.

- A maximum of 0.21E-9, 0.155E-06 $F.cm^{-2}$ for electric double layer and coating capacitance was observed. These values tell the modified coatings acts as a pseudo capacitor.

- Corrosion rate from weight loss studies for bare steel, standard epoxy, (0.5, 1, 1.5 wt %) lignin loadings are 46.868±1.2, 8.276±1.1, 3.626±0.8, 1.394±0.9, 0.1022±0.4 mm/year respectively, which confirms the better corrosion rate with the increase in lignin loadings. Similarly better self-healing behavior was observed from EIS analysis and immersion studies.

Conclusion drawn on self-healing corrosion inhibition coatings with pH-responsive activity of nano cellulose in two pack epoxy polyamide system.

- The importance of sonication to have uniform sized particles in preparation of cellulose nano fibers were confirmed with. TEM and SEM images also proves the hallow structure of nano cellulose.

- FTIR results revealed that CNB has similar peaks as that of benzotriazole and cellulose nano fiber ensuring the loading of benzotriazole.

- All the corrosion rate, polarization, impedance values were noted at different interval that is after 72 and 120 hours with immersion of mild steel (bare and coated after marking) in 3.5 wt% sodium chloride.

- Polarization studies have shown decreased in current density I_{cor} values from 6.037E-4, 3.206E-5, 8.779E-7, 4.8174E-8, 5.726E-10 $A/cm^2$with a corrosion potential of E_{corr} values of -0.972, -0.584, -0.518, -0.347, -0.002 volts respectively for bare, standard, 2, 4, 6% CNB after 120 hr.

- The impedance value after 120 hours of immersion for 6 wt% CNB has maximum value up to 1.2E+7.

- Electric double layer and coating capacitance values increases as CNB% increases in 2k polyamide epoxy coatings increases.

- A maximum of 0.251E-03, 0.155E-04$F.cm^{-2}$for electric double layer and coating capacitance was observed. These values confirm that the modified coatings can acts as a pseudo capacitor.

- Corrosion rate proved that corrosion rate is higher for 2, 4, 6 wt% CNB when compared to bare and standard after 120 hr of immersion time.

Conclusions drawn by comparing the Performance of a epoxy coatings modified with LNC and CNB.

- Sustainable eco-friendly hybrid organic coatings with high solid content came into existence which are capable of competing with the fourth generation coatings.
- The corrosion density got decreased to 3.703E-8, 5.726E-10 A/cm^2 for a corrosion potential of -0.292 , -0.002Volts for 1.5% LNC and 6% CNB coatings respectively
- The impedance value from bode and nyquist plot reveals for the two coating systems as 6.444E6, 1.258E7 for 1.5% LNC and 6% CNB coatings respectively.
- Modified epoxy Coatings act as a pseudo capacitor with a coating capacitance of 0.155E-06, 0.155E-04 F.$cm^{-2}$for 1.5% LNC and 6% CNB coatings respectively.
- The gravimetric analysis proved that the corrosion rate is nearly equal to both coating system for higher loadings of corrosion inhibitor that is for 1.5% LNC is 0.1022$\pm$0.4 and for 6% CNB is 1.76$\pm$0.6 mm/year.

6.2 Scope for future work

There is a large scope to continue the present work not only in the coatings but also in the building green concretes. Some of the possibilities are listed below.

- In preparation of green concrete the high build solid epoxy (especially phenolic based) hybrid coatings having high chemical resistant can give long life for mild steel during building a base in construction.
- Valorization of lignin and cellulose by preparation of Superabsorbent polymer (SAP) for the application in crack healing of concrete, and in paints.
- Cellulose based lignin hydrogel can be prepared for synthesis of bio-scaffold.

Bibliography:

Adapa PK, Tabil LG, Schoenau GJ, et al (2011) Quantitative Analysis of Lignocellulosic Components of Non-Treated and Steam Exploded Barley, Canola, Oat and Wheat Straw Using Fourier Transform Infrared Spectroscopy. J Agric Sci Technol B 1:177–188

Adsul SH, Soma Raju KRC, Sarada B V., et al (2018) Evaluation of self-healing properties of inhibitor loaded nanoclay-based anticorrosive coatings on magnesium alloy AZ91D. J Magnes Alloy 6:299–308. doi: 10.1016/j.jma.2018.05.003

Akbarzadeh E, Ibrahim MNM, Rahim AA (2012) Monomers of lignin as corrosion inhibitors for mild steel: study of their behaviour by factorial experimental design. Corros Eng Sci Technol 47:302–311. doi: 10.1179/1743278212y.0000000013

Akbarzadeh E, Ibrahim MNM, Rahim AA (2011) Corrosion inhibition of mild steel in near neutral solution by Kraft and Soda lignins extracted from oil palm empty fruit bunch. Int J Electrochem Sci 6:5396–5416

Almeida IF, Pereira T, Silva NHCS, et al (2014) Bacterial cellulose membranes as drug delivery systems: An in vivo skin compatibility study. Eur J Pharm Biopharm 86:332–336. doi: 10.1016/j.ejpb.2013.08.008

Awad MI (2006) Eco friendly corrosion inhibitors: Inhibitive action of quinine for corrosion of low carbon steel in 1 M HCl. J Appl Electrochem 36:1163–1168. doi: 10.1007/s10800-006-9204-1

Bagale UD, Desale R, Sonawane SH, Kulkarni RD (2018a) An Active Corrosion Inhibition Coating of Two Pack Epoxy Polyamide System using Halloysite Nanocontainer. Prot Met Phys Chem Surfaces 54:230–239. doi: 10.1134/S2070205118020144

Bagale UD, Desale R, Sonawane SH, Kulkarni RD (2018b) An Active Corrosion Inhibition Coating of Two Pack Epoxy Polyamide System using Halloysite Nanocontainer. Prot Met Phys Chem Surfaces 54:230–239. doi: 10.1134/s2070205118020144

Bagale UD, Sonawane SH, Bhanvase BA, et al (2018c) Green synthesis of nanocapsules for self-healing anticorrosion coating using ultrasound-assisted approach. Green Process Synth 7:147–159. doi: 10.1515/gps-2016-0160

Bansal N, Bhalla A, Pattathil S, et al (2016) Cell wall-associated transition metals improve alkaline-oxidative pretreatment in diverse hardwoods. Green Chem 18:1405–1415. doi: 10.1039/c5gc01748c

Chhabra A, Gohel A (2017) Recent observations of atmospheric carbon dioxide over India. Curr Sci 112:2364–2366

Devadasu S, Joshi S, Gogate P, Sonawane S (2019) INTENSIFICATION OF DELIGNIFICATION OF TECTONAGRANDIS SAW DUST AS SUSTAINABLE BIOMASS USING ACOUSTIC. Ultrason Sonochem 104914. doi: 10.1016/j.ultsonch.2019.104914

Division B, Science I, Division B, Science I Pretreatment of Biomass

Espinoza J, Torres P, Ramírez B, et al (2016) Antioxidant, antimicrobial, and antimutagenic

properties of technical lignins and their applications. BioResources 11:5452–5481. doi: 10.15376/biores.11.2.Espinoza_Acosta

Fan TT, Chen X, Wang JH, et al (2011) Effect of Low Concentration Alkali and Ultrasound Combination Pretreatment on Biogas Production by Stalk. Adv Mater Res 383–390:3434–3437. doi: 10.4028/www.scientific.net/amr.383-390.3434

Faustino H, Gil N, Baptista C, Duarte AP (2010) Antioxidant activity of lignin phenolic compounds extracted from kraft and sulphite black liquors. Molecules 15:9308–9322. doi: 10.3390/molecules15129308

Frankel GS (2016) Active Protective Coatings. 233:. doi: 10.1007/978-94-017-7540-3

G. C, F. A (2014) Corrosion Inhibitors – Principles, Mechanisms and Applications. Dev Corros Prot. doi: 10.5772/57255

García A, Alriols MG, Llano-Ponte R, Labidi J (2011) Ultrasound-assisted fractionation of the lignocellulosic material. Bioresour Technol 102:6326–6330. doi: 10.1016/j.biortech.2011.02.045

Halambek J, Berković K, Vorkapić-Furač J (2010) The influence of Lavandula angustifolia L. oil on corrosion of Al-3Mg alloy. Corros Sci 52:3978–3983. doi: 10.1016/j.corsci.2010.08.012

He Y, Boluk Y, Pan J, et al (2019) Corrosion protective properties of cellulose nanocrystals reinforced waterborne acrylate-based composite coating. Corros Sci 155:186–194. doi: 10.1016/j.corsci.2019.04.038

HUANG G, ZHANG C, CHEN Z (2006) Pulping of Wheat Straw with Caustic Potash-Ammonia Aqueous Solutions and Its Kinetics1 1 Supported by the Natural Science Foundation of Jiangxi Province (No. 0520003). Chinese J Chem Eng 14:729–733. doi: 10.1016/S1004-9541(07)60003-2

Hussin MH, Rahim AA, Mohamad Ibrahim MN, Brosse N (2015a) Improved corrosion inhibition of mild steel by chemically modified lignin polymers from Elaeis guineensis agricultural waste. Mater Chem Phys 163:201–212. doi: 10.1016/j.matchemphys.2015.07.030

Hussin MH, Shah AM, Rahim AA, et al (2015b) Antioxidant and anticorrosive properties of oil palm frond lignins extracted with different techniques. Ann For Sci 72:17–26. doi: 10.1007/s13595-014-0405-1

Kasaeian M, Ghasemi E, Ramezanzadeh B, et al (2018) Construction of a highly effective self-repair corrosion-resistant epoxy composite through impregnation of 1H-Benzimidazole corrosion inhibitor modified graphene oxide nanosheets (GO-BIM). Corros Sci 145:119–134. doi: 10.1016/j.corsci.2018.09.023

Leal DA, Riegel-Vidotti IC, Ferreira MGS, Marino CEB (2018) Smart coating based on double stimuli-responsive microcapsules containing linseed oil and benzotriazole for active corrosion protection. Corros Sci 130:56–63. doi: 10.1016/j.corsci.2017.10.009

Mohamed HA, Rehim MHA (2015) Surface active hyperbranched polyamide-ester as a corrosion inhibitor for carbon steel in both neutral and acidic media. Anti-Corrosion

Methods Mater 62:95–102. doi: 10.1108/ACMM-11-2013-1324

Montemor MF (2014) Functional and smart coatings for corrosion protection: A review of recent advances. Surf Coatings Technol 258:17–37. doi: 10.1016/j.surfcoat.2014.06.031

Mounguengui S, Saha Tchinda JB, Ndikontar MK, et al (2016) Total phenolic and lignin contents, phytochemical screening, antioxidant and fungal inhibition properties of the heartwood extractives of ten Congo Basin tree species. Ann For Sci 73:287–296. doi: 10.1007/s13595-015-0514-5

Nesterova T, Dam-Johansen K, Pedersen LT, Kiil S (2012) Microcapsule-based self-healing anticorrosive coatings: Capsule size, coating formulation, and exposure testing. Prog Org Coatings 75:309–318. doi: 10.1016/j.porgcoat.2012.08.002

Neumann GT, Pimentel BR, Rensel DJ, Hicks JC (2014) Correlating lignin structure to aromatic products in the catalytic fast pyrolysis of lignin model compounds containing β-O-4 linkages. Catal Sci Technol 4:3953–3963. doi: 10.1039/c4cy00569d

Ogunleye OO, Arinkoola AO, Eletta OA, et al (2020) Green corrosion inhibition and adsorption characteristics of Luffa cylindrica leaf extract on mild steel in hydrochloric acid environment. Heliyon 6:e03205. doi: 10.1016/j.heliyon.2020.e03205

Olad A, Nosrati R (2013) Preparation and corrosion resistance of nanostructured PVC/ZnO-polyaniline hybrid coating. Prog Org Coatings 76:113–118. doi: 10.1016/j.porgcoat.2012.08.017

Padilla-Martinez JP, Berrospe-Rodriguez C, Aguilar G, et al (2014) Optic cavitation with CW lasers: A review. Phys Fluids 26:16–20. doi: 10.1063/1.4904718

Patil RC, Radhakrishnan S (2006) Conducting polymer based hybrid nano-composites for enhanced corrosion protective coatings. Prog Org Coatings 57:332–336. doi: 10.1016/j.porgcoat.2006.09.012

Pinjari DV, Pandit AB (2010) Cavitation milling of natural cellulose to nanofibrils. Ultrason Sonochem 17:845–852. doi: 10.1016/j.ultsonch.2010.03.005

Qiu S, Chen C, Cui M, et al (2017) Corrosion protection performance of waterborne epoxy coatings containing self-doped polyaniline nanofiber. Appl Surf Sci 407:213–222. doi: 10.1016/j.apsusc.2017.02.142

Rahman OU, Shi S, Ding J, et al (2018) Lignin nanoparticles: Synthesis, characterization and corrosion protection performance. New J Chem 42:3415–3425. doi: 10.1039/c7nj04103a

Raja PB, Ismail M, Ghoreishiamiri S, et al (2016) Reviews on Corrosion Inhibitors: A Short View. Chem Eng Commun 203:1145–1156. doi: 10.1080/00986445.2016.1172485

Ramadoss G, Muthukumar K (2016) Ultrasonics Sonochemistry Mechanistic study on ultrasound assisted pretreatment of sugarcane bagasse using metal salt with hydrogen peroxide for bioethanol production. Ultrason Sonochem 28:207–217. doi: 10.1016/j.ultsonch.2015.07.006

Ramezanzadeh B, Attar MM (2011) Studying the effects of micro and nano sized ZnO particles on the corrosion resistance and deterioration behavior of an epoxy-polyamide coating on hot-dip galvanized steel. Prog Org Coatings 71:314–328. doi:

10.1016/j.porgcoat.2011.03.026

Ramezanzadeh B, Attar MM, Farzam M (2011) A study on the anticorrosion performance of the epoxy-polyamide nanocomposites containing ZnO nanoparticles. Prog Org Coatings 72:410–422. doi: 10.1016/j.porgcoat.2011.05.014

Ramli RA (2019) Slow release fertilizer hydrogels: A review. Polym Chem 10:6073–6090. doi: 10.1039/c9py01036j

Rauber D, Dier TKF, Volmer DA, Hempelmann R (2018) Electrochemical Lignin Degradation in Ionic Liquids on Ternary Mixed Metal Electrodes. Zeitschrift fur Phys Chemie 232:189–208. doi: 10.1515/zpch-2017-0951

Sathiyanarayanan S, Azim SS, Venkatachari G (2007a) Preparation of polyaniline-Fe2O3 composite and its anticorrosion performance. Synth Met 157:751–757. doi: 10.1016/j.synthmet.2007.08.004

Sathiyanarayanan S, Azim SS, Venkatachari G (2007b) Corrosion protection of magnesium ZM 21 alloy with polyaniline-TiO2 composite containing coatings. Prog Org Coatings 59:291–296. doi: 10.1016/j.porgcoat.2007.04.004

Selvaraj M, Maruthan K, Palraj S, Venkatachari G (2010) Preparation and characterization of thermally stable epoxy-titanate coatings. Prog Org Coatings 67:339–347. doi: 10.1016/j.porgcoat.2009.10.024

Shchukin DG, Lamaka S V., Yasakau KA, et al (2008) Active anticorrosion coatings with halloysite nanocontainers. J Phys Chem C 112:958–964. doi: 10.1021/jp076188r

Siva T, Kamaraj K, Karpakam V, Sathiyanarayanan S (2013) Soft template synthesis of poly(o-phenylenediamine) nanotubes and its application in self healing coatings. Prog Org Coatings 76:581–588. doi: 10.1016/j.porgcoat.2012.11.009

Sonawane S, Chaudhari P, Ghodke S, et al (2008) Combined effect of ultrasound and nanoclay on adsorption of phenol. Ultrason Sonochem 15:1033–1037. doi: 10.1016/j.ultsonch.2008.03.006

Subhedar PB, Gogate PR (2014) Alkaline and ultrasound assisted alkaline pretreatment for intensification of delignification process from sustainable raw-material. Ultrason Sonochem 21:216–225. doi: 10.1016/j.ultsonch.2013.08.001

Suryanarayana C, Rao KC, Kumar D (2008) Preparation and characterization of microcapsules containing linseed oil and its use in self-healing coatings. Prog Org Coatings 63:72–78. doi: 10.1016/j.porgcoat.2008.04.008

Theme S (2010) Solar membrane natural gas steam-reforming process 179–190. doi: 10.1002

Thesis a (2012) Ultrasonic Pretreatment for Anaerobic Digestion : a Study on Feedstock , Methane Yield , and Energy Balance

Trask RS, Williams HR, Bond IP (2007) Self-healing polymer composites: Mimicking nature to enhance performance. Bioinspiration and Biomimetics 2:. doi: 10.1088/1748-3182/2/1/P01

Velmurugan R, Muthukumar K (2012) Ultrasound-assisted alkaline pretreatment of sugarcane

bagasse for fermentable sugar production: Optimization through response surface methodology. Bioresour Technol 112:293–299. doi: 10.1016/j.biortech.2012.01.168

Vijayan P, AlMaadeed MA (2016) 'Containers' for self-healing epoxy composites and coating: Trends and advances. Express Polym Lett 10:506–524. doi: 10.3144/expresspolymlett.2016.48

Villa S, Riani P, Locardi F, Canepa F (2016) Functionalization of Fe3O4 NPs by silanization: Use of amine (APTES) and thiol (MPTMS) silanes and their physical characterization. Materials (Basel) 9:. doi: 10.3390/ma9100826

Wei Z, Yang JH, Zhou J, et al (2014) Self-healing gels based on constitutional dynamic chemistry and their potential applications. Chem Soc Rev 43:8114–8131. doi: 10.1039/c4cs00219a

White SR, Sottos NR, Geubelle PH, et al (2001) Autonomic healing of polymer composites. Nature 409:794–797. doi: 10.1038/35057232

Wypych G (2017) Additives and Chemical Structures Used in Self-Healing Technology. Self-Healing Mater 117–149. doi: 10.1016/b978-1-927885-23-9.50015-8

Xie S, Ragauskas AJ, Yuan JS (2016) Lignin Conversion: Opportunities and Challenges for the Integrated Biorefinery. Ind Biotechnol 12:161–167. doi: 10.1089/ind.2016.0007

Yabuki A, Kawashima A, Fathona IW (2014) Self-healing polymer coatings with cellulose nanofibers served as pathways for the release of a corrosion inhibitor. Corros Sci 85:141–146. doi: 10.1016/j.corsci.2014.04.010

Yabuki A, Shiraiwa T, Fathona IW (2016) pH-controlled self-healing polymer coatings with cellulose nanofibers providing an effective release of corrosion inhibitor. Corros Sci 103:117–123. doi: 10.1016/j.corsci.2015.11.015

Yadav M, Gope L, Sarkar TK (2016) Synthesized amino acid compounds as eco-friendly corrosion inhibitors for mild steel in hydrochloric acid solution: Electrochemical and quantum studies. Res Chem Intermed 42:2641–2660. doi: 10.1007/s11164-015-2172-5

Yi H, Yang Y, Gu X, et al (2015) Multilayer composite microcapsules synthesized by Pickering emulsion templates and their application in self-healing coating. J Mater Chem A 3:13749–13757. doi: 10.1039/c5ta02288f

Yiamsawas D, Baier G, Thines E, et al (2014) Biodegradable lignin nanocontainers. RSC Adv 4:11661–11663. doi: 10.1039/c3ra47971d

Yuan Z, Wen Y, Li G (2018) Production of bioethanol and value added compounds from wheat straw through combined alkaline/alkaline-peroxide pretreatment. Bioresour Technol 259:228–236. doi: 10.1016/j.biortech.2018.03.044

Zhao J, Lu Z, He X, et al (2017) One-Step Fabrication of Fe(OH)3@Cellulose Hollow Nanofibers with Superior Capability for Water Purification. ACS Appl Mater Interfaces 9:25339–25349. doi: 10.1021/acsami.7b07038

Zhong K, Zheng XL, Mao XY, et al (2012) Sugarcane bagasse derivative-based superabsorbent containing phosphate rock with water-fertilizer integration. Carbohydr Polym 90:820–826. doi: 10.1016/j.carbpol.2012.06.006

International Publications and Conferences and Book chapters

International Publications

1. Devadasu Sushmitha, Sourabh Joshi, Parag Gogate, Shirish Hari Sonawane, Srinath Suranani " Intensification of delignification of *tectona grandis* saw dust as sustainable biomass using acoustic cavitational devices" Ultrasonication and Sonochemistry,ISSN 1350-4177,63(2020), 104914, PP- 1-12. Elsevier, SCI-Indexed, Impact Factor-6.5. https://doi.org/10/1016/j.uiltsoch.2019.104914

2. Devadasu Sushmitha, Shirish Hari Sonawane, Srinath Suranani"Self-healing Corrosion Inhibition Coatings with PH-Responsive Activity by Incorporation of Nano Cellulose in Two pack epoxy polyamide system" Materials today Proceedings,ISSN 2214-7853, Scopus Indexed. https://doi.org/10.1016/j.matpr.2020.09.341

3. Devadasu Sushmitha, Uday Bagale, Shirish Hari Sonawane, Srinath Suranani "Development of Ultra-High Build Self-Healing Coatings Using Amino Silanized Lignin Nanocapsules".Materials today Proceedings,ISSN 2214-7853, Scopus Indexed. http://doi.org/10.1016/j.matpr.2021.02.576

International Conferences

1. D.Sushmitha, S.Srinath, S.Shirish "Ultrasound Assisted Pretreatment for efficient delignification of sawdust using sodium percarbonate", published in the proceeding of CHEMCON 2016, IIT-Madras, Dec- 27-30, 2016.

2. D.Sushmitha, S.Srinath "Optimization of Microwave assisted delignification process parameters using Response surface methodology, central composite design", RESEARCH CONCLAVE 2017, NITW, Warangal, during March 18-19, 2017.

3. D.Sushmitha, Anjani Mamidala, AkaknkshaMamidala, P.V. Nagaprapurna, Srinath Suranani"Investigation of a controlled release rate studies on Benzotriazole Loaded Electrospun Cellulose hallow Nano Fibers Proceedings of the ASEAO 2019 International Conference Singapore-, May 23 – 24, 2019.

4. D. Sushmitha, Uday bagale, Shirish Hari Sonawane, S.Srinath "Lignin Encapsulation by Pickering Emulsion and In-Situ Polymerization for Corrosion Inhibition of Mild Steel"

Energy and Environmental Technologies for Sustainable Development (CHEM-CONFLUX 20) MNIT Allahabad February 13-15, 2020.PP-87.

5. D.Sushmitha, S.Srinath "Evaluation of corrosion inhibition performance of encapsulated lignin and hollow cellulose as a carriers for self-healing of mild steel." International conference on recent advances in material chemistry, 5th ICRAMC-2021 on February 18-20 at SRM University, Tamil Nadu.

Book Chapters

1. D.Sushmitha, S.Srinath "Microwave assisted alkali-peroxide treated sawdust for delignification and its characterization" 2018. (Published in *springer book 2*Waste Valorization and Recycling, Volume 2, PP 527-537. ISBN 978-981-13-2783-4, DOI: https://doi.org/10.1007/978-981-13-2784-1.

2. Devadasu Sushmitha, Srinath Suranani"An Intensified and Integrated Biorefinery Approach for Bio-fuel Production."Inbook: Biochemical and Environmental Bioprocessing, chapter 5, July 2019.Taylor and franscis Group, CRC publication. Jerold, M. (Ed.), Sivasubramanian, V. (Ed.). (2020). Biochemical and Environmental Bioprocessing. Boca Raton: CRC **Press,** https://doi.org/10.1201/9780429198045**.**